I. THE CRYSTAL STRUCTURE OF TRIMESIC ACID

II. TOPICS IN CRYSTALLOGRAPHIC CALCULATIONS

Thesis by

David James Duchamp

In Partial Fulfillment of the Requirements

For the Degree of

Doctor of Philosophy

California Institute of Technology

Pasadena, California

1965

(Submitted May 14, 1965)

ACKNOWLEDGMENTS

For guidance during my graduate years, I am grateful to Dr. Richard E. Marsh, who was always available for discussions which were both educational and inspirational to me.

I acknowledge with thanks financial support from the National Science Foundation and the California Institute of Technology.

I wish to thank Professor J. H. Sturdivant, Professor Jürg Waser, Professor William P. Schaefer, and Dr. Sten Samson for their assistance on matters ranging from the use of x-ray apparatus to the teaching of freshmen.

My thanks also go to the members of the research group with which I have had the privilege of associating — especially to Dr. B. D. Sharma, Dr. R. H. Stanford, and Dr. C. M. Gramaccioli. In addition to discussing subjects of general interest with me, these gentlemen have allowed me to observe their work in detail, and thus broadened my research experience at Caltech.

I owe a special debt of gratitude to my father, C. J. Duchamp, whose support and encouragement has made my entire education possible.

Thanks also go to my wife, Annette, for her understanding and hard work during the preparation of this thesis.

I. THE CRYSTAL STRUCTURE OF TRIMESIC ACID
II. TOPICS IN CRYSTALLOGRAPHIC CALCULATIONS

By David James Duchamp

ABSTRACT

I. Trimesic acid (1, 3, 5-benzenetricarboxylic acid) crystallizes with a monoclinic unit cell of dimensions $\underline{a}$ = 26.52 A, $\underline{b}$ = 16.42 A, $\underline{c}$ = 26.55 A, and β = 91.53° with 48 molecules/unit cell. Extinctions indicated a space group of Cc or C2/c; a satisfactory structure was obtained in the latter with 6 molecules/asymmetric unit — $C_{54}O_{36}H_{36}$ with a formula weight of 1261 g. Of approximately 12,000 independent reflections within the CuK_{α} sphere, intensities of 11,563 were recorded visually from equi-inclination Weissenberg photographs.

The structure was solved by packing considerations aided by molecular transforms and two- and three-dimensional Patterson functions. Hydrogen positions were found on difference maps. A total of 978 parameters were refined by least squares; these included hydrogen parameters and anisotropic temperature factors for the C and O atoms. The final R factor was 0.0675; the final "goodness of fit" was 1.49. All calculations were carried out on the Caltech IBM 7040-7094 computer using the CRYRM Crystallographic Computing System.

The six independent molecules fall into two groups of three nearly parallel molecules. All molecules are connected by carboxyl-to-carboxyl hydrogen bond pairs to form a continuous array of six-molecule rings with a chicken-wire appearance. These arrays bend to assume two orientations, forming pleated sheets. Arrays in different orientations interpenetrate — three molecules in one orientation passing through the holes of three parallel arrays in the alternate orientation — to produce a completely interlocking network. One third of the carboxyl hydrogen atoms were found to be disordered.

II. Optical transforms as related to x-ray diffraction patterns are discussed with reference to the theory of Fraunhofer diffraction.

The use of a systems approach in crystallographic computing is discussed with special emphasis on the way in which this has been done at the California Institute of Technology.

An efficient manner of calculating Fourier and Patterson maps on a digital computer is presented. Expressions for the calculation of to-scale maps for standard sections and for general-plane sections are developed; space-group-specific expressions in a form suitable for computers are given for all space groups except the hexagonal ones.

Expressions for the calculation of settings for an Eulerian-cradle diffractometer are developed for both the general triclinic case and the orthogonal case.

Photographic materials on pp. 4, 6, 10, and 20 are essential and will not reproduce clearly on Xerox copies. Photographic copies should be ordered.

TABLE OF CONTENTS

PART I

THE CRYSTAL STRUCTURE OF TRIMESIC ACID

INTRODUCTION

Early in 1962 our attention was called to trimesic acid — 1, 3, 5-benzenetricarboxylic acid — by Professor Harden M. McConnell and Dr. G. R. Leibling. Their EPR experiments showed that trimesic acid crystals may be damaged by x-rays to produce a "relatively high concentration of stable, long-lived free radicals" (1). They pointed out that a crystal structure determination had never been reported for this compound. Knowledge of the crystal structure is essential to precise interpretation of the EPR phenomena described above.

D'everin (2) reported that trimesic acid forms rhombic crystals which are strongly double refractive. A literature survey showed no other reference to crystals of trimesic acid.

We were especially interested in trimesic acid because it has a high potential for hydrogen bond formation. Its high melting point (350°) suggests a tightly hydrogen-bonded structure. Determination of this structure is in line with other investigations being undertaken at this laboratory for the purpose of obtaining more and better information on the crystal structures of hydrogen-bonded compounds.

PRELIMINARY OBSERVATIONS

i) Unit cell and space group.

Large prismatic crystals of trimesic acid were furnished by Dr. Leibling. A preliminary investigation showed the crystals to be monoclinic with approximate cell dimensions $\underline{a} = \underline{c} = 26.5$ A, $\underline{b} = 16.35$ A, and $\beta = 91.6°$. (For final cell parameters see Table 2.) Reflections of the type $hk\ell$ are present only for $h + k = 2n$, and of the type $h0\ell$ only for $\ell = 2n$, $(h = 2n)$. These absences indicate that the space group is either Cc or C 2/c. The density measured by flotation methods is 1.46 g. cm.$^{-3}$, in good agreement with the value 1.45 g. cm.$^{-3}$ calculated on the basis of 48 molecules per unit cell — or 6 molecules per asymmetric unit if the space group is C 2/c.

The $h0\ell$ Weissenberg photographs show almost exact mm symmetry with the mirror planes along the [1 0 1] and the [1 0 $\bar{1}$] axes — making the $h0\ell$ reflections equivalent to the $\ell 0h$ reflections (see Figure 1). Only a few reflections deviate from this rule. In upper layers this mm pseudosymmetry disappears.

ii) Twinning.

Many crystals appear to twin internally about the [1 0 1] or [1 0 $\bar{1}$] planes. In twinned crystals the pseudo-mm $h0\ell$ symmetry features are propagated to different extents in the upper layers. Attempts to detect this twinning with a microscope were unsuccessful. Checking an upper level Weissenberg x-ray photograph for absence of reflections with $h + k = 2n + 1$ appears to be the only sure test.

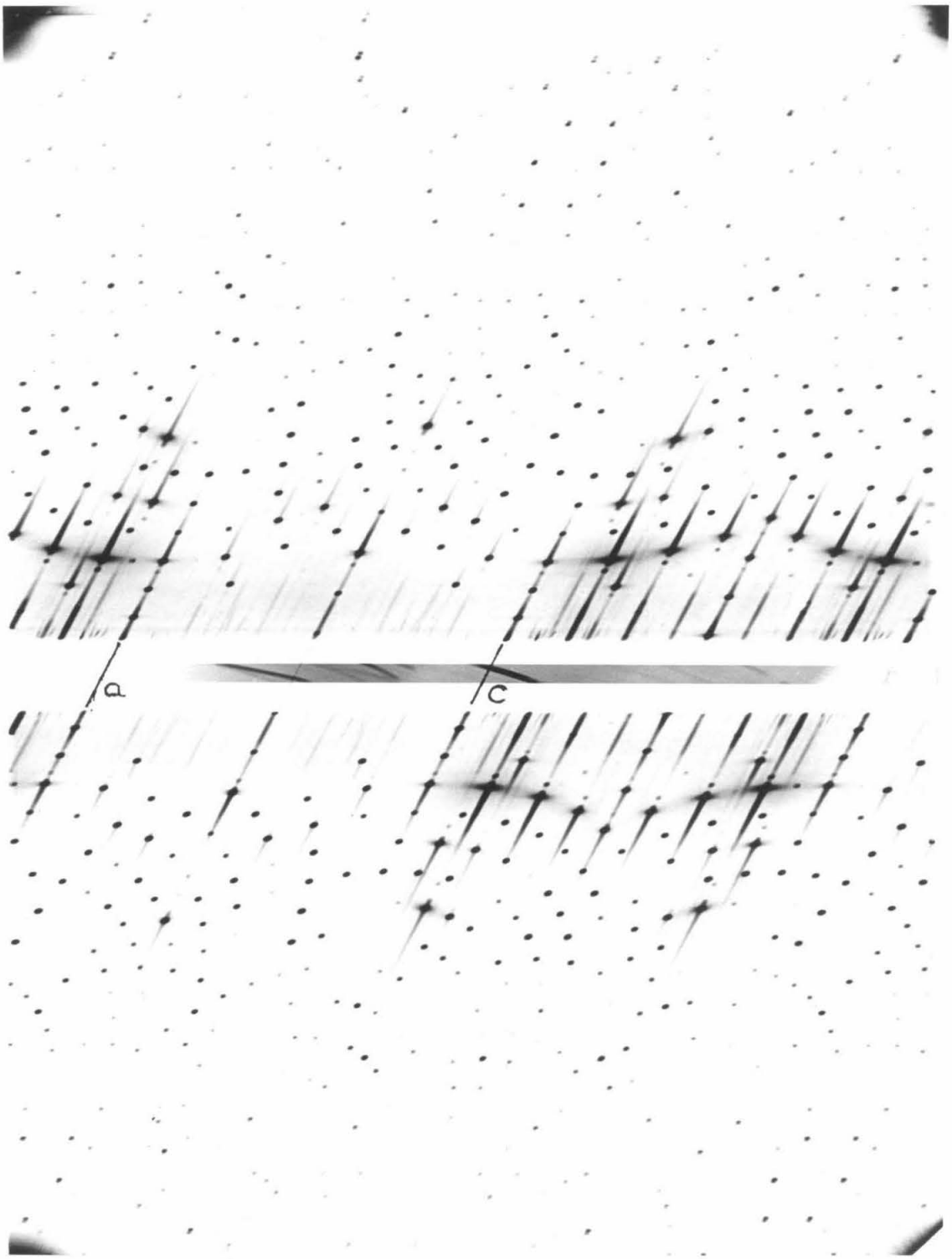

Figure 1. An h0ℓ Weissenberg photograph of trimesic acid.

iii) A disordered crystalline form of trimesic acid.

While trying to obtain untwinned crystals of trimesic acid, another crystalline form was encountered. Crystals of this form are slender needles, the needle axis constituting the b axis of a monoclinic unit cell. An oscillating-crystal photograph showed that the odd layers about b are much weaker than the even layers. Even-layer equi-inclination Weissenberg photographs have a normal appearance with the exception of obvious twinning about the b, c plane. Odd-layer photographs, however, show a peculiar smearing of spots along the reciprocal lattice festoons. The hlℓ photograph is shown in Figure 2. This smearing behavior is certainly caused by disorder. It was also found that the odd layers were about 15–20 times weaker than the even layers. Somewhat similar smearing behavior has been observed before — for example, in condensed phosphates (3) and in woolastonite ($CaSiO_3$) (4). A. J. C. Wilson (5) has discussed disordering in layer structures to some extent.

If all the weak smeared spots are considered true lattice reflections, the unit cell has approximate dimensions a = 26.2 A, b = 7.8 A, c = 21.9 A, and β = 102°. Reflections of the type hkℓ are present only for h + k = 2n and reflections of the type h0ℓ only for ℓ = 2n, indicating that the space group is either Cc or C 2/c. All reflections with both h and k odd fall on streaked festoons.

If all the weak smeared spots are considered not to be true lattice reflections, but instead the result of disorder a smaller unit cell may be chosen. The a and b axes are halved, and the "true"

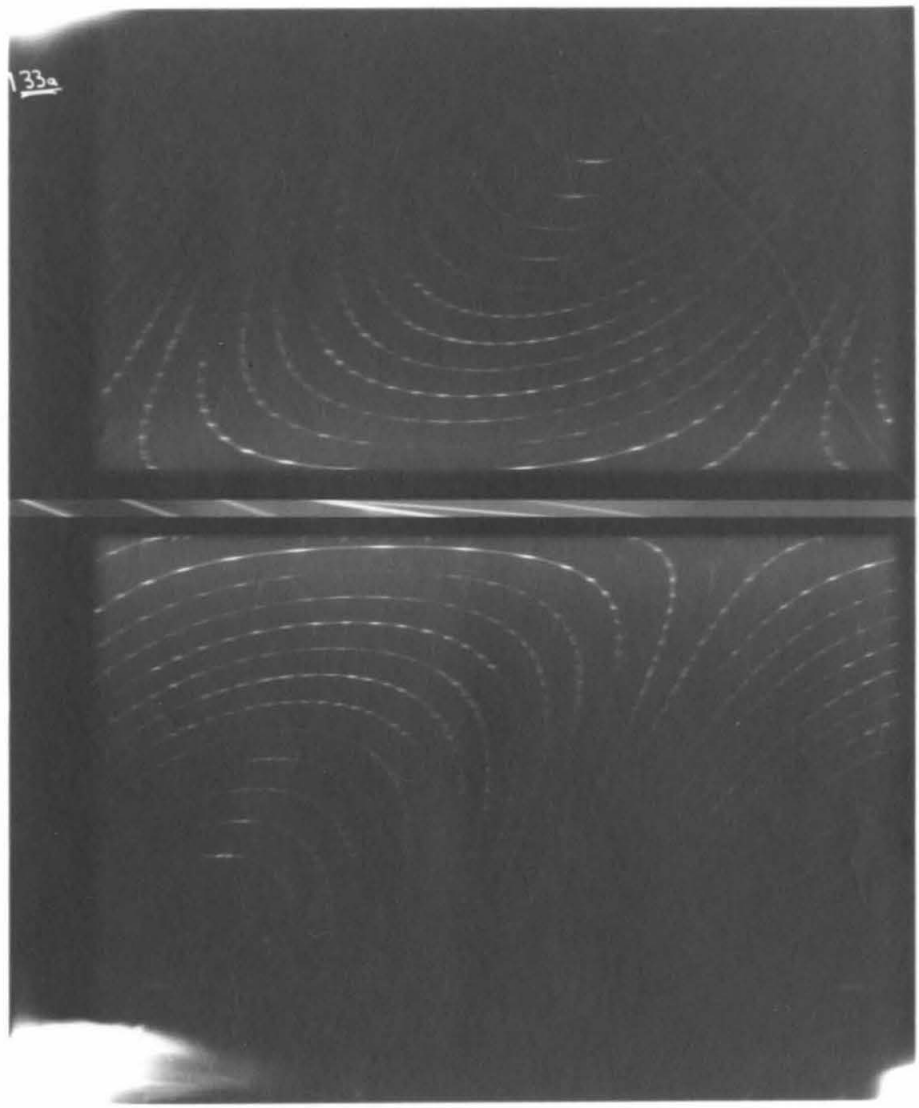

Figure 2. h1ℓ equi-inclination Weissenberg photograph showing disorder streaks. (Disordered crystalline form of trimesic acid.)

unit cell has approximate cell parameters: $\underline{a}' = 13.1$ A, $\underline{b}' = 3.9$ A, $\underline{c} = 21.8$ A, $\beta = 102°$. Defined according to this new cell, the h'k'ℓ reflections show no general absences, and the h'0ℓ reflections are still present only for $\ell = 2n$. An 0k'ℓ precession photograph indicated that the 0k'0 reflections are present only for $k' = 2n$. This indicates that the probable space group for the new cell is $P2_1/c$.

The short $\underline{b}'$ axis leads to the suspicion that the plane of the trimesic acid molecules may be perpendicular to the $\underline{b}'$ axis. Plotting the h0ℓ reciprocal lattice gives the pattern shown in Figure 3 (a). Comparing this to the transform of trimesic acid — shown in Figure 5 — confirmed the above assumption and showed that the six-membered ring of the molecule has the orientation shown in Figure 3 (b) with respect to the other axes.

The calculated density, 1.3 g. cm.$^{-3}$ (assuming no water of crystallization), seems to indicate four molecules of trimesic acid in the $\underline{a}', \underline{b}', \underline{c}$ cell. The presence or absence of water has not definitely been established yet, but water appears to be present. Perhaps the presence of water in a disordered array is causing the streaking phenomena. A more complete analysis of this disordering has not been undertaken.

iv) Problem size and feasibility.

Six molecules per asymmetric unit — this means the asymmetric unit has an empirical formula $C_{54}O_{36}H_{36}$ with a formula weight of 1260.9 g. Determination of the crystal structure of trimesic acid

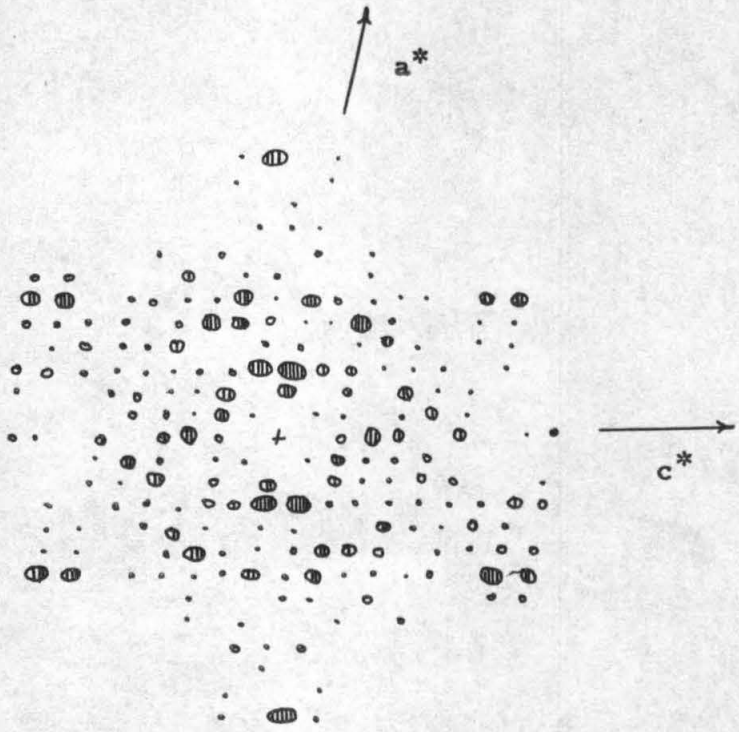

(a) Plot of h0ℓ reciprocal lattice.

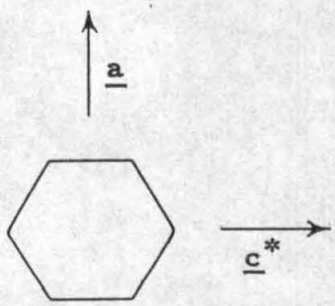

(b) Orientation of the six-membered ring.

Figure 3. Ring orientation in disordered form of *trimesic* acid.

thus required that the positions of 90 heavier atoms and 36 hydrogens be fixed. The most ambitious crystallographic investigation previous to this one was Vitamin B_{12}, $C_{63}H_{88}O_{14}N_{14}PCo$, with 1356 g. for the formula weight of the asymmetric unit (6). This structure was solved by the "heavy" atom method; trimesic acid has no heavy atoms. In addition the B_{12} structure determination took over 10 years and the efforts of many people. The questions were: first, could the crystal structure of trimesic acid be solved at all? and second, if it could be solved, would such a project be feasible for a doctoral dissertation?

In addition to solution of the structure, another problem to be faced was collection of data — there are about 12,000 independent reflections within the copper sphere. Computing would also be a problem. Refinement, in particular, with so many reflections and so many parameters had never before been done. For accurate hydrogen bonding information we would need a high accuracy determination with anisotropic thermal parameters and location of hydrogen atoms — all leading to a large computational problem.

In spite of these difficulties, the investigation was continued for a number of reasons. There are properties of the trimesic acid reciprocal lattice which indicated that the structure might be solvable in spite of the large size of the unit cell and the lack of a "heavy" atom. The transform of a six-membered ring appeared to be present on the rotation photograph about the b axis (see Figure 4). This indicated that the molecules might not be "randomly" oriented within one asymmetric unit; parallel molecules or similar orientation of certain

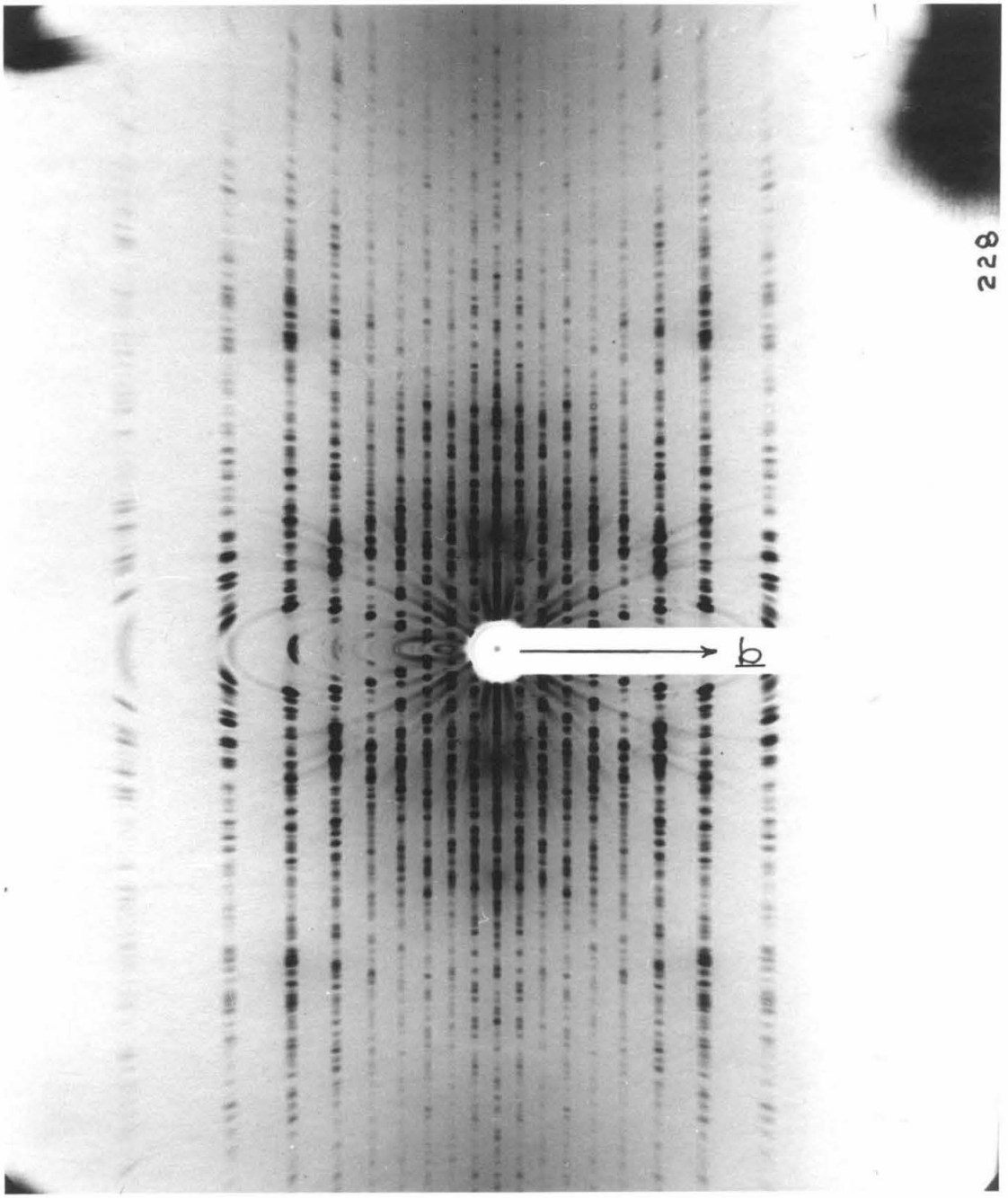

Figure 4. Rotation photograph about the b axis.

molecules with respect to given directions might be anticipated.

At this time, the Institute was in the process of acquiring powerful computing facilities which, if programmed correctly, would make the calculations feasible. In addition it was improbable that any other laboratory would attempt to solve this same structure (a reason particularly appealing to the author). With the discovery of the large size of the asymmetric unit, interest in the hydrogen bonding had increased. This structure is the largest ever attempted without a "heavy" atom, and in the final analysis, the main reason for going on was the same reason that sent men to the top of Mount Everest.

COLLECTION OF THREE-DIMENSIONAL DATA

i) Getting a crystal.

Among the crystals obtained from Dr. Leibling, the great majority were found to be twinned. The first crystal mounted was not twinned but was much too large for taking intensity photographs. Eventually two more untwinned crystals were found; since these were also too large, and since a spherical crystal is superior for collection of intensity data, a device for grinding crystals into spheres was constructed according to the plans given by Bond (7). A first attempt at sphere grinding produced two hemispherical crystals, x-ray photographs showing that cleavage had occurred perpendicular to the [1 0 $\bar{1}$] axis. A satisfactory sphere of diameter approximately 0.43 mm. was obtained from the last crystal.

ii) Data collection.

Three-dimensional intensity data were collected by the equi-inclination Weissenberg method using CuK_{α} radiation. A complete set of multiple-film photographs about the b and a axes was taken using the spherical crystal. The 0-layer about the [1 0 $\bar{1}$] axis was taken using the hemispherical crystal described previously. Using a standard intensity strip prepared from the spherical crystal, the intensities of reflections on layers 0-14 about the b axis, 0-4 about the a axis, and the 0 layer about the [1 0 $\bar{1}$] axis were estimated visually. (Data from the 0 layer about the [1 0 $\bar{1}$] axis were necessary because the set of even and the set of odd layers about the a and b

axes are not intercorrelated due to the absence of reflection with h + k odd.) Table 1 shows the number of reflections which were recorded. One will notice a large number of "less than" reflections — reflections which were too weak to observe. An attempt to observe some of these reflections through longer exposures did not yield much additional information. The absence of these reflections is probably due to the special properties of the crystal structure.

The films showed that quite a few intensities were affected by secondary reflection — the Renniger effect. Reflections so affected had a peculiar spot shape on the film and had different intensities when observed in different places. Reflections for which the films showed this effect to be important were given zero weight in the least squares.

iii) Precision unit cell parameters.

Precision h0ℓ and 0kℓ Weissenberg photographs using CuK_α radiation were taken using a Straumanis-type camera which has a radius of 180 π mm. and a film travel of approximately 23 mm. per 180° of rotation. On the h0ℓ photograph, 97 observations of reflection position were made, and on the 0kℓ photograph, 30 observations; all but 11 observations were for θ greater than 61°, with the $K_{\alpha 1}$ and $K_{\alpha 2}$ of the same reflection being considered as separate observations for high angle reflections. A set of cell parameters was calculated from these data using the CRYRM subprogram written for this purpose by G. Reeke (8). This subprogram minimizes the

Table 1. Summary of data collection.

Layer-Axis	Number of Reflections Recorded	Number of Recorded Reflections which were "Less Than"
0-b	454	86
1-b	903	315
2-b	881	279
3-b	886	231
4-b	868	304
5-b	851	264
6-b	838	175
7-b	806	173
8-b	776	226
9-b	737	221
10-b	711	227
11-b	663	229
12-b	626	210
13-b	560	124
14-b	509	121
0-a	284	35
1-a	521	94
2-a	557	103
3-a	547	107
4-a	554	113
0-[1 0 $\bar{1}$]	202	85

Table 2. Results of precision unit cell calculations.

a	26.5211	26.5201	26.5188
σ(a)	0.0006	0.0005	0.0004
b	16.4201	16.4197	16.4191
σ(b)	0.0004	0.0004	0.0003
c	26.5524	26.5514	26.5500
σ(c)	0.0005	0.0005	0.0004
β	91.527	91.528	91.529
$\sigma(\beta)$	0.0015	0.0015	0.0015
Eccentricity	0.00139	0.00046	left out
Absorption	−0.00032	left out	left out

Final Cell Parameters and Standard Deviations

$a = 26.520A \pm 0.002A$

$b = 16.420A \pm 0.001A$

$c = 26.551A \pm 0.002A$

$\beta = 91.528° \pm 0.002°$

function

$$\sum_{n=1}^{N} w_n(\sin^2\theta_{obs} - \sin^2\theta_{calc})^2 \left(\frac{4}{\lambda^2_n}\right)^2 .$$

The calculation was weighted with $\sqrt{w_n} = \frac{1}{\sin 2\theta}$. The results together with the final assumed cell parameters and standard deviations are summarized in Table 2.

iv) Data reduction.

Data reduction was carried out using the CRYRM Initial Data Processing Subprogram written by the author and Dr. C. M. Gramaccioli (reference 8, Chapter 4), (see also Part II of this thesis). The visually-estimated intensity values, directly as read from the films, were used as input to the subprogram. As each intensity reading was fed into the computer, it was assigned a standard deviation calculated by the following function:

$$\sigma(I) = \frac{1}{w_e}\left[0.833 + bI + \frac{0.1\,I^2}{(65.0 - I)^2}\right]\left[1 + 0.25\, e^{-50(0.5 - \sin^2\theta)^2}\right] \quad (1)$$

for $I < 65.0$

and $\sigma(I)$ = a very large number for $I \geq 65.0$; here $\sigma(I)$ is the standard deviation in intensity I, w_e is an external weight, b is a parameter, and θ is the Bragg angle.

In a first pass of the data (with b set arbitrarily at 0.1), film and pack factors were calculated by the expression

$$\log (k_{ab}) = \frac{\Sigma w_i \left[\log \left(\frac{I_a}{I_b} \right)_i \right]}{\Sigma w_i}$$

where k_{ab} is the factor between film a and film b, I_a is the reading from film a of a reflection i observed on both film a and film b, w_i is a weight calculated from the assigned standard deviations of I_a and I_b. The final overall film factor for normal incidence was 3.72 (Kodak Medical X-Ray Film). Also in this pass, values for b in equation 1 were calculated (for the method, see page 159). The b values resulting were: 0.0430 for axis a, 0.0594 for axis b, and 0.1657 for axis $[1\ 0\ \bar{1}]$. These parameters agreed with the author's empirical estimate of the quality of the data.

In a second pass, the intensity readings were assigned standard deviations according to equation 1 with b for each axis as calculated in the first pass. Data were scaled to the most intense film of each layer, using the pack factors and the overall average film factor as calculated in the first pass. The overall film factor was appropriate modified to take into account the angle of incidence of the x-rays to the film. Multiple observations within a layer were then averaged geometrically in the standard manner. The averages were then corrected for Lorentz and polarization effects. The standard deviation for each intensity was carried through the calculations by propagation-of-error methods to give a standard deviation

for each corrected intensity value.

In a third pass, scaling factors, $c_1, \cdots, c_n$, relating the different layers were calculated by a method which minimizes

$$\Sigma w_i[c_k I_{ik} - c_\ell I_{i\ell}]^2$$

where the summation is over all pairs of reflections I_{ik} and $I_{i\ell}$, and the weight, w_i, is calculated from the input standard deviations. Here too the standard deviations of each input reflection was carried through the calculations to give a standard deviation for each output reflection.

Approximate scale and overall temperature factors were then determined by the method of Wilson (9) using the CRYRM routine written by Mr. T. A. Beineke (reference 8, Chapter 5).

The final result (after correcting for indexing and card punching errors) was a set of 11563 independent observed structure factors of which 3172 were "less than" — too weak to be observed on the film. Each observed structure factor was accompanied by a quantity equal to the reciprocal of the estimated standard deviation in the square of the observed structure factor.

SOLUTION OF THE STRUCTURE

i) Introduction.

Because of the size of the structure — it being the largest number of atoms ever determined without the aid of a "heavy" atom — and because no one standard method was used in obtaining a trial structure, the solution of the structure will be discussed in more detail than is normal.

ii) Conclusions from rotation and h0ℓ Weissenberg photographs.

Whereas the h0ℓ photograph does show a six-fold type symmetry (see Figure 1), it is not the transform expected for a six-membered ring. This seems to rule out the plane of any of the six molecules being perpendicular to the b axis. The transform shown in the rotation photograph about the b axis (see Figure 4) is similar to the expected transform of a six-membered ring, suggesting that at least some of the molecules are oriented parallel to the b axis. A further approach by the molecular transform method was indicated.

iii) Molecular transform work.

Using the optical transform machine built by Professor J. H. Sturdivant, optical transforms of the trimesic acid molecule viewed normal to the plane (see Figure 5) and viewed with the plane in several tilted orientations were prepared. The optical method consists essentially of representing a molecule by holes punched to scale in a cardboard mask, shining coherent parallel light through these

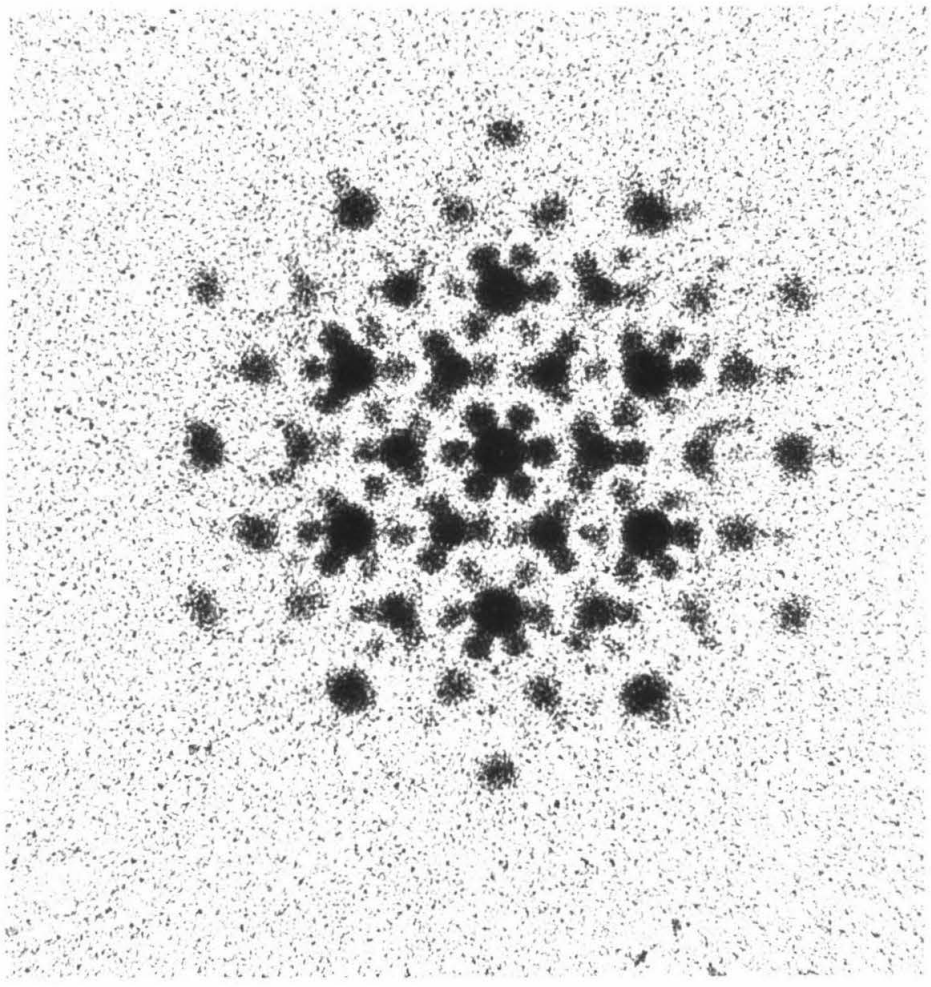

Figure 5. An optical transform of the trimesic acid molecule viewed normal to the plane.

Ring Orientation

holes, and observing the optical diffraction pattern (10). Optical transforms produced in this manner are comparable to the diffraction patterns produced by x-rays. Dark portions of the optical transform correspond to dense regions in the weighted reciprocal lattice.

Masks of trimesic acid were prepared using a scale of 0.26 inches per Angstrom with holes of diameter 5/64 inch. This is equivalent to the scale recommended by Lipson and Taylor (11) for good representation of the form factor of the carbon atom. Distances used were 1.39 A for the ring C–C bonds, 1.48 A for the ring to carboxyl C–C bonds, and 1.26 A for the C–O bonds – in agreement with the distances for benzoic acid as reported by Sims, Robertson, and Goodwin (12).

In order to sample the reciprocal lattice at various positions with respect to rotation about the b axis, 12 zero-level precession photographs of a crystal mounted about the b axis were taken systematically at intervals of about 15° rotation about b. Comparison of these photographs with the optical transforms confirmed that at least some of the molecules were oriented with their planes parallel to the b axis, and gave information about their orientation with respect to a and c. Conclusions are summarized in Figure 6.

iv) Two-dimensional Patterson work.

Since at least some of the rings appeared to be oriented on edge when viewed down the b axis, atoms might be expected to overlap in projection and behave similar to "heavy" atoms. This made

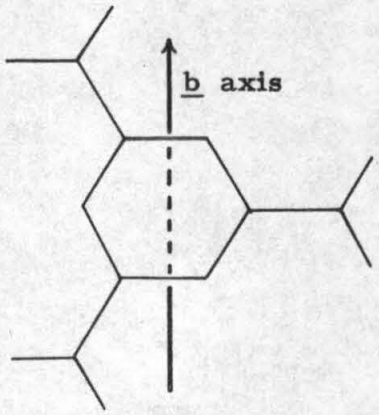

(a) Orientation of the trimesic acid ring with respect to the b axis direction.

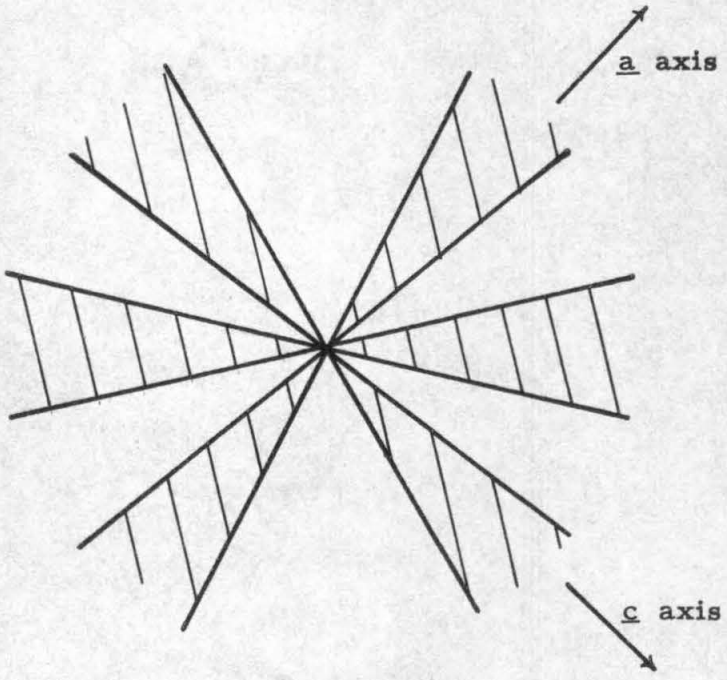

(b) Orientation with respect to rotation about the b axis direction. View is down the b axis. Shaded areas represent areas of probable ring orientation, as indicated by comparison of transforms and precession photographs.

Figure 6. Conclusions from molecular transform work.

projection work down the b axis appear feasible.

Preliminary Weissenberg h0ℓ data were collected. Reflections of the types hkℓ and $\bar{\ell}$kh were assumed to be equal in intensity. Patterson and sharpened Patterson projections were calculated; these maps are shown in Figures 6 and 7 respectively. The sharpening function used was

$$|F_{obs}|^2_{sharpened} = \frac{k^2(F_{obs})^2}{e^{-2B\left(\frac{\sin^2\theta}{\lambda^2}\right)}\Sigma n_i f_i^2}\left(\frac{\sin\theta}{\lambda}\right)^4 e^{-19.36\left(\frac{\sin^2\theta}{\lambda^2}\right)}$$

where n_i is the number of atoms of type i having atomic scattering factor f_i, k is a scale factor, and B is an overall temperature factor. The scale and overall temperature factors were estimated by Wilson's statistical methods (10).

Combination of the facts deduced from the Patterson projections and from the molecular transform work indicated that molecules probably lie in "chains" in the b axis direction — essentially as shown in Figure 8. This is in good agreement with the observed length of the b axis.

v) The structure in two dimensions.

A study of the possible packing of the molecules when viewed down the b axis was used to deduce a trial structure in two dimensions. The "chains" shown in Figure 9 and the possible orientations with respect to rotation about the b axis direction shown in Figure 6 were taken as a basis for this study. The Patterson

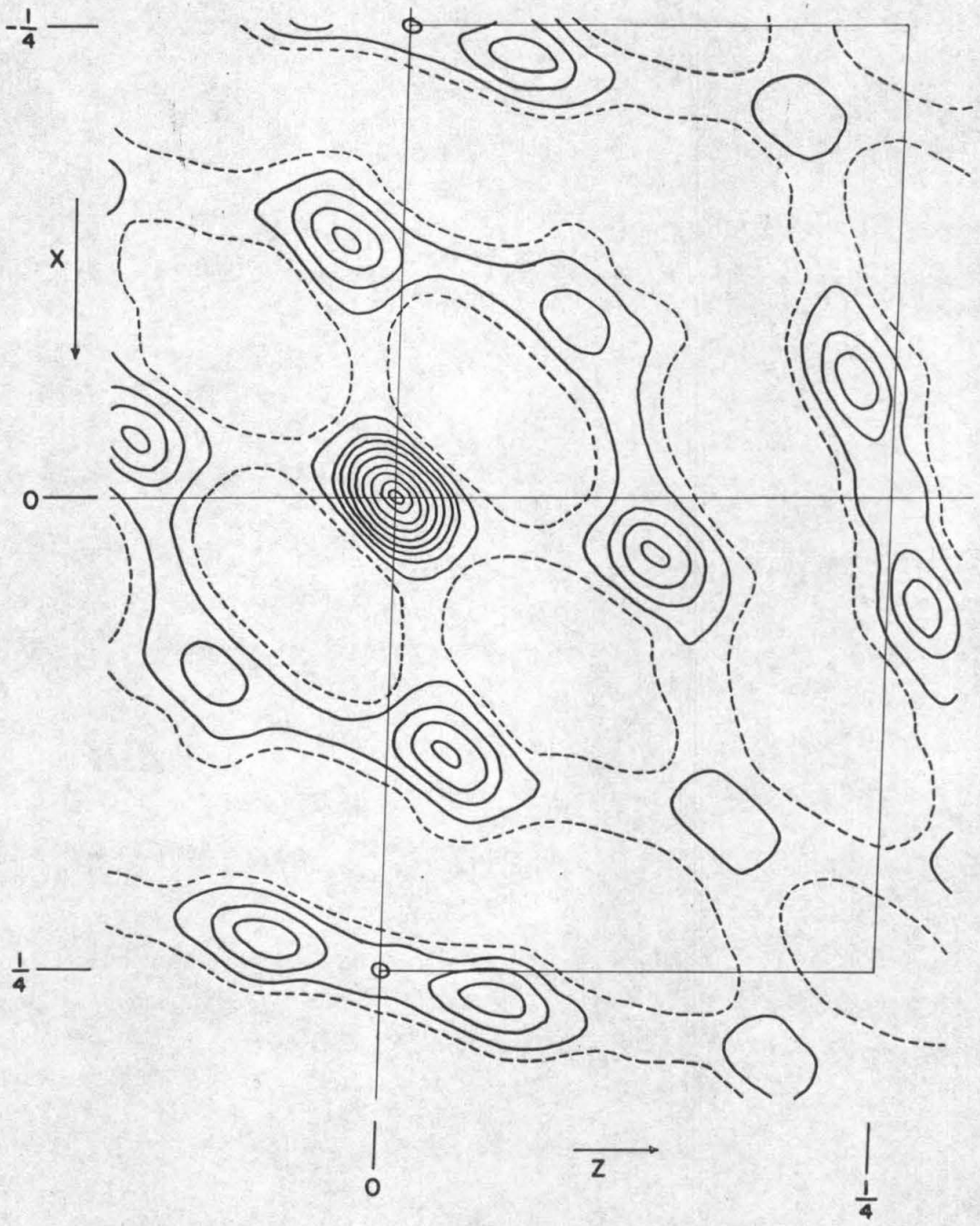

Figure 7. Two-dimensional Patterson map.

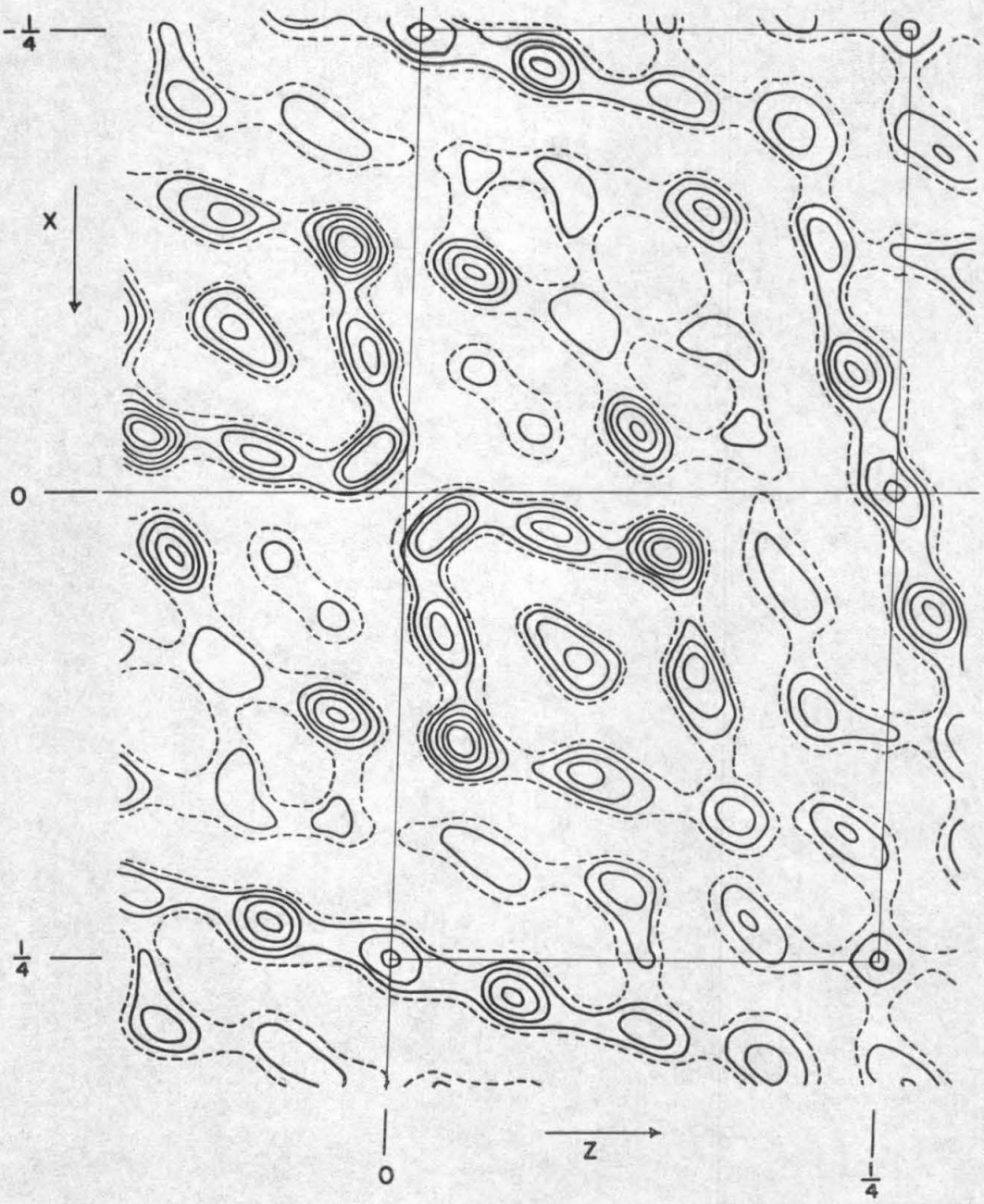

Figure 8. Two-dimensional sharpened Patterson map.

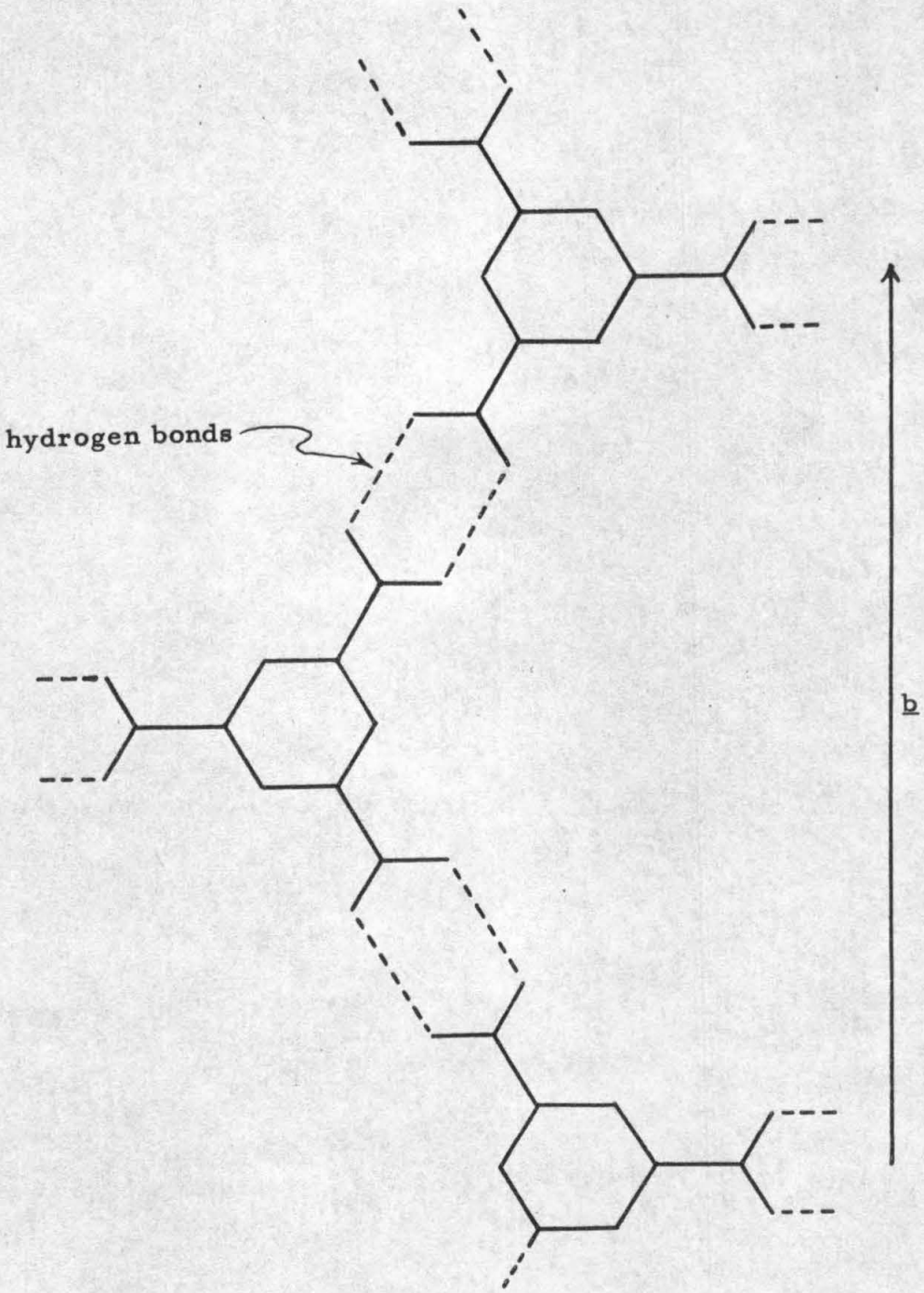

Figure 9. Proposed "chain" type array.

projections — both sharpened and regular — were used to check each step and to give hints as to how to proceed. During this study, the three-dimensional aspects of the structure were also considered.

The final model was checked by a structure-factor calculation and by an electron density projection. Calculated structure factors were in agreement with the observed structure factors, and the electron density projection was in agreement with the proposed structure. The structure as it was at this stage is shown in Figure 10. Some atoms are superimposed in this projection; a double circle indicates two atoms, and a single circle, one. The origin shown is shifted 1/4 in $\underline{x}$ from the final origin. The six molecules of the asymmetric unit are designated A, B, C, D, E, and F.

vi) Three-dimensional Patterson work.

When three-dimensional data were available, a three-dimensional "sharpened" Patterson map was calculated using the CRYRM Fourier-Patterson Subprogram written by the author. The sharpening function was the same as described for the two-dimensional case; the origin was also subtracted out.

By direct analysis of the three-dimensional Patterson map, $\underline{y}$ coordinates for the centers of the six rings were found. The keys to this analysis were the special peaks generated by parallel rings — including those related by symmetry elements. Whereas it could be seen from analysis of the Patterson that ring F was not centered at

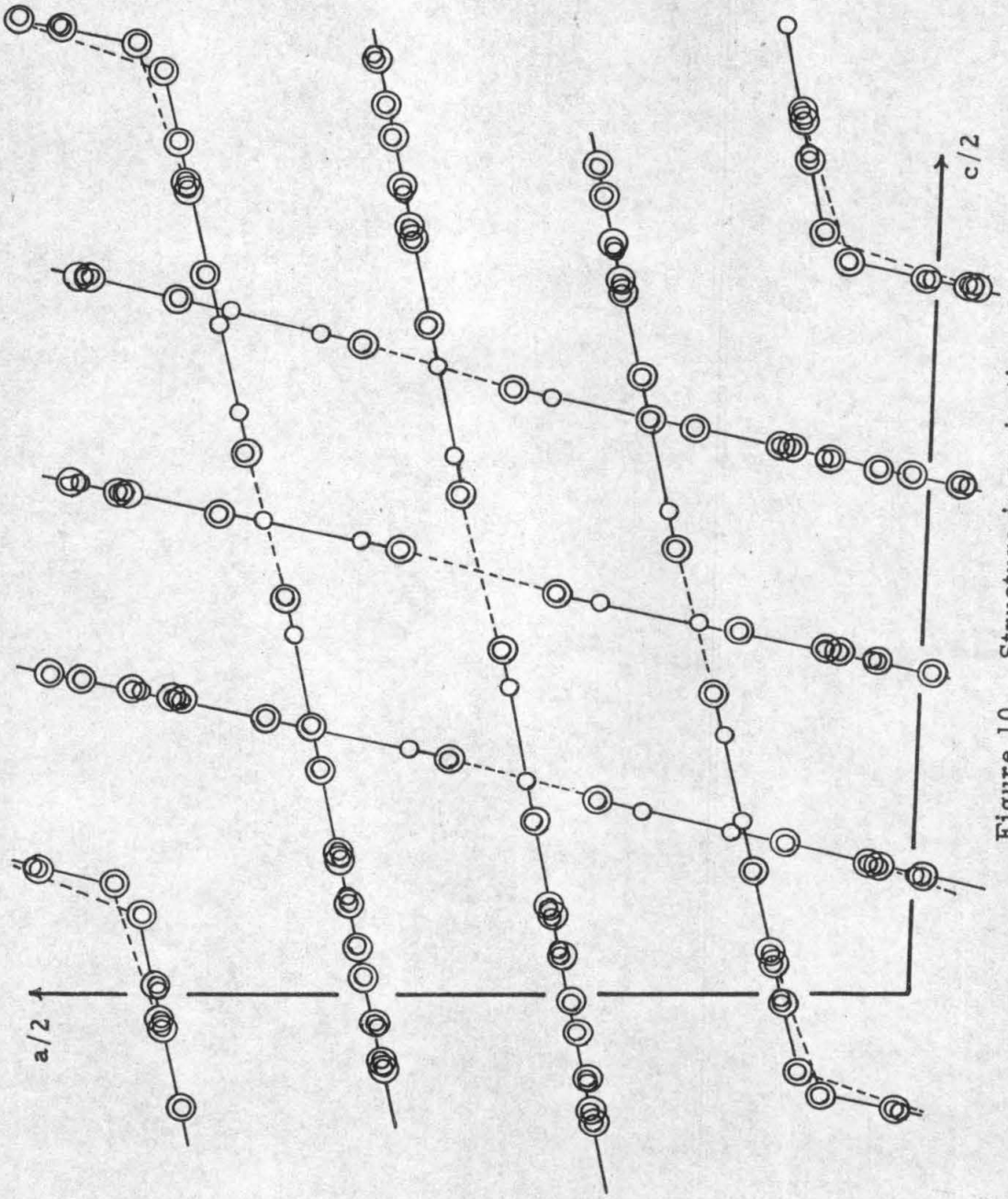

Figure 10. Structure in projection.

exactly y = 0.25, the direction of deviation from 0.25 could not be fixed; therefore the value 0.25 was assumed for the center of this ring. The results are summarized in Table 3, together with the y coordinate of the final ring centers. The final parameters deviate only slightly from those obtained by analysis of the Patterson map.

Only one problem remained: the structure as derived could be placed in the unit cell in either of two ways. The structure provides that molecules A and B are hydrogen-bonded to respective symmetry-related molecules. The Patterson map indicated that the symmetry element involved was a two-fold axis, which would require disordered hydrogen bonding. The symmetry element could also be a center of symmetry which is 0.25 in x and 0.25 in z from the two-fold axis. This orientation requires no disorder, but does not give a particularly favorable hydrogen-bonding orientation for ring A. The orientation first assumed was that from the Patterson — hydrogen bonding across a two-fold axis.

By assuming standard distances, y coordinates were calculated for the individual atoms. These were combined with the x and z coordinates from the two-dimensional work to give a trial structure with positions for all the 90 non-hydrogen atoms. A three-dimensional structure-factor calculation using all the data gave an agreement factor, R, of 0.51.

Table 3. Results of three-dimensional Patterson analysis.

	y Coordinate of Ring Center	
Ring	From Patterson	Final
A	-0.205	-0.203
B	0.250	0.249
C	0.295	0.297
D	-0.250	-0.251
E	-0.234	-0.225
F	0.25?	0.229

REFINEMENT OF THE STRUCTURE

i) Introduction.

The structure was refined on the Caltech IBM 7094 computer by Fourier and least-squares methods using the CRYRM Crystallographic Computing System (8). The refinement was begun in two dimensions, but quickly shifted to three dimensions. Hydrogen atoms and anisotropic thermal parameters — ignored at the beginning — were added at appropriate times. Rings A, B, C, D, E, and F were numbered separately according to the following scheme:

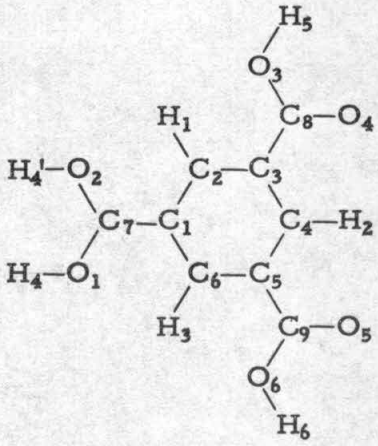

Hydrogen 4 — found to be disordered in all six molecules — is shown twice. Atomic scattering factors for carbon (valence), oxygen, and hydrogen were taken from the "International Tables for X-ray Crystallography" (13).

In the least-squares refinement (see reference 8, Chapter 6), the quantity minimized was $\Sigma w_i \left| |F_{obs}|^2 - |F_{calc}|^2 \right|^2$. The R factor was calculated by the standard expression

$$R = \frac{\Sigma \left| |F_{obs}| - |F_{calc}| \right|}{\Sigma |F_{obs}|} .$$

"Less than" reflections for which $|F_{calc}|$ was less than the minimum observable structure factor were not entered into the least squares or R factor calculations. When two successive least-squares cycles were calculated, the inverse matrix from the first cycle was also used for the second cycle. Because of the limited size of the computer memory of the IBM 7094, the largest matrix of parameters which could be calculated is about 200 × 200. This meant that the parameters of trimesic acid had to be split into separate matrices or that some of the parameters had to be left out of the refinement. The least squares subprogram provides for a variety of matrix setups. The matrix configuration at various stages of the refinement will be mentioned and discussed in hopes that the experience gained here may be useful in designing future refinements.

ii) Two-dimensional refinement.

Using only h0ℓ data, three cycles, A_1–A_3, of full-matrix least squares were run on the x and z coordinates from the trial two-dimensional model. In cases where two atoms overlapped in this projection, one atom with twice as many electrons was entered. Isotropic temperature factors were held at 3.4 A^2 for all atoms. After cycles A_1 and A_3 the shifts were plotted, and the coordinates were adjusted to give proper bond distances and to maintain the planarity of the rings; the orientation of the rings with respect to the b axis

was kept fixed. Even though this refinement proved to be rather unstable, the R factor for the h0ℓ reflections was reduced from 0.61 to 0.38 by this method. Following the least-squares refinement, an h0ℓ electron density projection map was calculated and analyzed for shifts.

The two-dimensional work produced significant shifts in the positions of the centers of the molecules. In addition, the planes of the carboxyl groups of C_8 and C_9 in both ring E and ring F were found to be twisted out of the planes of their respective benzene rings. This was evidence for the idea that even though the planes of molecules E and F are not parallel, they are bonded together in a chain array like that shown in Figure 9. Further two-dimensional refinement did not seem warranted.

iii) Three-dimensional refinement.

Since, as discussed previously, the origin originally derived forced disorder in some of the carboxyl hydrogens, the origin was shifted to the alternate position before beginning the three-dimensional refinement. Attempts at Fourier and least-squares refinement produced almost no improvement; in particular, reflections with $k + \ell$ odd continually showed poor agreement between observed and calculated structure factors. Calculations showed that only these reflections had been affected by the above-mentioned change in origin; since they had shown much better agreement in the first three-dimensional structure-factor calculation, the only course seemed to be to change back to the original origin.

With the corrected origin, structure factors and three-dimensional electron density maps in the planes of the molecules, using only data for which $|F_{calc}| > 45.0$ and $\sin^2\theta/\lambda^2 < 0.20$, were calculated. These maps indicated only small coordinate shifts.

Atomic coordinates from this analysis were refined by least squares using only very low angle data — the 1070 reflections for which $\sin^2\theta/\lambda^2 < 0.08$. The weighting scheme was $\sqrt{w_i} = 1/F_{obs}$ for $F_{obs} > 15.0$ and $\sqrt{w_i} = 1/\sqrt{15.0|F_{obs}|}$ for $F_{obs} < 15.0$. Isotropic temperature factors were held at 2.9 for all atoms. Two cycles, B_1 and B_2, were run with the coordinates of atoms of molecules A, C, E, and F in one full matrix; everything else was held fixed. This was followed by two cycles, B_3 and B_4, with the coordinates of atoms of molecules C, D, E, and F being refined; then two, B_5 and B_6, with molecules B, D, E, and F in the refinement. This refinement worked exceedingly well — the R factor for the data used, originally 0.32, was 0.167 after cycle B_5. The most significant shifts were in molecule F which moved as a unit to a position about 0.4 A from its input position.

Since many bond distances and angles were now in disagreement with the expected values, coordinates were shifted toward more reasonable values by the method of Waser (14), using a program furnished by Professor Waser and slightly modified by the author to accept CRYRM-type input. Essentially this method finds the "best" molecule consistent with the input coordinates and the expected distances. Each molecule was treated separately; carboxyl groups were allowed to rotate out of the planes of the molecules.

Using the coordinates so derived, refinement by least-squares was continued. Two cycles, C_1 and C_2, were run with a four-matrix arrangement — coordinates of atoms of molecules A and C, those of B and D, and those of E and F in three 90×90 matrices respectively, with the scale and isotropic temperature factors in a fourth matrix. Whereas coordinates refined satisfactorily, isotropic temperature parameter shifts were clearly of no value. To correct this, the weighting scheme was changed, and more data were included in the refinement. The weighting scheme adopted here and used for the remainder of the refinement was $\sqrt{w_i} = 1/\sigma(F_{obs}^2)$, where $\sigma(F_{obs}^2)$ is the standard deviation in F_{obs}^2 which was obtained during the initial data-reduction calculations. With the matrix arrangement for atomic coordinates changed to one matrix per molecule and with input isotropic temperature factors for all atoms held constant at 2.9, four more least-squares cycles, C_3—C_6, were run. All parameters refined satisfactorily, and the R factor for the 11,000 data used in the last two of these cycles was reduced to about 0.16.

At this time, anisotropic thermal parameters for all 90 atoms were introduced. Carbon atoms were allowed to refine anisotropically from their respective isotropic values; since the oxygen atoms were expected to show a strong anisotropy perpendicular to their respective rings, input anisotropic temperature parameters were calculated by hand for each oxygen atom. The anisotropic temperature factor expression used here is of the form

$$e^{-(h^2b_{11} + k^2b_{22} + {}^2b_{33} + hkb_{12} + h\ell b_{13} + k\ell b_{23})},$$

where h, k, and ℓ are the indices of the particular reflection, and the b_{ij} are the six anisotropic temperature parameters.

Four cycles of least squares, D_1—D_4, were calculated using a block matrix arrangement — the coordinates of each atom in a 3×3 matrix and the anisotropic thermal parameters for each atom in a 6×6 matrix. From cycle D_3 onward all 11563 recorded reflections were used in the refinement. The R factor after D_3 was 0.105.

Since hydrogen contributions were felt to be influencing many reflections, a three-dimensional difference electron density map was calculated. This map indicated unambiguously the locations of all the benzene-ring hydrogen atoms, but not of the carboxyl hydrogen atoms. The difference map had a rather high noise level, presumably from shifts remaining in the parameters of the heavier atoms.

An unsuccessful attempt was made to continue the refinement ignoring the carboxyl hydrogen atoms. A quick calculation showed that these hydrogen atoms probably contributed strongly to several important reflections. These hydrogens are involved in oxygen-to-oxygen hydrogen bonds, the question in each case being "to which oxygen is the hydrogen covalently bonded?" In order not to prejudice the answers to these questions, carboxyl hydrogens were placed at calculated points midway between the oxygens involved, and least-squares refinement was continued.

After five more cycles, D_5—D_9, of refinement of the carbon and oxygen parameters (the hydrogen parameters were held fixed), the R factor was 0.0788, but the coordinate shifts were oscillating.

To correct this, several low-angle large reflections which clearly showed extinction effects were given zero weight in the refinement, and the matrix arrangement for coordinates was changed to one matrix per molecule. Four more cycles, D_{10}–D_{13}, were then computed. In cycles D_{10} and D_{11}, some anisotropic temperature parameters were placed in selected large matrices; however, when results indicated that this change did not help the refinement, these parameters were placed in a block-matrix arrangement for the remainder of the refinement. In the case of coordinates, on the other hand, the author feels that the larger matrices helped significantly in settling down the refinement; for the remainder of the refinement, all heavy-atom coordinates of a simple molecule were included in a single matrix.

Attention was now given to the location of carboxyl hydrogen atoms. Using structure factors calculated without the carboxyl hydrogen atoms, three-dimensional difference electron-density sections were calculated in the least-squares planes through each set of four oxygen atoms involved in the hydrogen-bond pairs; only reflections for which $\sin^2 \theta/\lambda^2 < 0.28$ were included. These maps clearly showed the positions of H_5 and H_6 for all six molecules. For molecules A and B, H_4, which is required to be disordered by hydrogen bonding across a two-fold axis (the oxygen-to-oxygen hydrogen-bonded distance being too long for a symmetric hydrogen bond), appeared in two positions in each case. A half hydrogen atom at each position was used in succeeding calculations. For molecules C, D, E, and F, the maps showed a preferential orientation for each H_4;

disorder, however, appeared possible. In succeeding calculations, these hydrogen atoms initially were placed in single positions.

In least-squares cycles, E_1–E_{14}, which followed, hydrogen atom coordinates were refined in one 120 × 120 matrix; the matrix arrangement of carbon and oxygen parameters was as before. Beginning with cycle E_5 hydrogen temperature factors were refined in a separate 40 × 40 matrix. After cycle E_8 the scale factor was held fixed at a value indicated by the trend of the refinement. A distance and angle calculation using the coordinates from cycle E_{12} showed that hydrogens H_4 of rings C, D, E, and F — mentioned above as possibly being disordered — had moved in each case to positions intermediate between the two oxygen atoms of the O–H··· O hydrogen bonds. Difference electron density sections, with all atoms, including hydrogen atoms, subtracted out, suggested that the hydrogen atoms in question were disordered in a ratio of about 2/3 to 1/3 — the 2/3 hydrogen in each case being at the position originally assigned to a full hydrogen. Assuming this ratio, the parameters of these hydrogen atoms were refined in cycles E_{13} and E_{14}. After these cycles the refinement was stopped since all shifts were negligible except for one temperature factor and three positional parameters involving disordered hydrogens, which were about 1.5 standard deviations. All other parameter shifts were below standard deviations; most carbon and oxygen parameter shifts were below 0.1 standard deviations.

iv) Results of the refinement.

Final agreement indexes are shown in Table 4; for comparison,

Table 4. Final agreement indexes.

	All Atoms	Without Hydrogens
$R = \frac{\Sigma \left\| \lvert F_{obs} \rvert - \lvert F_{calc} \rvert \right\|}{\Sigma \lvert F_{obs} \rvert}$	6.75	7.97
Weighted $R = \frac{\Sigma w(\lvert F_{obs} \rvert^2 - \lvert F_{calc} \rvert^2)^2}{\Sigma w \lvert F_{obs} \rvert^4}$	2.52	7.05
Goodness of fit $= \left(\frac{\Sigma w(\lvert F_{obs} \rvert^2 - \lvert F_{calc} \rvert^2)^2}{m - s} \right)^{\frac{1}{2}}$	1.49	2.49
Number of "less than" reflections with calculated structure factors greater than the minimum observable structure factor.	86	111

the same indexes with the hydrogen atoms left out of the calculation are shown. The final "goodness of fit" or the "quadratic mean error" (15), which should approach unity at convergence if the weights are on an absolute scale, is 1.49, a value within the range usually obtained for a good refinement.

Final positional and temperature parameters are given in Table 5, together with their standard deviations. Standard deviations, σ_i, were calculated by the equation

$$\sigma_i = \left[(A^{-1})_{ii} \left[\frac{\Sigma w_i (k^2 F_{obs}^2 - F_{calc}^2)^2}{m - s} \right] \right]^{\frac{1}{2}}$$

where $(A^{-1})_{ii}$ is the diagonal element of the inverse least-squares matrix, m is the number of observations and s is the number of parameters. All carbon and nitrogen parameters are shown multiplied by 10^5; hydrogen coordinates are multiplied by 10^3. Table 6 gives for each reflection the observed structure factor and the structure factor calculated using parameters derived from the last cycle of least squares. "Less than" reflections are indicated by a negative sign on the observed structure factor. Reflections which were given a zero weight are indicated by an asterisk after the observed structure factor.

A composite drawing of the final electron density sections is shown in Figure 11. The upper part shows sections through the oxygen and carbon atoms; all were calculated in the best least-squares planes through the carbon atoms of each molecule, except sections

Table 5. Final atomic parameters and their standard deviations.

A

	x	y	z	b_{11}	b_{22}	b_{33}	b_{12}	b_{13}	b_{23}
C(1)	12593(13)	-20176(17)	27637(9)	88(5)	320(11)	92(4)	-1(14)	-3(8)	1(10)
C(2)	15241(13)	-12880(16)	26158(10)	87(5)	268(10)	112(4)	19(13)	-12(8)	10(10)
C(3)	20592(12)	-12979(16)	29187(9)	94(5)	252(10)	100(4)	-0(13)	-12(8)	-13(9)
C(4)	22976(13)	-20089(15)	29722(10)	87(5)	279(10)	102(4)	4(13)	-15(8)	-25(10)
C(5)	20350(13)	-27613(16)	29263(9)	96(5)	266(10)	98(4)	6(13)	-9(8)	-3(9)
C(6)	15150(13)	-27561(16)	28202(9)	95(5)	289(11)	100(4)	-12(13)	-19(8)	-3(10)
C(7)	07103(13)	-20154(18)	26525(10)	90(5)	315(12)	128(4)	42(14)	-20(9)	25(11)
C(8)	23250(13)	-05185(17)	29917(10)	105(5)	296(11)	117(4)	2(14)	-11(9)	-28(10)
C(9)	23085(13)	-35362(16)	30139(10)	95(5)	267(11)	131(4)	13(14)	-24(9)	-21(10)
O(1)	04872(10)	-26841(12)	26107(10)	100(4)	362(10)	350(6)	-74(12)	-81(10)	53(12)
O(2)	04936(9)	-13383(12)	25971(8)	101(4)	376(9)	243(5)	60(11)	-83(8)	15(10)
O(3)	20621(10)	01418(11)	25630(8)	153(5)	205(7)	258(4)	24(11)	-112(9)	-30(9)
O(4)	27865(9)	-05321(12)	30906(8)	109(4)	305(8)	218(4)	-24(11)	-41(8)	-76(9)
O(5)	27608(9)	-35137(11)	31480(8)	113(4)	302(9)	229(4)	54(11)	-71(8)	-10(9)
O(6)	20571(9)	-41949(10)	29584(8)	128(5)	258(8)	234(4)	-21(11)	-88(8)	7(9)
H(1)	136(1)	-089(2)	277(1)	4.2(0.9)					
H(2)	265(1)	-196(2)	305(1)	1.5(0.7)					
H(3)	131(1)	-321(2)	276(1)	2.8(0.8)					
H(4) 1/2	017(3)	-262(3)	252(3)	2.6(1.3)					
H(4') 1/2	020(3)	-142(3)	241(3)	5.4(1.8)					
H(5)	226(2)	055(2)	305(1)	6.4(1.0)					
H(6)	235(2)	-479(2)	306(1)	6.6(1.1)					

B

	x	y	z	b_{11}	b_{22}	b_{33}	b_{12}	b_{13}	b_{23}
C(1)	02749(12)	24954(16)	37586(9)	91(5)	317(11)	88(4)	10(14)	-10(8)	-0(9)
C(2)	05284(12)	17569(15)	40117(10)	99(5)	281(11)	89(4)	6(13)	-19(8)	14(9)
C(3)	04372(13)	17500(15)	45284(9)	100(5)	282(11)	94(4)	-5(13)	-15(8)	21(9)
C(4)	04884(13)	24745(15)	47908(9)	103(5)	309(11)	81(3)	11(14)	-16(8)	6(9)
C(5)	04358(13)	32166(16)	45341(9)	108(5)	298(11)	91(4)	-19(14)	-5(8)	9(9)
C(6)	03288(13)	32249(16)	40198(10)	112(6)	302(11)	94(4)	24(14)	-15(9)	25(10)
C(7)	01579(14)	24994(17)	32075(9)	130(6)	321(12)	82(4)	10(15)	-16(9)	-4(9)
C(8)	06135(13)	09685(16)	47995(10)	119(6)	311(12)	97(4)	-1(15)	-21(9)	7(10)
C(9)	08147(13)	39908(16)	48229(10)	120(6)	306(11)	99(4)	-22(15)	5(9)	-6(10)
O(1)	01063(12)	31734(12)	29904(7)	330(8)	392(9)	103(3)	18(15)	-87(9)	93(8)
O(2)	01081(11)	18238(12)	29881(7)	246(7)	413(9)	92(3)	26(14)	-69(8)	-60(8)
O(3)	04731(11)	05101(10)	45446(7)	229(6)	248(8)	138(3)	1(12)	-94(8)	-9(8)
O(4)	06233(10)	09845(11)	52609(6)	206(6)	332(8)	103(3)	4(12)	-61(7)	54(7)
O(5)	06464(10)	39626(11)	52768(7)	223(6)	301(8)	116(3)	-71(12)	-43(8)	-36(8)
O(6)	04491(10)	46468(10)	45706(7)	234(6)	245(7)	138(3)	12(12)	-99(8)	13(7)
H(1)	032(1)	124(1)	383(1)	1.0(0.6)					
H(2)	055(1)	244(2)	515(1)	1.5(0.7)					
H(3)	029(1)	367(2)	383(1)	2.3(0.7)					
H(4) 1/2	001(3)	310(2)	267(1)	-.1(1.1)					
H(4') 1/2	001(4)	199(3)	264(2)	3.1(1.5)					
H(5)	066(2)	-028(2)	475(1)	5.5(1.0)					
H(6)	062(2)	504(2)	483(1)	4.9(0.9)					

C

	x	y	z	b_{11}	b_{22}	b_{33}	b_{12}	b_{13}	b_{23}
C(1)	40451(13)	29796(16)	36130(9)	94(5)	285(11)	99(4)	-1(13)	-32(8)	-6(10)
C(2)	37910(13)	22390(16)	35601(10)	98(5)	265(11)	113(4)	12(13)	-24(9)	24(10)
C(3)	32771(13)	22355(16)	34572(9)	108(5)	240(10)	102(4)	-18(13)	-17(9)	-10(9)
C(4)	30157(13)	29665(16)	33758(9)	86(5)	288(11)	100(4)	3(13)	3(8)	-13(10)
C(5)	32775(12)	36985(16)	34255(9)	92(5)	250(10)	103(4)	1(13)	-18(8)	-7(9)
C(6)	37923(13)	37090(16)	35404(9)	101(5)	259(10)	103(4)	5(13)	-30(8)	-34(9)
C(7)	45961(13)	29680(17)	37253(10)	90(5)	306(11)	130(4)	-1(14)	-28(9)	39(11)
C(8)	30077(13)	14630(16)	33301(10)	98(5)	241(10)	123(4)	26(13)	2(9)	-2(10)
C(9)	29989(13)	44802(18)	33257(10)	95(5)	308(11)	119(4)	13(14)	-21(9)	-3(10)
O(1)	48560(9)	36338(12)	36896(8)	91(4)	367(9)	214(4)	-51(11)	-31(8)	41(9)
O(2)	48015(10)	23040(12)	38417(10)	106(5)	400(10)	357(6)	40(12)	-111(10)	186(12)
O(3)	32718(10)	08061(11)	33362(8)	124(5)	256(8)	232(4)	31(11)	-44(8)	-66(9)
O(4)	25455(9)	14769(12)	32310(8)	109(4)	309(9)	230(4)	-33(11)	-84(8)	-66(9)
O(5)	25415(9)	44580(12)	32072(8)	120(5)	271(8)	226(4)	50(11)	-72(8)	-19(9)
O(6)	32559(10)	51331(11)	33561(8)	142(5)	202(7)	284(5)	-58(11)	-124(9)	5(9)
H(1)	395(1)	179(1)	362(1)	1.2(0.6)					
H(2)	264(1)	299(2)	330(1)	1.5(0.7)					
H(3)	401(1)	423(2)	357(1)	3.8(0.8)					
H(4) 2/3	523(2)	356(4)	380(2)	5.8(1.4)					
H(4') 1/3	503(5)	218(8)	393(5)	3.1(3.1)					
H(5)	303(2)	018(2)	328(1)	4.8(0.9)					
H(6)	305(2)	556(2)	325(1)	4.8(0.9)					

D

	x	y	z	b_{11}	b_{22}	b_{33}	b_{12}	b_{13}	b_{23}
C(1)	11094(13)	-24797(15)	66524(9)	97(5)	298(11)	94(4)	4(13)	-23(8)	-11(9)
C(2)	10235(13)	-17709(15)	62866(9)	101(5)	271(10)	98(4)	-30(13)	-16(8)	-1(9)
C(3)	09084(12)	-17978(15)	57734(10)	93(5)	279(11)	97(4)	-2(13)	-15(8)	10(9)
C(4)	08675(13)	-25378(15)	55272(9)	113(6)	287(11)	88(3)	-25(14)	-6(8)	-7(9)
C(5)	09373(13)	-32589(15)	57983(9)	113(6)	246(10)	95(4)	-5(14)	-22(8)	-7(9)
C(6)	10604(13)	-32262(15)	63098(10)	115(6)	278(11)	100(4)	-21(14)	-39(9)	29(9)
C(7)	12171(13)	-24405(15)	71041(9)	120(6)	287(11)	87(3)	1(14)	-14(8)	-9(9)
C(8)	08055(13)	-10252(17)	54878(9)	123(6)	318(11)	93(4)	-34(15)	-18(9)	5(10)
C(9)	08428(13)	-40464(16)	55308(10)	127(6)	297(11)	98(4)	4(15)	-23(9)	-7(10)
O(1)	13466(12)	-30932(11)	73230(7)	289(7)	372(9)	101(3)	122(14)	-83(9)	55(8)
O(2)	11817(10)	-17724(11)	73222(7)	205(6)	381(8)	99(3)	58(13)	-32(8)	-89(8)
O(3)	08117(11)	-09696(10)	57446(7)	249(6)	243(7)	117(3)	9(12)	-83(8)	-7(7)
O(4)	07050(11)	-10643(11)	50268(6)	257(6)	317(8)	98(3)	-60(13)	-63(8)	28(8)
O(5)	07208(11)	-40397(11)	50791(7)	234(6)	343(9)	121(3)	-28(13)	-91(8)	-62(8)
O(6)	08792(11)	-46983(11)	57980(7)	258(7)	262(8)	140(3)	-56(13)	-46(9)	4(8)
H(1)	103(1)	-126(2)	645(1)	3.0(0.8)					
H(2)	078(1)	-247(2)	516(1)	2.4(0.8)					
H(3)	111(1)	-367(1)	649(1)	.2(0.5)					
H(4) 2/3	135(3)	-502(4)	769(2)	2.0(1.3)					
H(4') 1/3	114(6)	-194(7)	763(3)	4.8(2.6)					
H(5)	080(2)	-620(2)	559(1)	5.2(0.9)					
H(6)	072(2)	010(2)	552(1)	4.5(1.0)					

E

	x	y	z	b_{11}	b_{22}	b_{33}	b_{12}	b_{13}	b_{23}
C(1)	16293(13)	22778(18)	40641(9)	92(5)	284(10)	91(3)	28(13)	-25(8)	-19(9)
C(2)	16841(13)	30192(15)	43208(10)	117(6)	251(10)	104(4)	-16(14)	-24(9)	22(9)
C(3)	17922(12)	30171(15)	48363(9)	92(5)	248(10)	99(4)	4(13)	-16(8)	-14(9)
C(4)	18632(12)	22961(15)	50926(9)	101(5)	248(10)	88(3)	20(13)	-25(8)	-10(9)
C(5)	18000(12)	15990(15)	48398(9)	93(5)	243(10)	98(4)	14(13)	-11(8)	28(9)
C(6)	16775(12)	15964(15)	43277(10)	95(5)	266(10)	100(4)	27(13)	-9(8)	-28(9)
C(7)	15164(14)	22990(15)	35148(10)	114(6)	280(11)	90(4)	11(14)	-19(8)	-7(10)
C(8)	18889(15)	38006(16)	51148(10)	106(6)	252(10)	105(4)	-7(14)	-1(9)	5(9)
C(9)	19007(13)	07968(15)	51270(9)	94(5)	250(10)	99(4)	-14(13)	-3(8)	-24(9)
O(1)	13863(10)	16321(11)	33016(6)	160(5)	337(8)	97(3)	-1(11)	-51(7)	-62(7)
O(2)	15433(12)	29613(11)	32698(7)	306(7)	350(9)	104(3)	-78(14)	-79(9)	68(8)
O(3)	16943(9)	44462(10)	48729(7)	150(5)	205(7)	150(3)	-7(10)	-75(7)	13(7)
O(4)	20468(10)	38166(10)	55381(7)	183(5)	249(7)	108(3)	-58(11)	-44(7)	-27(7)
O(5)	21791(10)	07849(10)	54986(7)	189(5)	249(8)	120(3)	25(11)	-62(7)	21(7)
O(6)	16746(9)	01444(10)	49406(7)	146(5)	207(7)	151(3)	-20(10)	-70(7)	23(7)
H(1)	167(1)	348(1)	412(1)	.6(0.6)					
H(2)	192(1)	230(1)	546(1)	1.2(0.6)					
H(3)	166(1)	102(2)	414(1)	3.2(0.8)					
H(4) 2/3	130(3)	184(3)	293(2)	6.3(1.2)					
H(4') 1/3	152(6)	299(7)	268(4)	3.4(2.7)					
H(5)	178(1)	500(2)	506(1)	2.1(0.7)					
H(6)	181(1)	-029(2)	516(1)	2.3(0.7)					

F

	x	y	z	b_{11}	b_{22}	b_{33}	b_{12}	b_{13}	b_{23}
C(1)	15629(13)	-22050(16)	41205(10)	91(5)	290(11)	105(4)	-9(13)	-22(8)	22(10)
C(2)	18507(13)	-14975(16)	41534(10)	111(5)	241(10)	111(4)	18(14)	-19(9)	-2(10)
C(3)	23610(13)	-15392(15)	42785(9)	95(5)	253(10)	97(4)	23(13)	-18(8)	-18(9)
C(4)	25907(13)	-22680(15)	43572(9)	88(5)	261(10)	105(4)	5(13)	-26(8)	-2(9)
C(5)	23115(13)	-29946(15)	42989(9)	104(5)	213(10)	102(4)	2(13)	-29(8)	28(9)
C(6)	17982(13)	-29564(16)	41866(10)	107(5)	274(11)	105(4)	1(14)	-15(9)	21(10)
C(7)	10154(13)	-21472(17)	40035(10)	92(5)	311(11)	122(4)	10(14)	-23(9)	8(10)
C(8)	26636(13)	-07871(16)	43723(10)	116(6)	238(10)	111(4)	17(14)	-2(9)	-20(9)
C(9)	25754(13)	-37916(16)	43748(9)	105(5)	279(11)	94(4)	1(13)	-9(8)	13(9)
O(1)	07679(10)	-28115(12)	40315(10)	102(5)	383(10)	354(6)	-88(12)	-118(10)	170(12)
O(2)	08206(9)	-14798(11)	38864(8)	102(4)	329(8)	180(4)	58(10)	-58(7)	29(9)
O(3)	24810(10)	-01303(10)	41526(7)	169(5)	220(7)	154(3)	-9(11)	-97(8)	43(8)
O(4)	30406(9)	-07955(10)	46442(8)	113(4)	269(8)	206(4)	-6(10)	-78(8)	-35(9)
O(5)	29894(9)	-38275(10)	45824(7)	106(4)	240(7)	161(3)	26(10)	-30(7)	67(8)
O(6)	23231(9)	-44251(10)	42066(7)	148(5)	216(7)	148(3)	-5(11)	-73(7)	-9(7)
H(1)	170(1)	-108(2)	412(1)	2.4(0.7)					
H(2)	295(1)	-229(1)	443(1)	1.7(0.7)					
H(3)	159(1)	-340(2)	419(1)	2.4(0.7)					
H(4) 2/3	044(2)	-275(4)	396(3)	5.5(1.4)					
H(4') 1/3	056(4)	-143(7)	387(5)	3.0(2.8)					
H(5)	263(2)	084(2)	429(1)	5.7(1.0)					
H(6)	256(1)	-492(1)	428(1)	1.9(0.7)					

Table 6. Observed and calculated structure factors.

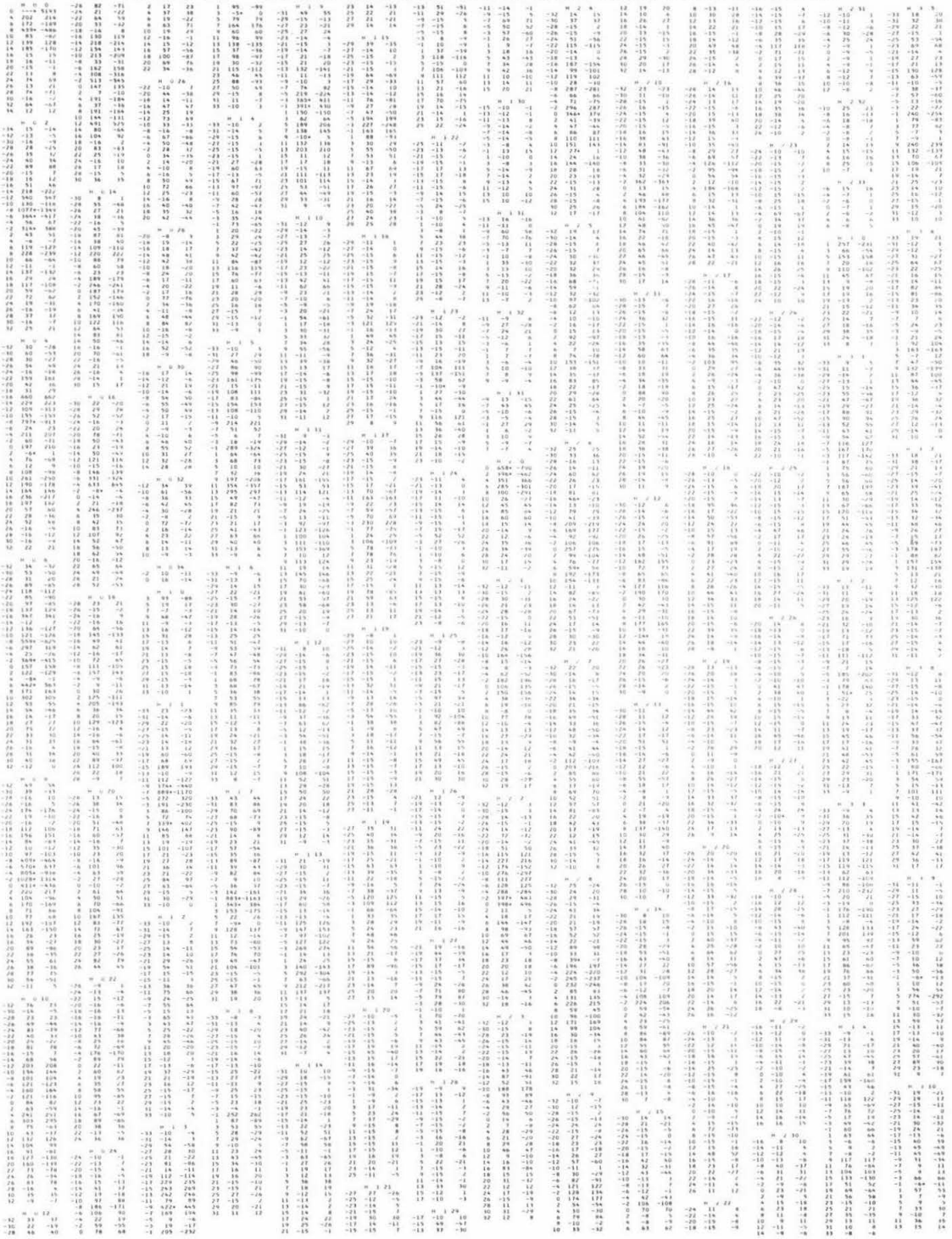

(Columns are h, F_{obs}, and F_{calc}.)

Table 6 (continued)

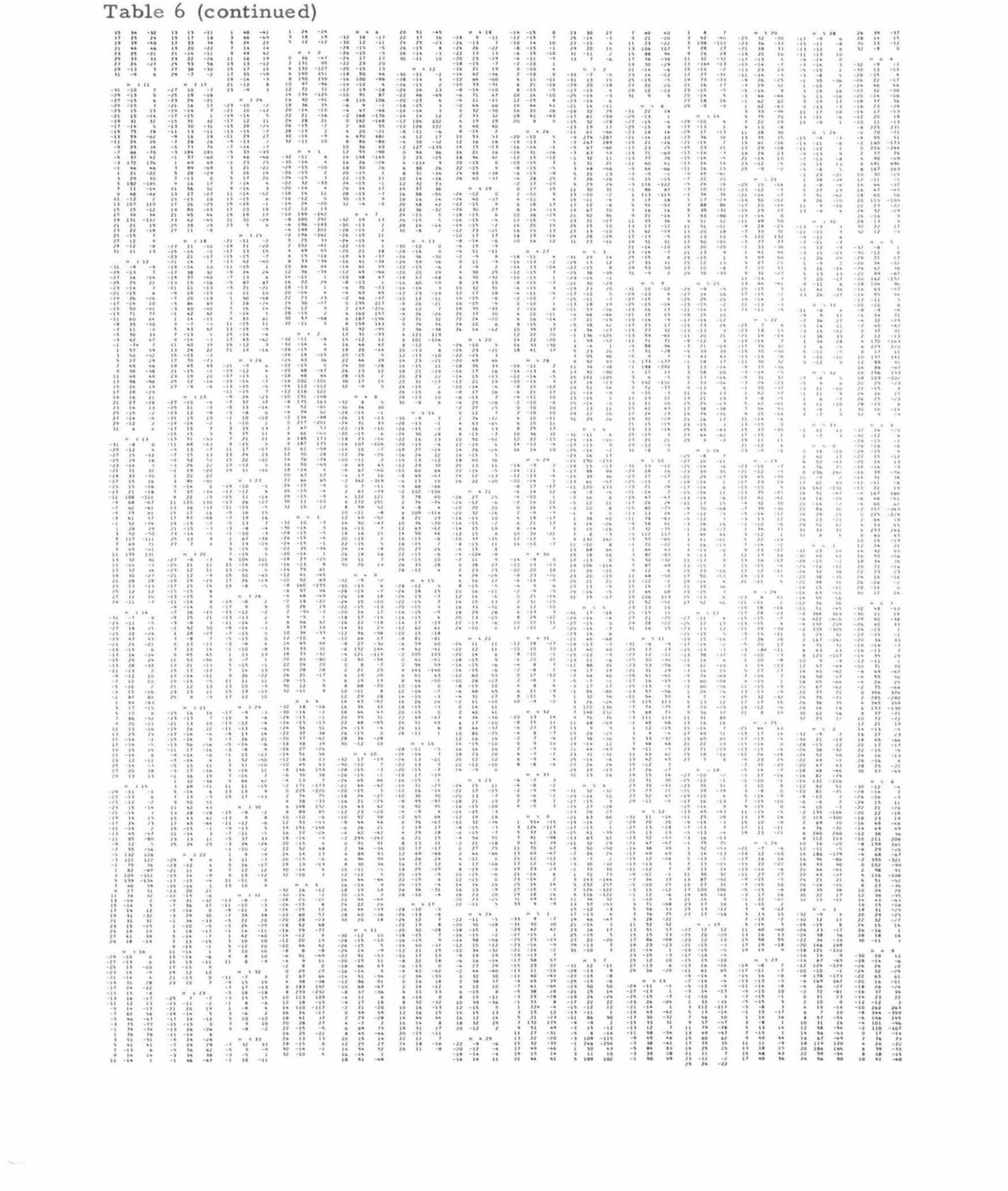

Table 6 (continued)

Table 6 (continued)

Table 6 (continued)

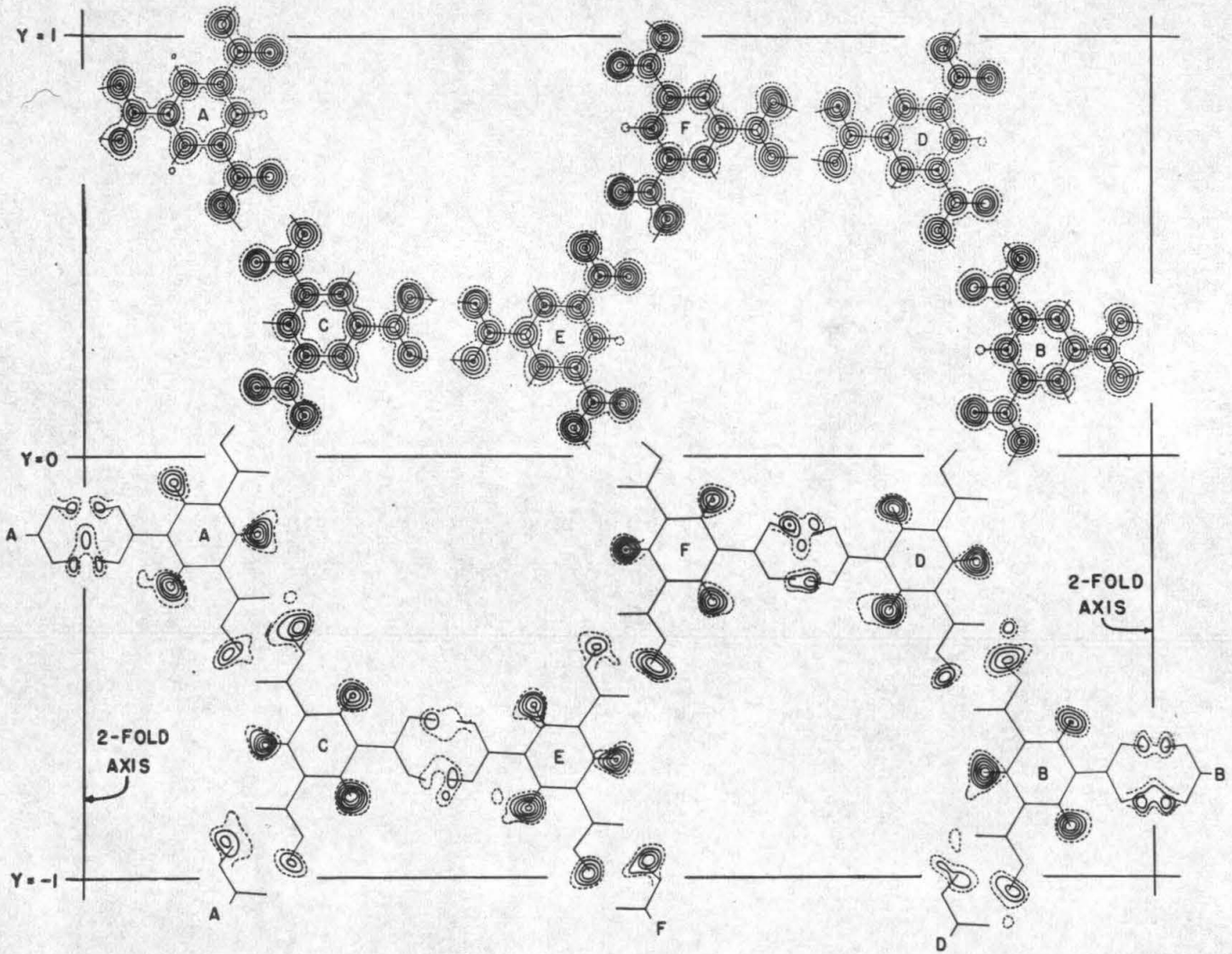

Figure 11. Final composite electron density and difference electron density maps. Contours in the upper part are at intervals of 2.0 eA^{-3} beginning with 1.0 eA^{-3} (dashed), in the lower, at intervals of 0.1 eA^{-3}, beginning with 0.1 eA^{-3} (dashed).

through those oxygens which deviated by more than 0.20 A from the respective planes were calculated in parallel planes through the centers of the atoms. The lower part shows difference electron density sections — the carbon and oxygen atoms being subtracted out to show the hydrogen atoms. Sections through the ring hydrogen atoms were calculated in the best least-squares planes through the carbon atoms of the respective molecules; sections through the carboxyl hydrogen atoms were calculated in the best least-squares planes through the four oxygen atoms involved in each carboxyl-to-carboxyl hydrogen-bond pair. When contouring the difference sections, noise at the positions of the carbon and oxygen atoms was ignored. Figure 12 shows the final h0ℓ projection electron density map.

v) General comments.

In light of this refinement, the author would like to make the following comments:

1. The complete refinement of large structures, such as this one, is well within the range of modern computers. In this refinement the last two cycles of least squares, which involved 11563 reflections and 978 parameters, required about two hours of calculation time on the IBM 7094 computer.

2. The multiple large matrix arrangement in least squares was found to work quite well.

3. Fourier techniques can be quite misleading in early stages of structure determination. In this refinement, at early stages when

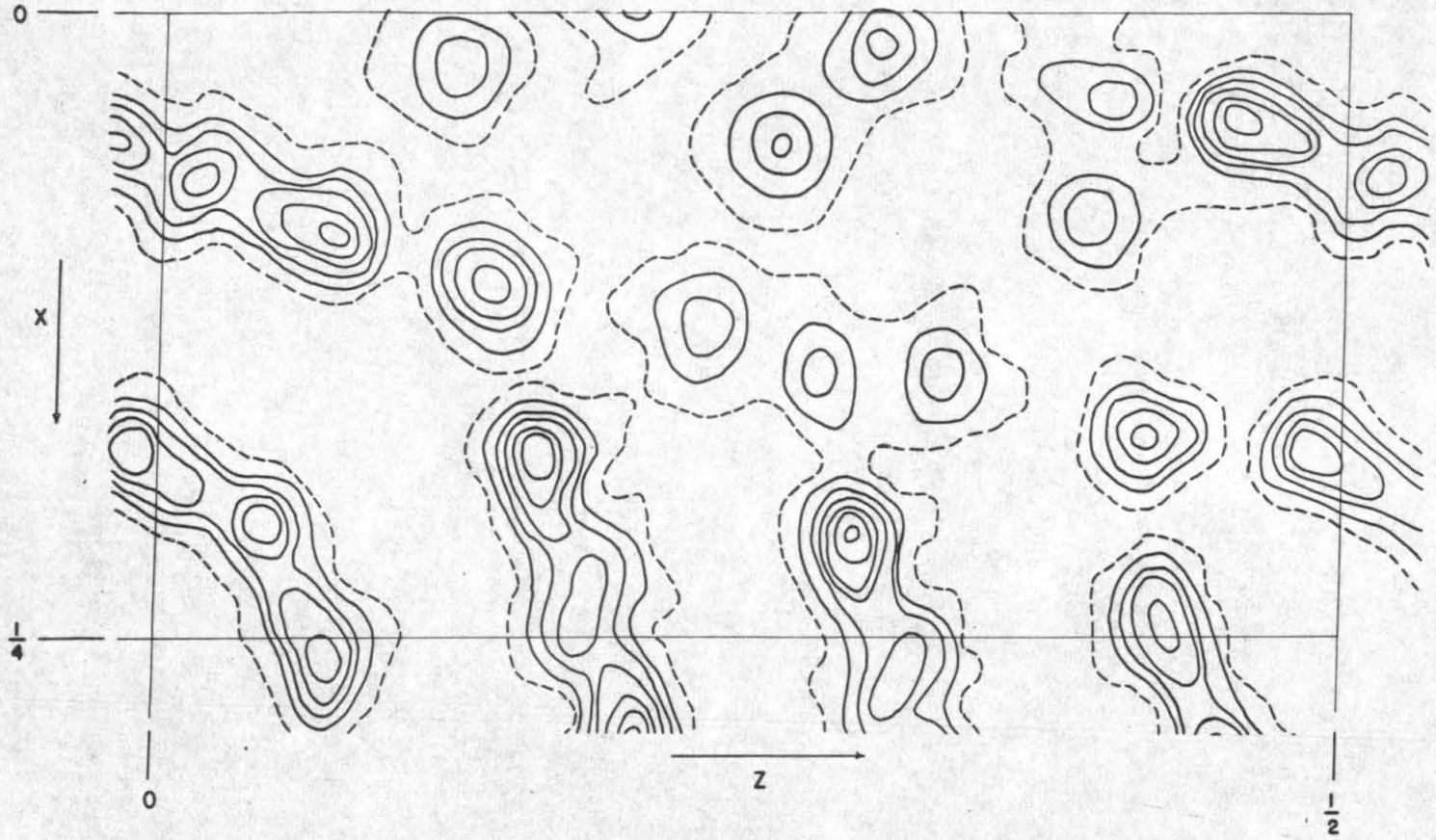

Figure 12. Final h0ℓ electron density projection. Contours are at intervals of 5.0 eA^{-2} beginning with the 5.0 eA^{-2} contour (dashed).

the molecules were incorrectly placed in the unit cell, beautiful, well-resolved electron-density maps were obtained even though reflections with $k + \ell$ odd showed great disagreement between observed and calculated structure factors. In fact, maps calculated immediately after positioning the molecules correctly did not appear to be significantly better than the incorrect ones.

4. Even with 11563 reflections the assumption often voiced — that it is not necessary to be careful with individual reflections since, with large amounts of data, random errors cancel out — does not apply. At one point in this refinement, one high-weight mis-indexed reflection was responsible for divergence of the refinement.

5. Introduction of hydrogen atoms was important to this refinement even though the ratio of hydrogen atoms to heavier atoms is only 2 to 5.

DISCUSSION OF THE STRUCTURE

i) Bond distances and angles.

Interatomic distances and angles were calculated using the CRYRM Distances, Angles and Planes Subprogram written by Mr. J. Lo (see reference 8, Chapter 8). The results are illustrated in Figure 13. For simplicity in this figure all the molecules are shown in the same plane even though the planes of molecules A, C, and E are significantly different from those of molecules B, D, and F. The asymmetric unit shown was picked because it best illustrates the hydrogen bonding (it is not the same as the asymmetric unit of Table 5). Interior angles of the benzene rings, which are not shown in this figure, may be found in Table 7.

The standard deviations in the positions of carbon and oxygen atoms as shown in Table 5 are in all cases about 0.002 to 0.003 A. Assuming isotropic uncorrelated errors allows calculation of a value of about 0.004 A for standard deviations in bond lengths involving carbon and oxygen atoms, with a limit of error — assumed at three standard deviations — of 0.012 A. Similarly the standard deviation in bonds from carbon or oxygen to hydrogen (not disordered) are about 0.03 A with a limit of error of about 0.1 A. In the case of 1/2 and 2/3 hydrogens, these values are about 0.06 A and 0.2 A respectively; with 1/3 hydrogens, these values are about 0.13 A and 0.4 A respectively.

Estimated standard deviations in bond angles were calculated by propagation of bond length errors through the law of cosines. For

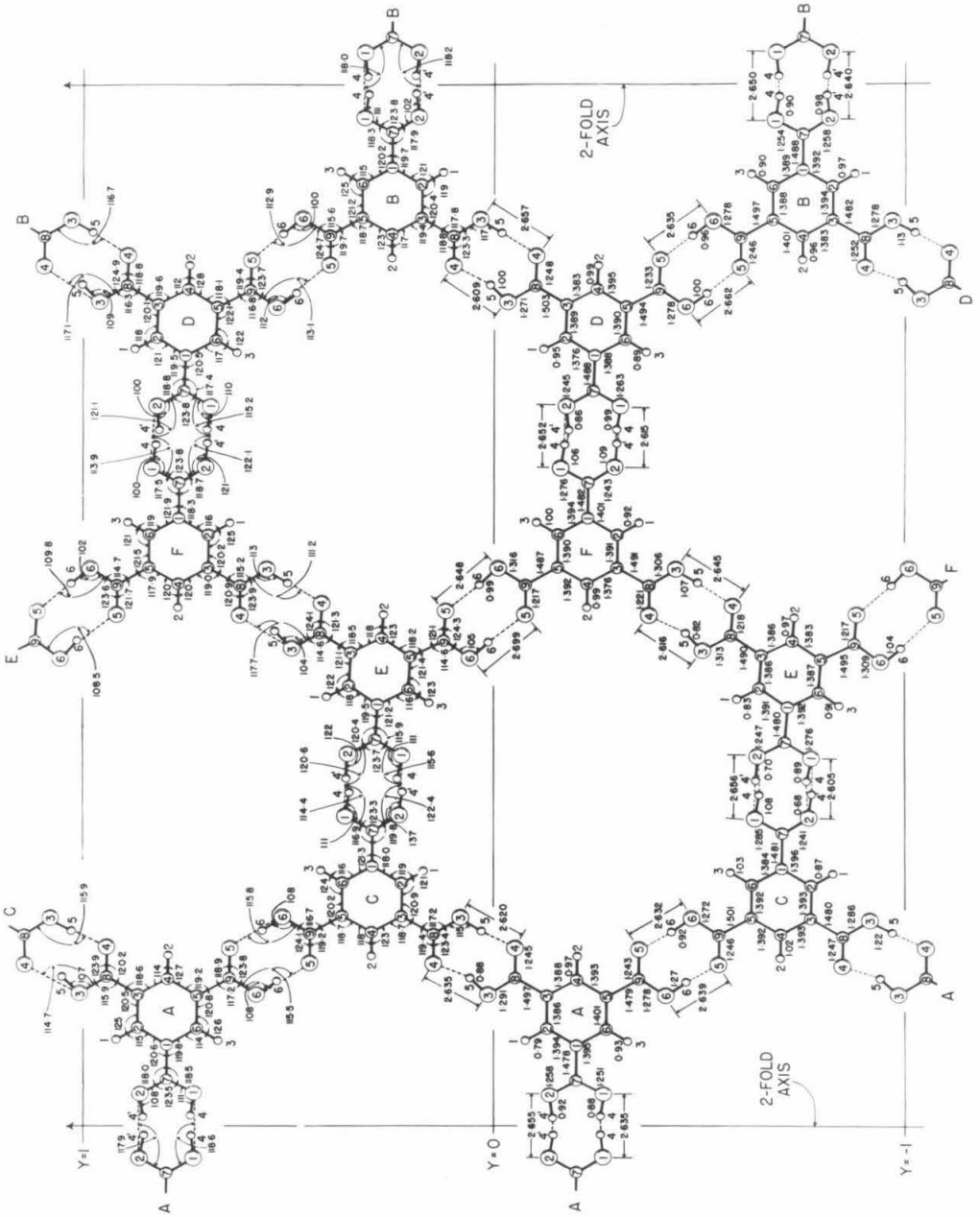

Figure 13. Bond distances and angles.

Table 7. Interior angles of the benzene rings (in degrees).

	A	B	C	D	E	F	Ave
$C_6-C_1-C_2$	119.6	120.2	120.6	119.9	119.3	119.8	119.9
$C_1-C_2-C_3$	120.1	119.9	119.6	120.3	120.3	119.5	120.1
$C_2-C_3-C_4$	120.8	120.2	120.3	120.3	120.2	120.7	120.4
$C_3-C_4-C_5$	119.6	119.8	119.2	119.6	119.7	119.8	119.6
$C_4-C_5-C_6$	119.9	120.1	121.0	119.7	120.4	120.4	120.2
$C_5-C_6-C_1$	120.0	119.9	119.3	120.2	120.1	119.6	119.9

C—C—C and C—C—O angles of about 120°, the standard deviation is about 0.4° with a limit of error of about 1.2°. For the C—C—H and the C—O—H (not disordered) angles which are shown in the figure, the standard deviation is about 3° with a limit of error of about 9°. For the C—O—H angles involving 1/2 or 2/3 hydrogens, the values are 6° and 18° respectively; for the 1/3 hydrogens, the values are 13° and 39° respectively.

In Table 8, average values are presented for certain interatomic distances and angles. For purposes of comparison, the largest and smallest values observed for the quantity being averaged are also presented. The carboxyl groups which involve disordered hydrogens were not included in the averaging. The C—O distances in the carboxyl groups of C(8) and C(9) of rings E and F are significantly different from the corresponding distances in rings A, B, C, and D; the difference is presumably related to the large out-of-plane twisting of these carboxyl groups which results from the hydrogen bonding between rings E and F, which do not lie in parallel planes.

The O···O hydrogen bond distances have values ranging from 2.605 A to 2.699 A. These distances are significantly different from one another; the value observed within this range for a particular distance is probably governed by the arrangement of molecules in the unit cell.

The distances and angles found here for trimesic acid compare favorably with those found in benzoic acid (12), where the carboxyl group was reported to deviate only slightly from the plane of the

Table 8. Average distances and angles.

(Subscripts c and r denote ring and carboxyl respectively.)

Distances	Largest	Smallest	Average	Number of Observations
C_r-C_r	1.401 A	1.376 A	1.390 A	36
C_r-C_c	1.503	1.478	1.489	18
C_r-H_r	1.03	0.79	0.94	18
C_c-O_c* (short)				
Rings A, B, C, D	1.252	1.233	1.245	8
Rings E, F	1.221	1.217	1.218	4
C_c-O_c* (long)				
Rings A, B, C, D	1.291	1.271	1.279	8
Rings E, F	1.316	1.306	1.319	4
O_c-H_c*	1.27	0.82	1.02	12
Angles				
$C_r-C_r-C_r$	121.0°	119.2	(120.0°)	36
$C_r-C_r-C_c$	122.1	117.9	(120.0)	36
$C_r-C_c-O_c$ (short)*	121.7	118.8	120.0	12
$C_r-C_c-O_c$ (long)*	117.8	114.6	116.1	12
$O_c-C_c-O_c$	124.9	123.3	123.9	18
$C_r-C_r-H_r$	128	112	(120)	36
$C_c-O_c-H_c$*	117	100	110	8

*Carboxyl groups of C(7) of all molecules are not included in these calculations since the hydrogens of these carboxyl groups are disordered.

benzene ring — similar to most of the trimesic acid carboxyl groups. The C—O distances within the carboxyl group of benzoic acid are 1.24 A and 1.29 A, and the O—O hydrogen bond distance is 2.64 A — well within the range given above.

In the case of mellitic acid, benzene hexacarboxylic acid, the carboxyl groups, which of course cannot be in the plane of the benzene ring, were reported by Darlow (16) to have a wide range of values for the C—O distances. These values are in general similar to those found in trimesic acid for the out-of-plane carboxyl groups of rings E and F.

ii) Temperature factors.

The magnitudes and direction cosines of the principal axes of the thermal ellipsoids of the heavy atoms are shown in Table 9. These were calculated from the anisotropic temperature parameters listed in Table 5 by the method of Waser (17) using the CRYRM subprogram written for this purpose by Mrs. B. Stroll (see reference 8, Chapter 12). The oxygen atoms were found to have large amplitudes in directions perpendicular to their respective planes.

The large out-of-plane amplitudes of these atoms undoubtedly cause errors in the observed carbon to oxygen bond lengths, and these distances should probably be increased by about 0.02 A in the average case — a value obtained by assuming a riding motion. The significance of this number, however, can be questioned. If one considers 0(1) and 0(2) of molecule A (the carbon to oxygen distances here are expected to be equal), one finds that O_1 has the larger

	A				B				C				D				E				F			
C(1)	3.45	-012	1000	013	3.43	-108	-994	029	3.27	-650	-178	756	3.26	-312	-887	348	3.37	-387	643	671	3.33	-509	-741	451
	2.65	-539	-019	856	2.72	-761	100	661	3.04	-153	983	106	3.05	-677	459	593	2.95	-368	-765	538	2.74	-492	668	571
	2.41	842	005	517	2.31	639	-050	750	2.20	744	047	646	2.30	666	050	726	2.34	845	-039	510	2.16	706	-068	686
C(2)	3.26	-290	109	958	3.07	-354	842	416	3.47	-491	204	860	3.23	-717	584	399	3.51	-716	-136	704	3.64	-816	194	566
	2.95	-326	-945	016	3.01	-768	-512	406	2.90	473	879	050	2.83	-272	-737	626	2.82	608	362	690	2.70	578	305	741
	2.33	900	-306	285	2.28	532	-176	813	2.42	731	-432	508	2.41	641	341	670	2.55	344	-922	168	2.42	019	-933	360
C(3)	3.02	-531	-298	807	3.20	-486	721	507	3.30	-816	109	589	3.07	-348	804	491	3.18	-622	-495	623	3.04	-552	-308	789
	2.71	-384	919	099	2.91	-695	-661	300	2.77	372	-652	650	2.91	-557	-591	597	2.59	-222	854	475	2.65	-307	939	163
	2.46	756	257	582	2.43	530	-207	808	2.44	442	750	480	2.40	754	-066	634	2.38	751	-157	621	2.38	775	153	592
C(4)	3.23	-282	-697	666	3.35	-230	-973	023	3.15	-049	-940	339	3.36	-779	622	100	3.23	-526	-099	859	3.19	-791	-346	526
	2.81	-395	710	593	3.01	-901	221	397	2.78	-073	341	939	2.95	-586	-767	279	2.81	-015	994	107	2.60	-258	936	245
	2.30	874	096	453	2.16	367	-071	917	2.43	996	-022	059	2.42	225	158	955	2.22	850	-043	501	2.21	555	-058	815
C(5)	2.96	-574	-505	659	3.32	-471	865	186	3.12	-542	-130	844	3.37	-894	014	471	3.43	-708	140	711	2.98	-363	439	831
	2.84	-274	861	437	2.90	-835	-501	250	2.69	-153	987	058	2.67	115	-959	257	2.56	640	541	528	2.73	-735	-677	056
	2.53	772	-071	611	2.51	284	-038	950	2.39	826	098	533	2.41	432	284	844	2.15	299	-829	464	2.27	572	-591	553
C(6)	3.17	-458	798	404	3.41	-643	-765	054	3.47	-609	-358	724	3.82	-751	354	578	3.33	-650	317	708	3.27	-474	-656	600
	3.07	-445	-588	688	3.22	-637	563	543	2.76	-510	860	010	2.90	-384	-921	079	2.98	512	854	077	2.61	093	626	772
	2.40	770	136	603	2.45	424	-315	838	2.31	608	363	690	2.35	538	-163	812	2.64	561	-413	702	2.50	876	-421	213
C(7)	3.77	-178	355	922	3.75	-937	-292	219	3.99	-293	424	865	3.45	-963	-090	278	3.62	-372	104	932	3.41	-882	-291	393
	3.51	-425	-869	265	3.43	-288	956	056	3.16	-262	-898	362	3.10	111	-991	068	3.36	-146	-988	056	2.99	-282	956	085
	2.29	887	-345	282	2.25	200	011	974	2.35	920	-120	349	2.37	244	097	958	2.42	917	-115	358	2.41	376	036	915
C(8)	3.55	-317	-539	789	3.55	-889	193	439	3.48	-097	-041	997	3.82	-755	613	251	3.40	-817	-253	540	3.09	-740	204	660
	3.05	-479	801	371	3.35	-201	-979	030	2.91	809	578	081	3.20	-558	-787	278	3.08	557	-114	807	2.89	645	-054	745
	2.78	819	260	490	2.56	412	-062	898	2.44	587	-809	008	2.52	343	070	927	2.50	-149	961	238	2.70	-189	-978	097
C(9)	3.88	-341	-210	925	3.53	779	-625	023	3.56	-412	-304	870	3.76	-922	-103	397	3.07	-476	766	445	2.96	168	-648	738
	2.83	057	968	242	3.15	-640	-761	124	3.31	-027	946	322	3.20	119	-993	018	2.98	-750	-611	272	2.70	-834	309	480
	2.48	938	-135	293	2.78	027	111	992	2.51	911	-110	374	2.60	367	064	918	2.52	458	-205	853	2.46	528	695	474
O(1)	10.16	-196	066	983	9.61	-981	003	218	6.20	-184	191	969	8.66	-962	-198	215	10.88	-253	237	944	4.87	-910	-168	403
	4.10	347	-929	123	4.58	078	921	380	3.97	214	-950	223	4.13	-099	897	433	3.85	211	-933	286	3.78	280	-924	254
	2.39	917	365	134	2.30	175	-390	899	2.40	959	249	108	2.27	255	-395	875	2.36	944	272	161	2.25	306	344	879
O(2)	7.27	-298	-010	962	7.24	-965	-126	256	10.34	-225	241	950	6.03	-931	-306	223	5.44	-349	034	945	9.04	-968	150	229
	4.22	281	955	090	4.50	168	-970	169	4.23	-433	-893	136	4.04	348	-910	218	3.80	394	912	103	3.82	212	920	323
	2.33	912	-297	257	2.25	202	206	952	2.31	873	-380	282	2.57	111	280	950	2.31	850	-409	309	2.53	138	-361	918
O(3)	8.13	-430	-055	912	7.15	-916	-009	426	6.83	-243	-150	965	7.46	-957	-019	316	6.12	-757	082	668	5.43	-715	038	717
	3.57	899	059	409	3.26	400	-118	898	3.35	943	196	244	2.93	291	-099	944	3.15	642	274	698	3.09	699	037	696
	2.16	-077	997	027	2.67	039	993	111	2.64	-228	969	100	2.61	010	995	100	2.28	118	-958	257	2.18	-001	-999	053
O(4)	6.43	-205	-189	965	6.10	-957	044	312	6.77	-237	-117	970	6.96	-968	158	222	6.34	-374	-076	934	5.40	-958	082	299
	3.39	-605	796	044	3.76	146	927	342	3.51	517	-856	009	3.35	187	973	134	2.98	521	-842	128	3.07	170	-605	773
	2.70	769	575	257	2.43	250	-373	887	2.63	822	504	242	2.56	169	-171	966	2.64	767	535	334	2.43	230	792	559
O(5)	6.86	-314	-064	955	6.54	-969	161	213	6.81	-338	-077	947	7.16	-939	007	368	4.82	-258	221	947	5.76	-928	-042	396
	3.51	499	838	209	3.57	016	-714	699	3.31	698	648	286	4.01	154	-885	436	3.06	849	517	089	3.13	306	481	813
	2.59	807	-543	210	2.71	247	681	683	2.59	631	-758	148	2.59	307	466	821	2.25	461	-827	308	2.55	213	-876	428
O(6)	7.14	-369	028	939	7.31	-916	-010	425	8.82	-385	025	933	7.48	-975	067	236	5.33	-717	-010	716	5.34	-690	086	737
	3.16	899	-242	340	3.26	388	227	883	3.35	894	-239	355	3.78	209	-029	972	3.07	693	-113	693	3.10	722	013	672
	2.52	235	970	058	2.61	100	-974	202	2.11	230	971	063	2.80	072	997	012	2.32	072	994	086	2.21	-050	-996	072

Table 9. Principal axes of the thermal ellipsoids. Columns are the magnitudes, B, and the direction cosines ($\times 10^3$) with respect to crystallographic axes, a, b, and c respectively.

amplitude of vibration and also the smaller distance — in agreement with the expected correction; however, calculation of the difference between the corrections to be applied to the O_1 and O_2 to carbon distances gives 0.015 A which is much greater than the difference necessary to make the two distances equal. A similar situation is observed with O_1 and O_2 of molecule B. These observations suggest that the value given above for correcting the carbon to oxygen bond lengths may be too large.

iii) Planarity of the molecules.

The least-squares planes through atoms $C_1, \cdots, C_9$ of each of the rings and the deviations of atoms from these planes are given in Table 10. Table 11 gives the same information for planes calculated through atoms $C_1, \cdots, C_6$. The planes are calculated by the method of Shomaker, Waser, Marsh, and Bergman (18) using the CRYRM Distances, Angles, and Planes Subprogram. Direction cosines are given relative to the crystallographic a, b, and c axes.

The results show that molecules A, C, and E are almost exactly parallel; similarly molecules B, D, and F are almost exactly parallel. Also, the normals to the best planes through all the molecules are very nearly perpendicular to the b axis. Furthermore the angles formed by the plane normals of molecules A, C, and E with the a axis are very nearly the same as the corresponding angles formed by the plane normals of B, D, and F with the c axis; this arrangement explains the pseudo mm symmetry observed in projection down the b axis.

Table 10. Least-squares planes through atoms C(1), ···, C(9).

Direction Cosines	A	B	C	D	E	F
cos(a)	−.2095	−.9824	−.2384	−.9771	−.2252	−.9806
cos(b)	+.0120	−.0020	+.0062	−.0197	+.0215	−.0146
cos(c)	+.9829	+.2128	+.9771	+.2376	+.9797	+.2211
Origin to plane distance	6.4751	1.4014	6.8289	1.3684	9.7026	−1.9073
Deviations						
C(1)	−.002	−.002	+.018	−.021	+.004	+.001
C(2)	+.001	+.005	+.034	−.003	−.057	−.008
C(3)	−.016	+.013	+.040	−.022	−.038	+.013
C(4)	−.035	+.034	+.053	−.047	+.003	−.003
C(5)	−.018	+.015	+.024	−.034	−.007	+.030
C(6)	−.011	+.003	−.003	−.031	+.009	+.048
C(7)	+.013	−.008	−.039	+.039	+.029	−.028
C(8)	+.031	−.030	−.076	+.045	+.052	−.008
C(9)	+.038	−.030	−.051	+.068	+.005	−.045
O(1)	+.015	+.001	−.277	−.138	+.226	+.201
O(2)	+.002	−.000	+.126	+.246	−.136	−.246
O(3)	+.089	−.066	−.234	+.164	−.387	+.254
O(4)	+.032	−.055	−.040	+.015	+.534	−.256
O(5)	+.137	−.116	−.069	+.099	+.296	−.550
O(6)	+.012	−.004	−.128	+.162	−.305	+.450
H(1)	−.009	−.086	+.083	+.081	−.033	−.096
H(2)	−.022	+.064	+.100	−.055	−.027	+.065
H(3)	−.052	+.000	−.044	−.040	+.123	−.003

Table 11. Least-squares planes through atoms C(1), ···, C(6).

Direction Cosines	A	B	C	D	E	F
cos(a)	−.1989	−.9843	−.2262	−.9787	−.2241	−.9806
cos(b)	+.0090	−.0020	+.0171	−.0295	+.0418	+.0006
cos(c)	+.9849	+.2021	+.9795	+.2287	+.9792	+.2216
Origin to plane distance	6.5365	1.2893	7.0457	1.2363	9.6147	−1.8295
Deviations						
C(1)	−.004	+.002	+.008	−.009	+.019	−.013
C(2)	+.004	+.001	+.002	+.010	−.018	−.004
C(3)	+.001	−.006	−.010	−.001	−.000	+.019
C(4)	−.006	+.007	+.008	−.009	+.017	−.016
C(5)	+.007	−.004	+.001	+.010	−.017	−.001
C(6)	−.002	−.001	−.009	−.001	−.001	+.016
C(7)	−.005	+.012	−.031	+.037	+.044	−.043
C(8)	+.053	−.056	−.148	+.060	+.117	+.018
C(9)	+.075	−.058	−.070	+.131	−.031	−.095
O(1)	−.006	+.028	−.249	−.135	+.218	+.169
O(2)	−.025	+.026	+.130	+.228	−.099	−.244
O(3)	+.100	−.086	−.309	+.163	−.301	+.296
O(4)	+.068	−.095	−.128	+.043	+.599	−.230
O(5)	+.187	−.158	−.104	+.173	+.260	−.600
O(6)	+.045	−.024	−.126	+.228	−.362	+.383
H(1)	−.013	−.084	+.049	+.076	+.020	−.080
H(2)	+.017	+.027	+.043	−.008	−.012	+.053
H(3)	−.046	+.002	−.033	−.007	+.097	−.049

The benzene rings of molecules A, B, C, and D are planar. Most of the carboxyl carbons in these molecules, however, deviate slightly, but significantly, from the planes of the ring atoms; the deviations of the carboxyl oxygens are even more pronounced in some cases. In going from the plane of the benzene ring to the plane of the carboxyl group there seems to be both a component of rotation about the C–C bond connecting the two and a component of rotation about an axis in the plane of the molecule, but perpendicular to this C–C bond. In effect the carboxyl groups "droop" over the edges of the benzene rings – much like a piece of paper droops when extended over the edge of a table. With molecules A, B, C, and D the "drooping" component seems to be the more important for all the carboxyl groups except the O_1–C_7–O_2 groups of molecules C and D where the rotation component is the more important.

The benzene rings of molecules E and F appear to be very slightly nonplanar. This slight nonplanarity is probably related to the large out-of-plane deviations of the carboxyl groups of these molecules. For these carboxyl groups the component of rotation about the C–C bond is the more important in describing the deviations from the planes of the respective molecules, but here also the "drooping" component is important.

iv) Packing of the molecules and hydrogen bonding.

This section contains the most interesting part of the structural results obtained from this investigation. The intermolecular hydrogen bonding is in all cases through carboxyl-to-carboxyl double hydrogen

bonds, all carboxyl groups being fully hydrogen bonded. The hydrogen-bonding interconnections between the various molecules was shown in Figure 13. To be three dimensionally correct, this figure should be folded about 70° between molecules E and F.

If one proceeds — without knowledge of the crystal structure of trimesic acid — to construct a model by linking together various coplanar trimesic acid rings, one obtains an infinite net, I, which is very similar in appearance to common "chicken wire."

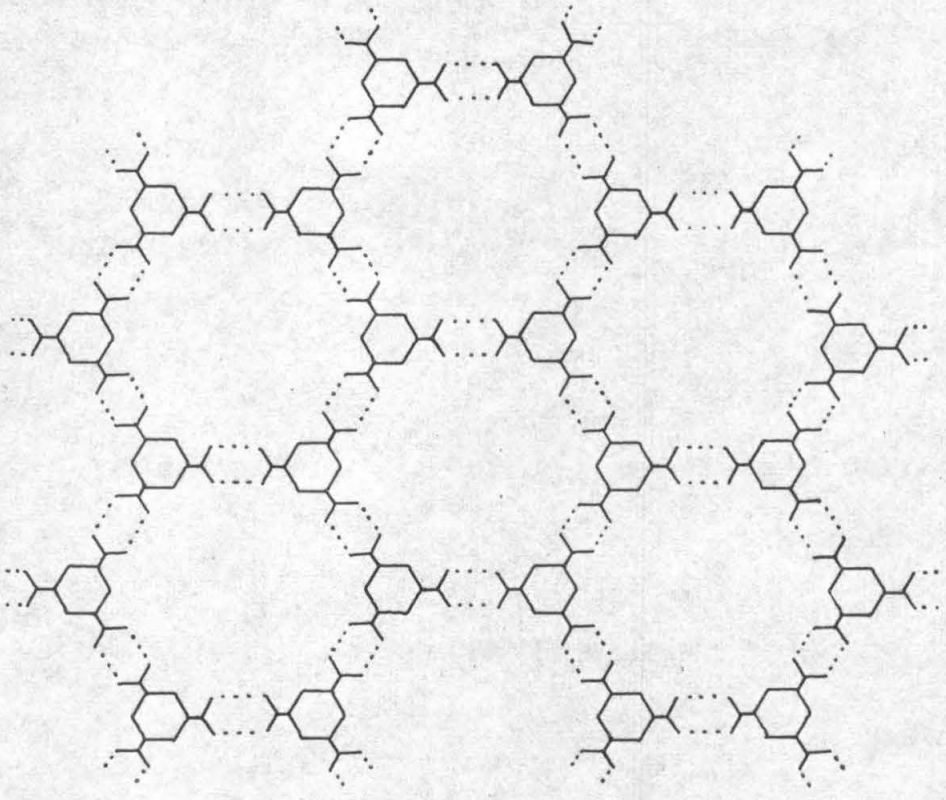

I

As can be seen, stacking of parallel nets of this type leaves large

holes in the structure at the centers of the large six-molecule rings.

All molecules in trimesic acid are arranged in infinite arrays of the type shown above. The problem of the holes is solved by allowing interpenetrating arrays as shown in II. In trimesic acid

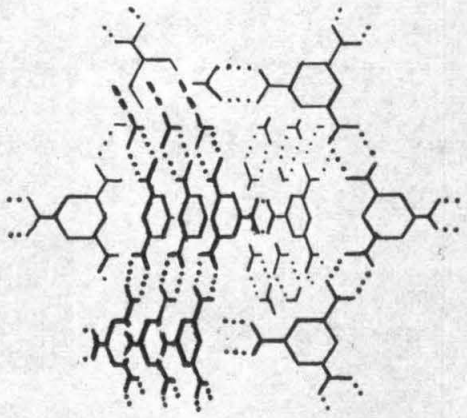

II

there are three parallel interpenetrating arrays passing through each group of three parallel large six-molecule rings.

If one proceeds with model construction in three dimensions based only upon the assumption of interpenetrating nets, one encounters another problem with holes in the structure which arises, in effect, from the fact that the large six-molecule rings are only wide enough for passage of three parallel interpenetrating nets. In

trimesic acid this problem is solved by allowing the two sets of interpenetrating nets to exchange directions every six molecules, III.

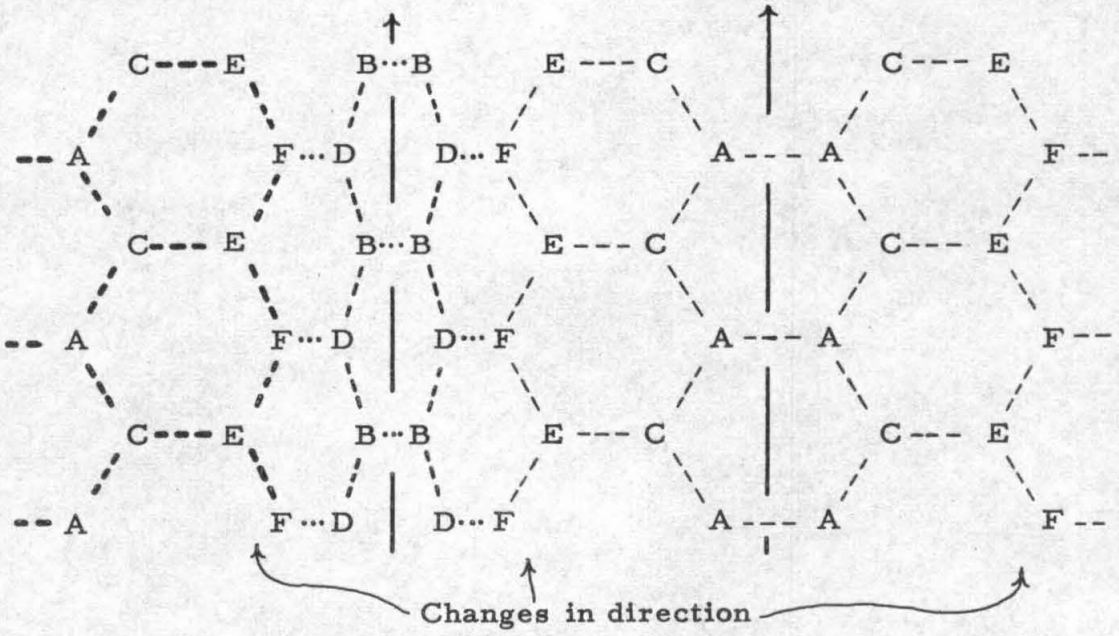

III

One direction is given by molecules A, C, and E, the other by molecules B, D, and F; the change in direction occurs in the connection between molecules E and F.

The packing is shown schematically in projection down the b axis in Figure 14. The difference in height along the b axis between light and dark molecules is $\Delta y = 0.50$, approximately. The molecules designated A, B, C, D, E, and F correspond to the asymmetric unit shown in Table 5. The pleated-sheet type hydrogen-bonding array described above can be seen by following the chain. The groups of three parallel molecules are easily visible. Another important feature is that the molecules which are hydrogen bonded

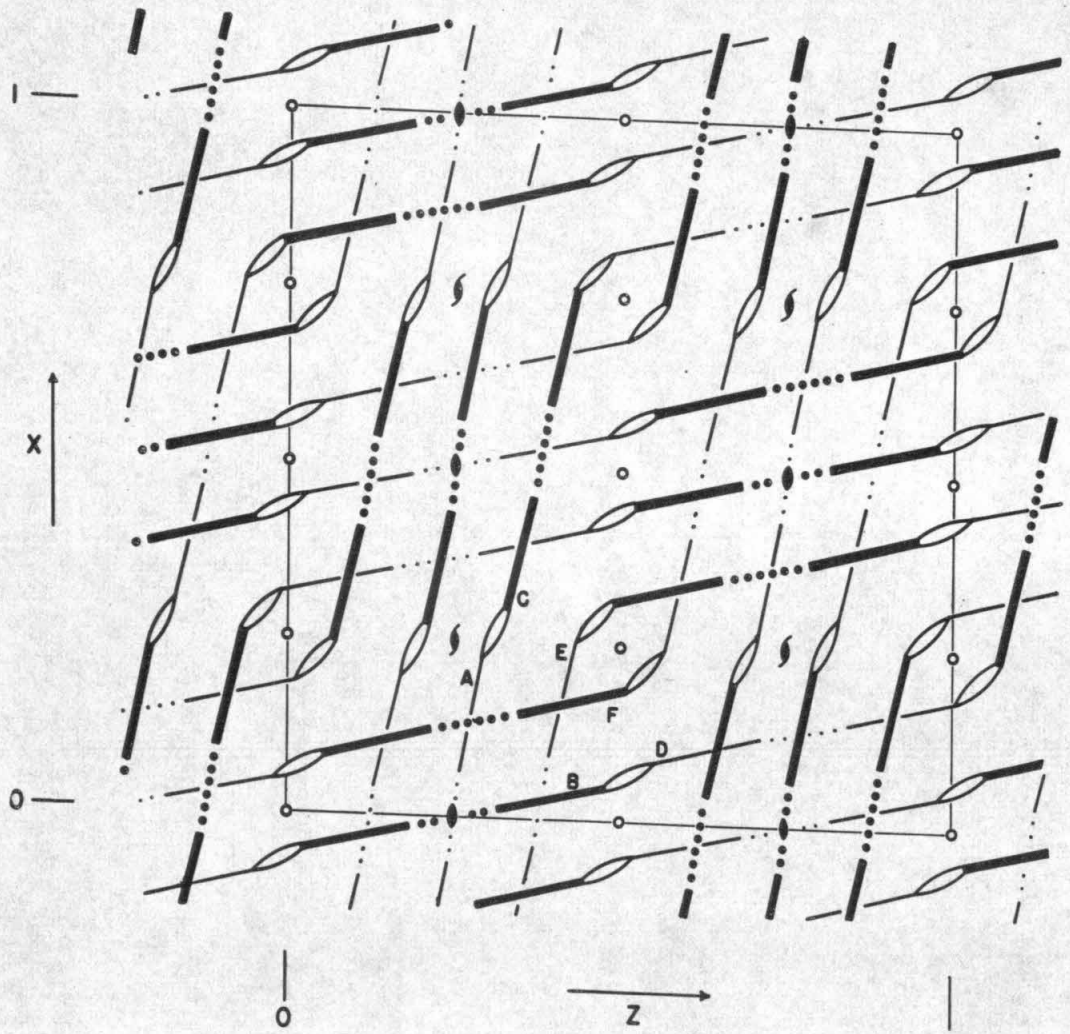

Figure 14. Schematic view of packing view down the b axis. Dotted lines represent single carboxyl links between molecules, ( ) figures represent double links.

together are, except for the E to F connection, parallel but not coplanar. The out-of-plane deviations of the carboxyl groups noted previously may be readily explained in terms of a tendency of carboxyl groups linked by hydrogen bonds to line up and closely approach one another.

There are two groups of three nearly parallel molecules — one involving molecules E, A, and C' (related to C by a 2_1 axis), the other involving molecules F, B, and D' (related to D by a center of symmetry). The dihedral angles between the planes of adjacent molecules (see Table 11) are 2.6° for A and E, 3.8° for A and C', 1.6° for F and B, and 2.5° for B and D'.

v) Disorder in the hydrogen bonding.

As pointed out previously, disorder in the hydrogen bonding of the $O_1-C_7-O_2$ carboxyl groups of molecules A and B is required by the hydrogen bonding across a two-fold axis. For the corresponding carboxyl groups of molecules C, D, E, and F, an approximate 2/3 to 1/3 disorder has been given. The fact that the hydrogens of these carboxyl groups failed to refine correctly when entered into the least-squares as whole hydrogens, coupled with the appearance of difference electron density maps, see Figure 11, show fairly conclusively that these carboxyl hydrogens are disordered. The refinement assuming the 2/3 to 1/3 ratio was satisfactory; however, this ratio is only our best evaluation of the situation and should be considered only an estimate.

Disorder in the hydrogen bonding of other carboxyl groups does not seem likely, but small amounts may not be ruled out. By taking the accentric space group Cc instead of the centric one which has been used, one may remove the restriction for the carboxyl groups of A and B; however, this new space group would not explain the disorder for the other molecules. There being no other indications to suggest a change in space group, it is highly unlikely that anything is to be gained by pursuing the matter further.

vi) A check on the least-squares standard deviations.

As Table 8 shows, there are a large number of observations of certain distances and angles, in particular those related to the benzene rings, which may be expected on sound chemical grounds to be equal. It is therefore appropriate that we determine empirical standard deviations from the sets of observations of these quantities and compare the results with the standard deviations obtained from the least squares. Such a comparison would check the reliability of standard deviations obtained from the least-squares refinement.

A consistent and unbiased estimate of the variance of the distribution of a variable x for which n random samples, $x_1, \cdots, x_n$, are available is given by the equation (19).

$$M_2 = \sigma^2_{\text{estimated}} = \frac{\sum_i (x_i - \bar{x})^2}{n - 1}$$

where $\bar{x}$ = sample mean = $\frac{\sum_i (x_i)}{n}$.

Furthermore, the standard deviation D of a value estimated by this method for σ^2 may be shown to be expressed by the following equation:

$$D^2 = \frac{2}{n-1} \sigma^4 .$$

If we substitute our estimated σ for the population σ in the equation above, we may calculate a value of D which is certainly necessary when comparing our estimated standard deviations with those obtained from the least squares.

The distribution of the C_r-C_r and the C_r-H_r distances and of the $C_r-C_r-C_r$ and $C_r-C_r-H_r$ angles were examined by the method described above; only these quantities were chosen because the other distances and angles listed in Table 8 might possibly have systematic deviations from one another which would give an erroneous estimate of the standard deviation.

The results of the analysis are shown in Table 12, together with the standard deviations calculated from positional standard deviations derived from the least-squares refinement. The agreement between the two sets of standard deviations is very good; in all cases they are the same to within three standard deviations of $\sigma_{estimated}$. The only trend is that the least-squares standard deviations are slightly lower; however, this trend could be due to systematic differences between the observed quantities which would tend to raise values of $\sigma_{estimated}$. In this light $\sigma_{estimated}$ may be properly called an upper limit of the corresponding least squares standard deviation. To summarize, the author feels that this experiment verifies the standard deviations obtained from the least-squares refinement.

Table 12. Comparison of standard deviations.

	Distances		Angles	
	C_r-C_r	C_r-H_r	$C_r-C_r-C_r$	$C_r-C_r-H_r$
$\sigma^2_{estimated}$	0.000034 A^2	0.0042 A^2	0.18°^{2}	16°^{2}
D = expected standard deviation of $\sigma^2_{estimated}$	0.000008	0.0014	0.04	4
n	36	18	36	36
$\sigma_{estimated}$	0.0058 A	0.06 A	0.43°	4°
Standard deviation of $\sigma_{estimated}$	0.0007	0.01	0.05	0.5
$\sigma_{least\ squares}$	0.004 A	0.03 A	0.4°	3°

References to Part I

1. G. R. Leibling, Ph. D. Dissertation, 72, California Institute of Technology, Pasadena (1965).

2. L. D'everin, Bull. soc. vand. sci. natur., 59, 417 (1937) as reported in C. A., 34, 4320 (1940).

3. J. W. Gryden, G. Donnary, and H. M. Ondik, Acta Cryst., 11, 38 (1958).

4. J. W. Jeffery, Acta Cryst., 6, 821 (1953).

5. A. J. C. Wilson, "X-ray Optics," Chap. 5-7, Methuen, London, 1949.

6. D. C. Hodgkin, et al., Proc Roy. Soc., A266, 440-517 (1962).

7. W. L. Bond, Rev. Sci. Instr., 22, 344 (1951).

8. D. J. Duchamp, "User's Guide to the CRYRM Crystallographic Computing System," Chap. 10, California Institute of Technology, Pasadena, 1964.

9. A. J. C. Wilson, Nature, 150, 152 (1942).

10. See for example A. W. Hanson, H. Lipson, and C. A. Taylor, Proc. Roy. Soc., A218, 371 (1953).

11. H. Lipson and C. A. Taylor, Acta Cryst., 4, 458 (1951).

12. G. A. Sims, J. M. Robertson, and T. H. Goodwin, Acta Cryst., 8, 157 (1955).

13. "International Tables for X-ray Crystallography," Vol. III, 202-203, The Kynoch Press, Birmingham, 1962.

14. J. Waser, Acta Cryst., 16, 1091 (1963).

15. E. Whittaker and G. Robinson, "The Calculus of Observations," 241-245, Blackie and Son Limited, London, 1924.

16. S. F. Darlow, Acta Cryst., 14, 159 (1961).

17. J. Waser, Acta Cryst., 8, 731 (1955).

18. V. Schomaker, J. Waser, R. Marsh, and G. Bergman, Acta Cryst., 12, 600 (1959).

19. See for example H. Cramer, "Methods of Mathematical Statistics," 341-352, Princeton, 1946.

PART II

TOPICS IN CRYSTALLOGRAPHIC CALCULATIONS

OPTICAL TRANSFORMS AND X-RAY TRANSFORMS

The use of optical transforms in determination of crystal structures has been discussed many times in the literature (1). The method consists of preparing an optical transform by photographing the diffraction pattern produced by shining parallel, monochromatic light through holes in a cardboard mask — the holes in the mask representing atoms of a molecule — and then comparing this transform with the x-ray diffraction pattern of a crystal in order to obtain information about the orientation of the molecules in the crystal. However, a discussion of the detailed relationship between the optical and the x-ray diffraction patterns is not readily available. Also nothing has been mentioned about the effect of different size holes.

The expression for the x-ray transform is the well-known equation

$$F(hk) = \sum_{n}^{\text{all atoms}} f_n e^{2\pi i(hx_n + ky_n)} \qquad (1)$$

in which h and k are Cartesian coordinates in transform space and f_n is the x-ray scattering factor (temperature modified) for atom n which has coordinates $\underline{x}_n$ and $\underline{y}_n$. In the following a similar expression is derived for diffraction of light by holes in a mask. A reference which has been particularly useful is the classic work

on optics by Born and Wolf (2).

Fraunhofer diffraction of monocromatic radiation by a single circular aperture may be represented by

$$U_j(p,q) = \frac{1}{\lambda}\sqrt{\frac{E_j}{D_j}} \iint_{D_j} e^{-i\frac{2\pi}{\lambda}(p\xi + q\eta)}\, d\xi\, d\eta \qquad (2)$$

where $U_j(p,q)$ is the complex magnitude from aperture j at point p, q in transform space, E_j is the total energy incident on the aperture, D_j is the area of the aperture, ξ and η are Cartesian coordinates in the plane of the aperture, and the integration is over all ξ and η within the area of the aperture.

Let E' be the energy per unit area incident upon the aperture; and let us assume that the incident energy is directly dependent upon the area of the aperture. Then the total pattern from a number of different-sized non-overlapping circular apertures in the same plane is

$$U(p,q) = \sum_{j}^{\text{all apertures}} U_j(p,q) = \frac{\sqrt{E'}}{\lambda}\sum_j \iint_{D_j} e^{-i\frac{2\pi}{\lambda}(p\xi + q\eta)}\, d\xi\, d\eta \ .$$

Let $(\xi_1, \eta_1), (\xi_2, \eta_2), \cdots, (\xi_N, \eta_N)$ be the coordinates of the centers of the apertures $1, \cdots, N$. Then for each aperture let $\xi = \xi_j + \xi_j'$, $\eta = \eta_j + \eta_j'$. Substituting in the above gives

$$U(p,q) = \frac{\sqrt{E'}}{\lambda} \sum_j \iint_{D_j} e^{-i \frac{2\pi}{\lambda} [p(\xi_j + \xi_j') + q(\eta_j + \eta_j')]} \, d\xi_j' \, d\eta_j' \, .$$

Therefore

$$U(p,q) = \frac{E'}{\lambda} \sum_j \left\{ \underbrace{e^{-i \frac{2\pi}{\lambda} (p\xi_j + q\eta_j)}}_{\text{Superposition of coherent diffraction patterns}} \underbrace{\iint_{D_j} e^{-i \frac{2\pi}{\lambda} (p\xi_j' + q\eta_j')} \, d\xi_j' \, d\eta_j'}_{\text{Single aperture}} \right\}.$$

Evaluation of the term under the integral leads to

$$U(p,q) = \frac{\sqrt{E'}}{\lambda} \sum_j \left\{ e^{-i \frac{2\pi}{\lambda} (p\xi_j + q\eta_j)} \, 2\pi a_j^2 \, \frac{J_1(\frac{2\pi}{\lambda} a_j w)}{\frac{2\pi}{\lambda} a_j w} \right\}$$

where w is the radial distance, $w = p^2 + q^2$, and a_j is the radius of aperture j. Rearranging gives

$$U(p,q) = \frac{2\pi\sqrt{E'}}{\lambda} \sum g_j(w) \, e^{-\frac{2\pi i}{\lambda} (p\xi_j + q\eta_j)} \tag{3}$$

where

$$g_j(w) = a_j^2 \, \frac{J_1(\frac{2\pi}{\lambda} a_j w)}{\frac{2\pi}{\lambda} a_j w} \tag{4}$$

is the "scattering factor" for a circular aperture of radius a_j.

Equation 3 is analogous to equation 1 — the scattering factor for a given atom being replaced by equation 4. In Figure 1, $g_j(w)$ is plotted as a function of w. The shape of the curve is quite similar to that expected for the x-ray scattering factor. The two curves will fit fairly well if the size of the hole in the mask is chosen so that $g_j(w) = 0$ corresponds approximately to the edge of the copper sphere.

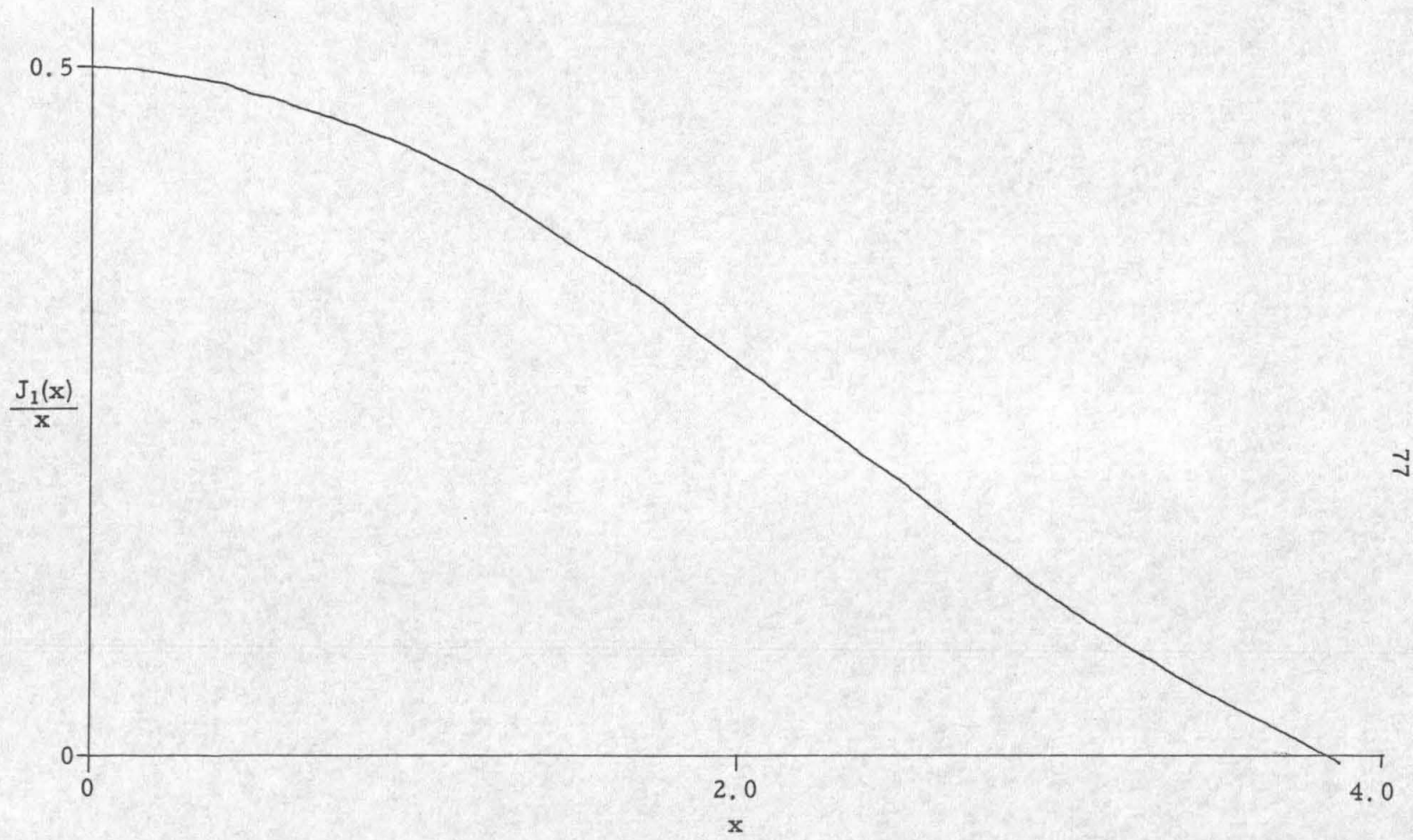

Figure 1. Plot showing the shape of the "scattering factor" of a circular aperture.

A SYSTEMS APPROACH TO CRYSTALLOGRAPHIC COMPUTING

As larger and larger crystallographic problems are undertaken and as more powerful (and complicated) computers become available, the mountain of details involved in crystallographic calculations grows. Also the compiler-executer systems of the more powerful computers — for example, IBJOB on the IBM 7090-7094 computers — impose excessive restrictions on the amount of memory which is available for a calculation, on the kind and number of programs which can be used in a given job on the computer, on the number and kind of temporary storage units available, on the input and output of information, and on simple changes to large programs. All of the restrictions enumerated above may be eliminated or reduced, and in addition advantages in efficiency and ease of operation may be gained, by using a systems approach in setting up crystallographic programs. Most crystallographic calculations — for example, Fourier and least-squares calculations — use well-known expressions, and may thus be programmed once, and these programs used over and over for routine calculations. One disadvantage of using a systems approach is that the programming, which must be done using symbolic machine language, is more difficult than programming in a compiler language, for example, FORTRAN; however, the extra difficulty is not as serious as one might believe and is more than compensated for by the extra power and efficiency which become possible.

In preparing crystallographic programs for Caltech's IBM 7094-7040 computing system, we have used a systems approach, the

end result being the CRYRM Crystallographic Computing System. Instructions for the use of this computing system are available in the "User's Guide to the CRYRM Crystallographic Computing System" (3) and will not be repeated in the thesis. A general description of the philosophy involved follows in this section, and some of the special mathematical expressions which were used are discussed in later sections.

A chart showing the level of control within the 7094 computer is given in Figure 2. The basic monitor, IBSYS, part of which remains in memory at all times, provides communication between the different systems. The different systems programs, such as CRYRM, are given control at the user's request. CRYRM, part of which remains in memory at all times during crystallographic calculations, consists of a crystallographic monitor, which calls in various subprograms as needed, and input-output and fractional subroutines for use by the different subprograms. It also provides for continuity of operation between jobs and for accounting. The systems program and all subprograms are stored on the installation's system library and need not be loaded each time by the user.

Intercompatible subprograms providing for a great variety of options have been written. In the usual case the crystallographer enters his reflection data by cards into the computer only once; these data are preserved on magnetic tape between computer runs. When using CRYRM, the user — in a single run of the computer and with a minimum number of cards — calls for various subprograms

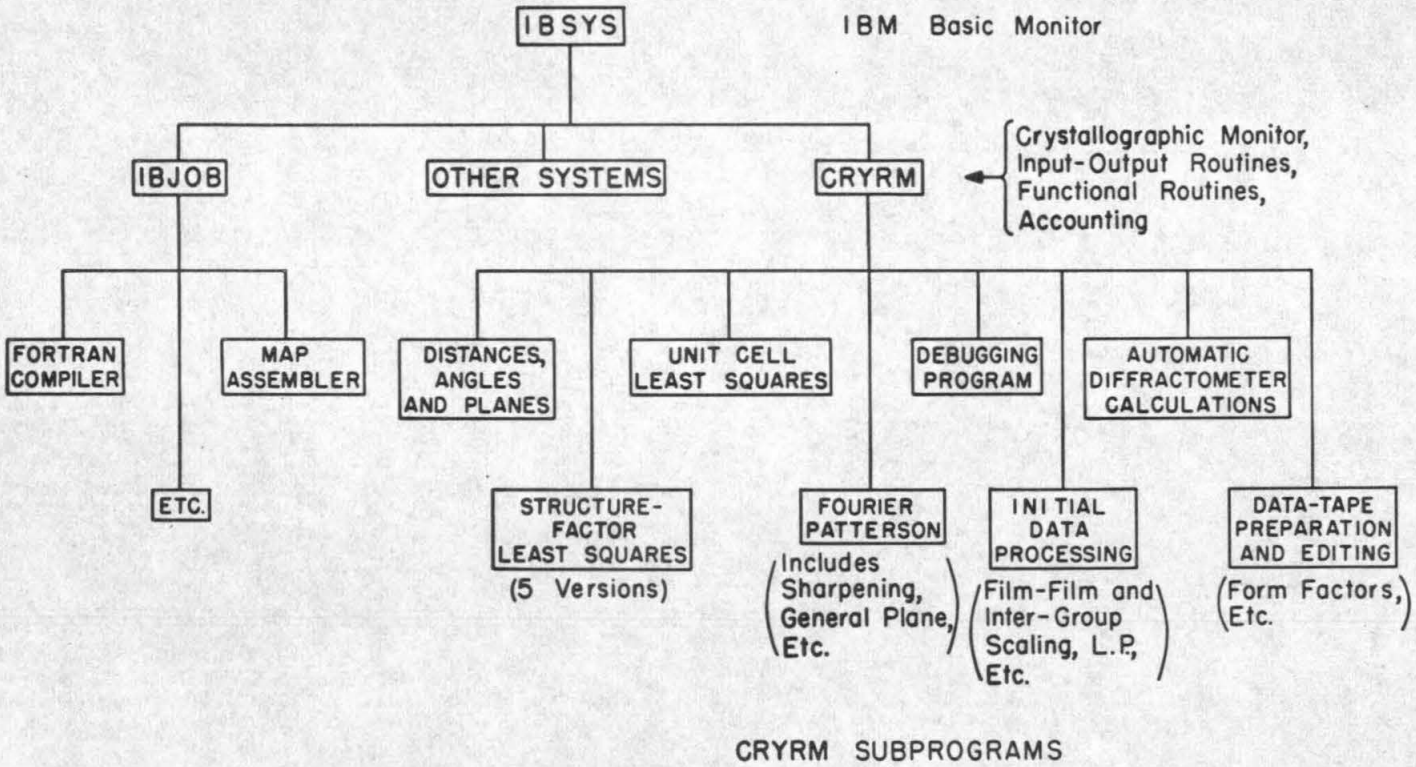

Figure 2. Level of control chart.

successively, the output from one subprogram automatically becoming the input to the next. As a subprogram is called in, the user, if he desires, may make small changes in the program very easily. In practice the CRYRM Crystallographic Computing System has been found to be very efficient and very easy to use. It has greatly speeded up many crystallographic investigations and indeed has even made some of them possible — trimesic acid, for example.

The author presented a paper on this subject at the July 26–31, 1964, annual meeting of the American Crystallographic Society in Bozeman, Montana (4).

COMPUTER CALCULATION OF FOURIER AND PATTERSON MAPS

i) Introduction.

Methods and expressions are presented which allow a computer to be programmed to calculate Fourier and Patterson maps given only the space group number, unit cell, and the asymmetric reflection data as determined by the Laue group. Methods leading to maps on an inches-per-Angstrom scale are also discussed, together with the efficient calculation of general plane sections. The methods described were used in writing the CRYRM Fourier and Patterson Subprogram.

ii) Performance of the summation.

The Fourier expression of a particular space group may be broken down in the usual manner to sums of certain trigonometric triple products, which then may be separated into three successive summations — one each in the h, k, and ℓ dimensions. Structure factors are processed one by one by a first-dimension summation routine which accumulates the sums in four regions, one for each possible double product — (cos)(cos), (cos)(sin), (sin)(cos), or (sin)(sin) — in the second and third dimension summations. One first-dimension summation is necessary whenever the slowest varying coordinate x, y, or z, changes between map points, as for example, between sections of a three-dimensional map. Projections down the crystallographic axes may be calculated by replacing the first-dimension routine by a routine which selects only reflections which have the corresponding index equal to zero, and appropriately

adjusts the scale.

iii) Definition of map points.

Provided a very fast sine and cosine subroutine of sufficient accuracy is available, a summation of Fourier series need not be done, as in the past, only at integral intervals of the lattice translations. Once the x coordinate, for example, of a map point is known, tables of $\sin(2\pi hx)$ and $\cos(2\pi hx)$ as a function of h may be calculated then used to find the trigonometric functions for given reflections by quick table lookup. This technique, becoming more efficient as the number of reflections grows, allows maps to be calculated on a prespecified inches-per-Angstrom scale, which may be contoured directly on the computer output.

a) Sections with one coordinate constant.

For sections (and projections) the following expressions may be used to calculate the interval in fractional coordinates between map points for setting up a to-scale map. We assume a rectangular array of points will be printed with P_h points/inch in the horizontal direction and P_v points/inch in the vertical direction and a scale of S inches/Angstrom. For a section of constant y with z constant in the horizontal direction

$$\Delta x_h = \frac{1}{P_h S \underline{a}} \quad , \quad \Delta z_h = 0 \quad ,$$

$$\Delta x_v = - \frac{\cos \beta}{P_v S \underline{a} \sin \beta} \quad ,$$

and $$\Delta z_v = \frac{1}{P_v S \underline{c} \sin\beta} ,$$

where Δx_h and Δx_v are the x increments in going between points in the horizontal and vertical directions respectively, similarly for z, and β is the angle between the $\underline{a}$ and $\underline{c}$ crystallographic axes.

b) General-plane sections.

A general plane may be defined by the direction cosines of the plane normal and by a point in the plane. Much time may be saved in the calculation of a general-plane section if the calculation is set up so that one of the fractional coordinates, x, y, or z, is held constant in the horizontal direction in the plane. Then if the index corresponding to this constant coordinate is chosen for the first-dimension summation, this summation need be performed only once for each row of the map instead of once for each point, as is usual. In the following discussion expressions are developed for the computation of the fractional coordinate intervals between points in the general plane. It is assumed that the first-dimension summation parameter is x in this discussion.

The situation is diagrammed in Figure 3 in which certain vectors are defined. In addition let

$\underset{\sim}{a}_1 = \frac{\hat{a}}{|a|}$,

$\underset{\sim}{a}_2 = \frac{\hat{b}}{|b|}$,

$\underset{\sim}{a}_3 = \frac{\hat{c}}{|c|}$,

where $\hat{a}$, $\hat{b}$, $\hat{c}$ are the unit cell triple and α_1, α_2, α_3 are the unit cell angles,

$\underset{\sim}{n}$ = normal to the molecular plane,

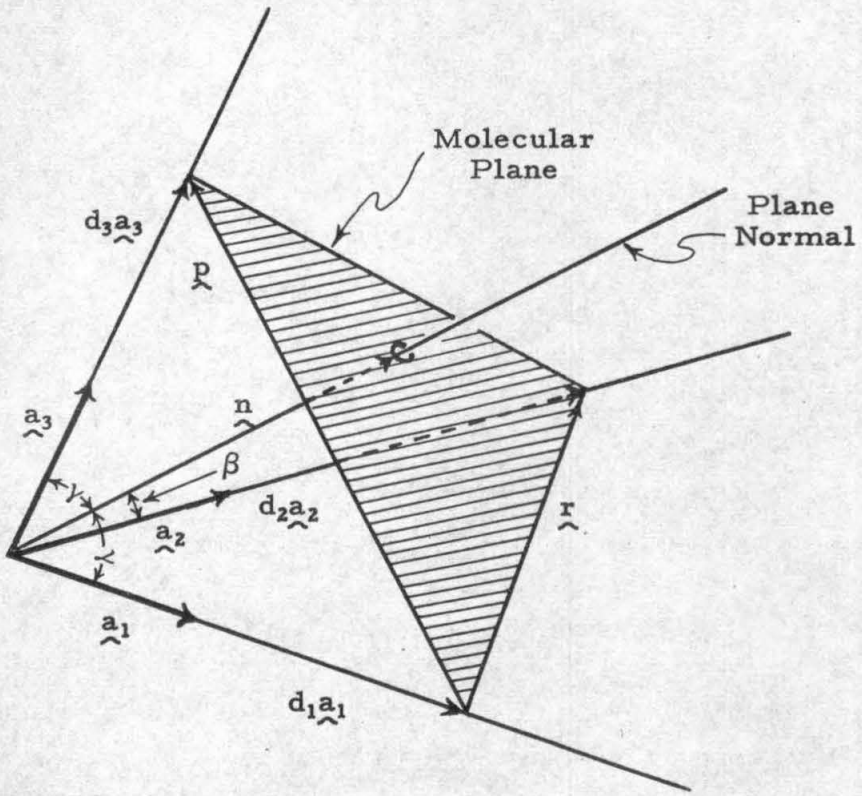

Figure 3. The general plane.

α = angle between $\underset{\wedge}{a}$ and $\underset{\wedge}{n}$,

β = angle between $\underset{\wedge}{b}$ and $\underset{\wedge}{n}$,

γ = angle between $\underset{\wedge}{c}$ and $\underset{\wedge}{n}$,

d_1 = intercept of the molecular plane on $\underset{\wedge}{a}_1$,

d_2 = intercept of the molecular plane on $\underset{\wedge}{a}_2$,

d_3 = intercept of the molecular plane on $\underset{\wedge}{a}_3$, and

$\begin{matrix}\cos\alpha \\ \cos\beta = \\ \cos\gamma\end{matrix}$ direction cosines of the plane with respect to the crystallographic $\underset{\wedge}{a}$, $\underset{\wedge}{b}$, and $\underset{\wedge}{c}$ axes respectively.

By the definition of the vector cross product,

$$\underset{\wedge}{n} \parallel \underset{\wedge}{r} \times \underset{\wedge}{p} \ ,$$

where

$$\underset{\wedge}{r} = d_2\underset{\sim}{a}_2 - d_1\underset{\sim}{a}_1$$
$$\underset{\wedge}{p} = d_3\underset{\sim}{a}_3 - d_1\underset{\sim}{a}_1 \ .$$

Expanding gives

$$\underset{\wedge}{r} \times \underset{\wedge}{p} = d_2d_3(\underset{\sim}{a}_2 \times \underset{\sim}{a}_3) - d_2d_1(\underset{\sim}{a}_2 \times \underset{\sim}{a}_1) - d_1d_3(\underset{\sim}{a}_1 \times \underset{\sim}{a}_3) \ .$$

Let

$$\underset{\wedge}{a}^1 = \underset{\wedge}{a}_2 \times \underset{\wedge}{a}_3$$
$$\underset{\wedge}{a}^3 = \underset{\wedge}{a}_1 \times \underset{\wedge}{a}_2$$
$$\underset{\wedge}{a}^2 = \underset{\wedge}{a}_3 \times \underset{\wedge}{a}_1 \ .$$

Then

$$\underset{\sim}{n} \;||\; d_2 d_3 \underset{\sim}{a}^1 + d_1 d_3 \underset{\sim}{a}^2 + d_1 d_2 \underset{\sim}{a}^3 \ .$$

Dividing through by $\frac{d_1 d_2 d_3}{|n|}$ gives

$$\underset{\sim}{n} \;||\; \frac{|n|}{d_1} \underset{\sim}{a}^1 + \frac{|n|}{d_2} \underset{\sim}{a}^2 + \frac{|n|}{d_3} \underset{\sim}{a}^3 \ .$$

But since

$$\cos \alpha = \frac{|n|}{d_1} \ , \quad \cos \beta = \frac{|n|}{d_2} \ , \quad \cos \gamma = \frac{|n|}{d_3} \ ,$$

we have that

$$n \;||\; \cos \alpha \, a^1 + \cos \beta \, a^2 + \cos \gamma \, a^3 \equiv n' \ .$$

Next, consider a vector $\underset{\sim}{m}$ in the plane of $\underset{\sim}{a}_2$ and $\underset{\sim}{a}_3$, parallel to the molecular plane.

Since $$\underset{\sim}{m} \cdot \underset{\sim}{n}' = 0 \ ,$$

it follows immediately that

$$\underset{\sim}{m} \;||\; \cos \gamma \, \underset{\sim}{a}_2 - \cos \beta \, \underset{\sim}{a}_3 \equiv \underset{\sim}{m}' \ .$$

We define translations in the direction of $\underset{\sim}{m}'$ to be translations in the molecular plane in the horizontal direction. It is immediately seen that the x coordinates of points are invariant under the above translation.

Next, consider a vector $\underset{\sim}{s}$ normal to both $\underset{\sim}{m}'$ and $\underset{\sim}{n}'$. Let

$$\underset{\sim}{s} = s_1\underset{\sim}{a}_1 + s_2\underset{\sim}{a}_2 + s_3\underset{\sim}{a}_3 \ .$$

If we denote

$$\cos \alpha = m_1$$

$$\cos \beta = m_2$$

$$\cos \gamma = m_3$$

we have

$$\underset{\sim}{n}' \cdot \underset{\sim}{s} = m_1s_1 + m_2s_2 + m_3s_3 = 0 \ ,$$

and

$$\underset{\sim}{m}' \cdot \underset{\sim}{s} = (m_3\underset{\sim}{a}_2 - m_2\underset{\sim}{a}_3) \cdot (s_1\underset{\sim}{a}_1 + s_2\underset{\sim}{a}_2 + s_3\underset{\sim}{a}_3)$$

$$= v_1s_1 + v_2s_2 + v_3s_3 = 0 \ ,$$

where

$$v_1 = m_3 \cos \alpha_3 - m_2 \cos \alpha_2$$

$$v_2 = m_3 - m_2 \cos \alpha_1$$

$$v_3 = m_3 \cos \alpha_1 - m_2 \ .$$

Solving the above equations gives

$$s_1 : s_2 : s_3 = v_3m_2 - m_3v_2 : m_3v_1 - v_3m_1 : m_1v_2 - v_1m_2 \ .$$

Denote

$$s_1' = v_3m_2 - m_3v_2,$$

$$s_2' = m_3v_1 - v_3m_1, \text{ and}$$

$$s_3' = m_1 v_2 - v_1 m_2 \ .$$

Therefore

$$\underset{\sim}{s} \ || \ s_1' \underset{\sim}{a}_1 + s_2' \underset{\sim}{a}_2 + s_3' \underset{\sim}{a}_3 \equiv \underset{\sim}{s}' \ .$$

We define translations in the direction of s' to correspond to vertical translations in the molecular plane.

The computation of translation parameters between map points follows directly. In the horizontal direction with P_h points/inch and a map scale of S inches/Angstrom, the changes in the y and z parameters expressed in fractional coordinates are

$$\Delta y_h = \frac{\cos \gamma}{(P_h)(S)(r)\,|\underline{b}|} \ ,$$

and

$$\Delta z_h = - \frac{\cos \beta}{(P_h)(S)(r)\,|\underline{c}|} \ ,$$

where

$$r = |\underset{\sim}{m}'| = \sqrt{\cos^2 \gamma + \cos^2 \beta - 2 \cos \beta \cos \gamma \cos \alpha_1} \ .$$

Similarly in the vertical direction, P_v points/inch produces changes in the x, y, and z, coordinates given by

$$\Delta x_v = \frac{s_1'}{(P_v)(S)(q)\,|\underset{\sim}{a}|} \ ,$$

$$\Delta y_v = \frac{s_2'}{(P_v)(S)(q)\,|\underset{\sim}{b}|} \ ,$$

and $$\Delta z_v = \frac{s_3'}{(P_v)(S)(q)\,|\underset{\sim}{c}|} ,$$

where

$$q = |\underset{\sim}{s}'| = \sqrt{s_1'^2 + s_2'^2 + s_3'^2 + 2s_1's_2' \cos \alpha_3 + 2s_1's_3' \cos \alpha_2 + 2s_2's_3' \cos \alpha_1}.$$

A special case must be considered since if cos γ and cos β = 0, the plane is undefined by the above expressions. In this special case the general-plane section reduces to a section with x constant giving expressions analogous to those of (a).

iv) Reflection data storage.

If calculation of three-dimensional and general-plane sections is to be efficient, all the reflection data must be stored in the computer memory during the calculation. Phasing and multiplication by volume factors, etc., may be conveniently done when the data are stored. Only the asymmetric unit of data, as dictated by the Laue group, need be stored; centering, if present, also reduces the storage space required. One convenient way for storing data is to divide the data into groups of constant h index, then to store reflections within each group in a large matrix in which the k index counts the rows and the ℓ index the columns (counting from zero). In this manner only one storage location per reflection is required for centric space groups, two storage locations per reflection for acentric ones.

From the unit cell parameters $\underline{a}$, $\underline{b}$, $\underline{c}$, α, β, and γ the maximum values which the h, k, and ℓ indices may assume within the sphere of reflection of radiation with wavelength λ may be calculated directly from Bragg's law, for example,

$$h_{max}^{0} = \frac{2\underline{a}}{\lambda} \quad .$$

Within a layer of constant h index, the maximum magnitude which the ℓ index assumes in the positive direction, $\ell_{max}(+)$, and in the negative direction $\ell_{max}(-)$ and likewise $k_{max}(+)$ and $k_{max}(-)$ may be calculated from ℓ_{max}^{0} and k_{max}^{0} by the following expressions

$$\ell_{max}(+) = [\cos(90° - \beta)\cos\phi + \sin(90° - \beta)\sin\phi]\ell_{max}^{0} \quad ,$$

$$\ell_{max}(-) = [\cos(90° - \beta)\cos\phi - \sin(90° - \beta)\sin\phi]\ell_{max}^{0} \quad ,$$

$$k_{max}(+) = [\cos(90° - \gamma)\cos\phi + \sin(90° - \gamma)\sin\phi]k_{max}^{0} \quad ,$$

and $$k_{max}(-) = [\cos(90° - \gamma)\cos\phi - \sin(90° - \gamma)\sin\phi]k_{max}^{0} \quad ,$$

where $\sin\phi = \frac{h\lambda}{2\underline{a}}$, and $\cos\phi = \sqrt{1 - \sin^2\phi}$.

The above may be easily derived by consideration of the sphere of reflection. The values obtained from this calculation for each h may be used, together with knowledge of the definition of the asymmetric unit of data, to dimension the matrices for reflection storage.

v) Fourier expressions for different space groups.

In order that the computer may calculate Fourier summations

given only the space group number, the expressions for different space groups must be coded into the program. Since the expressions as given in the International Tables (5) are not suitable for this, Fourier expressions for all space groups, excluding the hexagonal and trigonal space groups, have been derived in a triple product formulation. Also A and B are used for the real and imaginary components for structure factors of acentric space groups, since this formulation is more efficient for computers than the magnitude and phase angle formulation.

First we define symbols for all possible trigonometric triple products (with signs) involving hx, ky, and ℓz as shown in Table 1. Then beginning with the general Fourier trigonometric expression, assuming Fridel's law,

$$\rho(x,y,z) = \frac{2}{V} \Sigma A_{hk\ell} \cos(hx+ky+\ell z) + \Sigma B_{hk\ell} \sin(hx+ky+\ell z)$$

by use of trigonometric identities we obtain

$$\rho(x,y,z) = \frac{2}{V} \Sigma A_{hk\ell}(C+D+E+F) + \Sigma B_{hk\ell}(K+L+M+N) \ . \qquad (1)$$

If we now separate the summations into reflection groups as defined by signs of indices and require a positive sign on all indices within each triple product, we obtain

$$\rho(x,y,z) = \frac{2}{V} \Sigma[A_{hk\ell}(C + D + E + F)$$

$$+ A_{\bar{h}k\ell}(C - D - E + F)$$

Table 1. Definition of triple products.

Symbol	Triple Product		
C	$+\cos 2\pi hx$	$\cos 2\pi ky$	$\cos 2\pi \ell z$
D	$-\sin 2\pi hx$	$\sin 2\pi ky$	$\cos 2\pi \ell z$
E	$-\sin 2\pi hx$	$\cos 2\pi ky$	$\sin 2\pi \ell z$
F	$-\cos 2\pi hx$	$\sin 2\pi ky$	$\sin 2\pi \ell z$
G	$-\cos 2\pi hx$	$\cos 2\pi ky$	$\cos 2\pi \ell z$
H	$+\sin 2\pi hx$	$\sin 2\pi ky$	$\cos 2\pi \ell z$
I	$+\sin 2\pi hx$	$\cos 2\pi ky$	$\sin 2\pi \ell z$
J	$+\cos 2\pi hx$	$\sin 2\pi ky$	$\sin 2\pi \ell z$
K	$-\sin 2\pi hx$	$\sin 2\pi ky$	$\sin 2\pi \ell z$
L	$+\cos 2\pi hx$	$\cos 2\pi ky$	$\sin 2\pi \ell z$
M	$+\sin 2\pi hx$	$\cos 2\pi ky$	$\cos 2\pi \ell z$
N	$+\cos 2\pi hx$	$\sin 2\pi ky$	$\cos 2\pi \ell z$
O	$+\sin 2\pi hx$	$\sin 2\pi ky$	$\sin 2\pi \ell z$
P	$-\cos 2\pi hx$	$\cos 2\pi ky$	$\sin 2\pi \ell z$
Q	$-\sin 2\pi hx$	$\cos 2\pi ky$	$\cos 2\pi \ell z$
R	$-\cos 2\pi hx$	$\sin 2\pi ky$	$\cos 2\pi \ell z$

$$+ A_{hk\bar{\ell}}(C - D + E - F)$$

$$+ A_{hk\ell}(C + D - E - F)$$

$$+ B_{hk\ell}(L + K + M + N)$$

$$+ B_{\bar{h}k\ell}(L - K - M + N)$$

$$+ B_{h\bar{k}\ell}(L - K + M - N)$$

$$+ B_{hk\bar{\ell}}(- L - K + M + N)] \qquad (2)$$

Expression 2 is used only for derivation purposes when for example $F_{hk\ell}$ is related to $F_{h\bar{k}\bar{\ell}}$ by the symmetry of the space group. In space P1, no simplification is possible; the triple product formulation is given by 1. If, for example, one finds in a centric space group that $A_{hk\ell} = -A_{h\bar{k}\bar{\ell}}$, as for example in $P2_1/c$ for $k + \ell = 2n + 1$, then inspection of 2 shows that 1 reduces to

$$\rho(x,y,z) = \frac{4}{V} \Sigma A_{hk\ell} (D + F) \quad .$$

In tetragonal and cubic space groups, symmetry occurs which if taken into account in the trigonometric expressions would require trigonometric terms involving hy, kz, etc., which are not included in Table 1. It is more convenient and just as efficient to use such relations at the time of the first-dimension summation to generate equivalent reflections from those of the asymmetric unit — the trigonometric expressions being set up to expect a complete octant of data for Laue groups 4/mmm, $2/m\bar{3}$, and m3m and a complete quadrant for Laue group 4/m.

The expressions derived in this manner are given in Table 2, together with the data required. The volume factors which are required are 2/V for Laue Group $\bar{1}$, 4/V for Laue groups 2/m and 4/m, and 8/V for all others. Also in Table 2, for each space group, bounds are given which define one possible asymmetric unit; it is useful and quite easy to include this information in the computer, and to provide an option for changing these numbers if the user prefers a different asymmetric unit. Lower bounds are assumed zero unless otherwise indicated.

For monoclinic space groups, only the b axis unique orientations are considered, and "additional" space groups with different a and c orientations are provided. Where a choice of origin existed in higher symmetries, the origin was taken at the center of symmetry.

Data generation is discussed separately for each Laue group involved.

a) Laue group 4/m.

Only data for which h, k, and ℓ are all positive are required for an asymmetric unit of data; however, the Fourier expressions require also reflections of the type $\bar{h}k\ell$. For each reflection of indices $hk\ell$ a reflection with indices $\bar{k}h\ell$ may be generated in a space-group-dependent manner as shown in Table 3.

b) Laue group 4/mmm.

An asymmetric unit of data includes only 1/16 of the sphere of reflection, for example, all $hk\ell$ reflections for which $h \geqq k$; the Fourier expressions require all reflections with h, k, and ℓ all

Space Group	Laue Group	Data Required	Parity Tests	A(hkl) Factor	B(hkl) Factor	Bounds x	Bounds y	Bounds z
1 P1	$\bar{1}$	$hkl, \bar{h}\bar{k}l, h\bar{k}l, \bar{h}k\bar{l}$		C+D+E+F	K+L+M+N	1	1	1
2 $P\bar{1}$	1	$hkl, \bar{h}\bar{k}l, h\bar{k}l, \bar{h}k\bar{l}$		C+D+E+F	–	1	$\frac{1}{2}$	1
3 P2	2/m	$hkl, \bar{h}kl$		C+E	K+N	$\frac{1}{2}$	1	1
4 $P2_1$	2/m	$hkl, \bar{h}kl$	$k = 2n$ $k = 2n+1$	C+E D+F	K+N L+M	1	$\frac{1}{2}$	1
5 C2	2/m	$hkl, \bar{h}kl$ with $h+k = 2n$		C+E	K+N	$\frac{1}{2}$	$\frac{1}{2}$	1
5A A2	2/m	$hkl, \bar{h}kl$ with $k+\ell = 2n$		C+E	K+N	$\frac{1}{2}$	$\frac{1}{2}$	1
6 Pm	2/m	$hkl, \bar{h}kl$		C+E	L+M	1	$\frac{1}{2}$	1
7 Pc	2/m	$hkl, \bar{h}kl$	$\ell = 2n$ $\ell = 2n+1$	C+E D+F	L+M K+N	1	$\frac{1}{2}$	1
7A Pa	2/m	$hkl, \bar{h}kl$	$h = 2n$ $h = 2n+1$	C+E D+F	L+M K+N	1	$\frac{1}{2}$	1
7N Pn	2/m	$hkl, \bar{h}kl$	$h+\ell = 2n$ $h+\ell = 2n+1$	C+E D+F	L+M K+N	1	$\frac{1}{2}$	1
8 Cm	2/m	$hkl, \bar{h}kl$ with $h+k = 2n$		C+E	L+M	1	$\frac{1}{2}$	1
8A Am	2/m	$hkl, \bar{h}kl$ with $k+\ell = 2n$		C+E	L+M	1	$\frac{1}{2}$	1
9 Cc	2/m	$hkl, \bar{h}kl$ with $h+k = 2n$	$\ell = 2n$ $\ell = 2n+1$	C+E D+F	L+M K+N	1	$\frac{1}{2}$	1
9A Aa	2/m	$hkl, \bar{h}kl$ with $k+\ell = 2n$	$h = 2n$ $h = 2n+1$	C+E D+F	L+M K+N	1	$\frac{1}{2}$	1
10 P2/m	2/m	$hkl, \bar{h}kl$		C+E	–	$\frac{1}{2}$	$\frac{1}{2}$	1
11 $P2_1/m$	2/m	$hkl, \bar{h}kl$	$k = 2n$ $k = 2n+1$	C+E D+F	– –	1	$\frac{1}{2}$	1
12 C2/m	2/m	hkl, hkl with $h+k = 2n$		C+E	–	$\frac{1}{2}$	$\frac{1}{2}$	1
12A A2/m	2/m	$hkl, \bar{h}kl$ with $k+\ell = 2n$		C+E	–	1	$\frac{1}{2}$	$\frac{1}{2}$
13 P2/c	2/m	$hkl, \bar{h}kl$	$\ell = 2n$ $\ell = 2n+1$	C+E D+F	– –	$\frac{1}{2}$	$\frac{1}{2}$	1
13A P2/a	2/m	$hkl, \bar{h}kl$	$h = 2n$ $h = 2n+1$	C+E D+F	– –	1	$\frac{1}{2}$	$\frac{1}{2}$
13N P2/n	2/m	$hkl, \bar{h}kl$	$h+\ell = 2n$ $h+\ell = 2n+1$	C+E D+F	– –	$\frac{1}{2}$	1	1
14 $P2_1/c$	2/m	$hkl, \bar{h}kl$	$k+\ell = 2n$ $k+\ell = 2n+1$	C+E D+F	– –	1	$\frac{1}{2}$	1
14A $P2_1/a$	2/m	$hkl, \bar{h}kl$	$h+k = 2n$ $h+k = 2n+1$	C+E D+F	– –	1	$\frac{1}{2}$	1
14N $P2_1/n$	2/m	$hkl, \bar{h}kl$	$h+k+\ell = 2n$ $h+k+\ell = 2n+1$	C+E D+F	– –	1	$\frac{1}{2}$	1
15 C2/c	2/m	$hkl, \bar{h}kl$ with $h+k = 2n$	$\ell = 2n$ $\ell = 2n+1$	C+E D+F	– –	$\frac{1}{2}$	$\frac{1}{2}$	1
15A A2/a	2/m	$hkl, \bar{h}kl$ with $k+\ell = 2n$	$h = 2n$ $h = 2n+1$	C+E D+F	– –	1	$\frac{1}{2}$	$\frac{1}{2}$
16 P222	mmm	hkl		C	K	$\frac{1}{2}$	$\frac{1}{2}$	1
17 $P222_1$	mmm	hkl	$\ell = 2n$ $\ell = 2n+1$	C F	K M	$\frac{1}{2}$	$\frac{1}{2}$	1
18 $P2_12_12$	mmm	hkl	$h+k = 2n$ $h+k = 2n+1$	C D	K L	$\frac{1}{2}$	$\frac{1}{2}$	1
19 $P2_12_12_1$	mmm	hkl	$h+k = 2n, k+\ell = 2n$ $h+k = 2n, k+\ell = 2n+1$ $h+k = 2n+1, k+\ell = 2n$ $h+k = 2n+1, k+\ell = 2n+1$	C F E D	K M N L	$\frac{1}{2}$	$\frac{1}{2}$	1
20 $C222_1$	mmm	hkl with $h+k = 2n$	$\ell = 2n$ $\ell = 2n+1$	C F	K M	$\frac{1}{2}$	$\frac{1}{2}$	1
21 C222	mmm	hkl with $h+k = 2n$		C	K	$\frac{1}{2}$	$\frac{1}{2}$	1
22 F222	mmm	hkl with unmixed indices		C	K	$\frac{1}{2}$	$\frac{1}{2}$	1
23 I222	mmm	hkl with $h+k+\ell = 2n$		C	K	$\frac{1}{2}$	$\frac{1}{2}$	1
24 $I2_12_12_1$	mmm	hkl with $h+k+\ell = 2n$	$h = 2n, k = 2n, \ell = 2n$ $h = 2n, k = 2n+1,$ $\ell = 2n+1$ $h = 2n+1, k = 2n,$ $\ell = 2n+1$ $h = 2n+1, k = 2n+1,$ $\ell = 2n$	C E D F	K N L M	$\frac{1}{2}$	$\frac{1}{2}$	1
25 Pmm2	mmm	hkl		C	L	$\frac{1}{2}$	$\frac{1}{2}$	1
26 $Pmc2_1$	mmm	hkl	$\ell = 2n$ $\ell = 2n+1$	C F	L N	$\frac{1}{2}$	$\frac{1}{2}$	1
27 Pcc2	mmm	hkl	$\ell = 2n$ $\ell = 2n+1$	C D	L K	$\frac{1}{2}$	$\frac{1}{2}$	1
28 Pma2	mmm	hkl	$h = 2n$ $h = 2n+1$	C D	L K	$\frac{1}{2}$	1	1
29 $Pca2_1$	mmm	hkl	$h = 2n, \ell = 2n$ $h = 2n, \ell = 2n+1$ $h = 2n+1, \ell = 2n$ $h = 2n+1, \ell = 2n+1$	C E D F	L M K N	$\frac{1}{2}$	1	1
30 Pnc2	mmm	hkl	$k+\ell = 2n$ $k+\ell = 2n+1$	C D	L K	$\frac{1}{2}$	1	$\frac{1}{2}$
31 $Pmn2_1$	mmm	hkl	$h+\ell = 2n$ $h+\ell = 2n+1$	C F	L N	$\frac{1}{2}$	$\frac{1}{2}$	1
32 Pba2	mmm	hkl	$h+k = 2n$ $h+k = 2n+1$	C D	L K	$\frac{1}{2}$	1	1
33 $Pna2_1$	mmm	hkl	$h+k = 2n, \ell = 2n$ $h+k = 2n, \ell = 2n+1$ $h+k = 2n+1, \ell = 2n$ $h+k = 2n+1, \ell = 2n+1$	C E D F	L M K N	$\frac{1}{2}$	1	1
34 Pnn2	mmm	hkl	$h+k+\ell = 2n$ $h+k+\ell = 2n+1$	C D	L K	$\frac{1}{2}$	1	1
35 Cmm2	mmm	hkl with $h+k = 2n$		C	L	$\frac{1}{2}$	$\frac{1}{2}$	1
36 $CmC2_1$	mmm	hkl with $h+k = 2n$	$\ell = 2n$ $\ell = 2n+1$	C F	L N	$\frac{1}{2}$	$\frac{1}{2}$	1
37 Ccc2	mmm	hkl with $h+k = 2n$	$\ell = 2n$ $\ell = 2n+1$	C D	L K	$\frac{1}{2}$	$\frac{1}{2}$	1
38 Amm2	mmm	hkl with $k+\ell = 2n$		C	L	$\frac{1}{2}$	$\frac{1}{2}$	1
39 Abm2	mmm	hkl with $k+\ell = 2n$	$k = 2n$ $k = 2n+1$	C D	L K	$\frac{1}{2}$	$\frac{1}{2}$	1
40 Ama2	mmm	hkl with $k+\ell = 2n$	$h = 2n$ $h = 2n+1$	C D	L K	$\frac{1}{2}$	$\frac{1}{2}$	1
41 Aba2	mmm	hkl with $k+\ell = 2n$	$h+k = 2n$ $h+k = 2n+1$	C D	L K	$\frac{1}{2}$	$\frac{1}{2}$	1
42 Fmm2	mmm	hkl with unmixed indices		C	L	$\frac{1}{2}$	$\frac{1}{2}$	$\frac{1}{2}$
43 Fdd2	mmm	hkl with unmixed indices	$h+k+\ell = 4n$ $h+k+\ell = 4n+1$ $h+k+\ell = 4n+2$ $h+k+\ell = 4n+3$	C $\frac{C+D+K+P}{2}$ D $\frac{C+D+O+L}{2}$	L $\frac{C+H+K+L}{2}$ K $\frac{G+D+K+L}{2}$	$\frac{1}{2}$	$\frac{1}{2}$	1
44 Imm2	mmm	hkl with $h+k+\ell = 2n$		C	L	$\frac{1}{2}$	$\frac{1}{2}$	1
45 Iba2	mmm	hkl with $h+k+\ell = 2n$	$\ell = 2n$ $\ell = 2n+1$	C D	L K	$\frac{1}{2}$	$\frac{1}{2}$	1

Table 2. Fourier expressions for different space groups.

Space Group	Laue Group	Data Required	Parity Tests	A(hkℓ) Factor	B(hkℓ) Factor	Bounds x	Bounds y	Bounds z
46 Iam2	mmm	hkℓ with h+k+ℓ = 2n	h = 2n	C	L	¼	1	¼
			h = 2n+1	D	K			
47 Pmmm	mmm	hkℓ		C	–	¼	¼	¼
48 Pnnn	mmm	hkℓ	h+k = 2n, k+ℓ = 2n	C	–	$-\frac{1}{4}$ to ¼	1	¼
			h+k = 2n, k+ℓ = 2n+1	D	–			
			h+k = 2n+1, k+ℓ = 2n	F	–			
			h+k = 2n+1, k+ℓ = 2n+1	E	–			
49 Pccm	mmm	hkℓ	ℓ = 2n	C	–	¼	¼	¼
			ℓ = 2n+1	D	–			
50 Pban	mmm	hkℓ	h = 2n, k = 2n	C	–	¼	1	¼
			h = 2n, k = 2n+1	E	–			
			h = 2n+1, k = 2n	F	–			
			h = 2n+1, k = 2n+1	D	–			
51 Pmma	mmm	hkℓ	h = 2n	C	–	¼	¼	1
			h = 2n+1	E	–			
52 Pnna	mmm	hkℓ	h = 2n, k+ℓ = 2n	C	–	¼	¼	1
			h = 2n, k+ℓ = 2n+1	D	–			
			h = 2n+1, k+ℓ = 2n	F	–			
			h = 2n+1, k+ℓ = 2n+1	E	–			
53 Pmna	mmm	hkℓ	h+ℓ = 2n	C	–	¼	¼	1
			h+ℓ = 2n+1	F	–			
54 Pcca	mmm	hkℓ	h = 2n, ℓ = 2n	C	–	¼	¼	1
			h = 2n, ℓ = 2n+1	D	–			
			h = 2n+1, ℓ = 2n	E	–			
			h = 2n+1, ℓ = 2n+1	F	–			
55 Pbam	mmm	hkℓ	h+k = 2n	C	–	¼	1	¼
			h+k = 2n+1	D	–			
56 Pccn	mmm	hkℓ	h+k = 2n, h+ℓ = 2n	C	–	¼	1	¼
			h+k = 2n, h+ℓ = 2n+1	D	–			
			h+k = 2n+1, h+ℓ = 2n	F	–			
			h+k = 2n+1, h+ℓ = 2n+1	E	–			
57 Pbcm	mmm	hkℓ	k = 2n, ℓ = 2n	C	–	¼	1	¼
			k = 2n, ℓ = 2n+1	F	–			
			k = 2n+1, ℓ = 2n	D	–			
			k = 2n+1, ℓ = 2n+1	E	–			
58 Pnnm	mmm	hkℓ	h+k+ℓ = 2n	C	–	¼	1	¼
			h+k+ℓ = 2n+1	D	–			
59 Pmmn	mmm	hkℓ	h = 2n, k = 2n	C	–	$-\frac{1}{4}$ to ¼	$-\frac{1}{4}$ to ¼	¼
			h = 2n, k = 2n+1	F	–			
			h = 2n+1, k = 2n	E	–			
			h = 2n+1, k = 2n+1	D	–			
60 Pbcn	mmm	hkℓ	h+k = 2n, ℓ = 2n	C	–	¼	¼	1
			h+k = 2n, ℓ = 2n+1	F	–			
			h+k = 2n+1, ℓ = 2n	E	–			
			h+k = 2n+1, ℓ = 2n+1	D	–			
61 Pbca	mmm	hkℓ	h+k = 2n, k+ℓ = 2n	C	–	¼	¼	¼
			h+k = 2n, k+ℓ = 2n+1	F	–			
			h+k = 2n+1, k+ℓ = 2n	E	–			
			h+k = 2n+1, k+ℓ = 2n+1	D	–			
62 Pnma	mmm	hkℓ	h+ℓ = 2n, k = 2n	C	–	¼	¼	1
			h+ℓ = 2n, k = 2n+1	D	–			
			h+ℓ = 2n+1, k = 2n	E	–			
			h+ℓ = 2n+1, k = 2n+1	F	–			
63 Cmcm	mmm	hkℓ with h+k = 2n	ℓ = 2n	C	–	¼	1	¼
			ℓ = 2n+1	F	–			
64 Cmca	mmm	hkℓ with h+k = 2n	k+ℓ = 2n	C	–	¼	1	¼
			k+ℓ = 2n+1	F	–			
65 Cmmm	mmm	hkℓ with h+k = 2n		C	–	¼	¼	¼
66 Cccm	mmm	hkℓ with h+k = 2n	ℓ = 2n	C	–	¼	¼	¼
			ℓ = 2n+1	D	–			
67 Cmma	mmm	hkℓ with h+k = 2n	h = 2n	C	–	¼	¼	1
			h = 2n+1	F	–			
68 Ccca	mmm	hkℓ with h+k = 2n	k = 2n, ℓ = 2n	C	–	¼	¼	1
			k = 2n, ℓ = 2n+1	D	–			
			k = 2n+1, ℓ = 2n	E	–			
			k = 2n+1, ℓ = 2n+1	F	–			
69 Fmmm	mmm	hkℓ with unmixed indices		C	–	¼	¼	¼
70 Fddd	mmm	hkℓ with unmixed	h+k: 4n; k+ℓ: 4n; ℓ+h: 4n	C	–	¼	$-\frac{1}{4}$ to ¼	1
			4n; 4n+2; 4n+2	D	–			
			4n+2; 4n; 4n+2	F	–			
			4n+2; 4n+2; 4n	E	–			
			4n; 4n; 4n+2	$\frac{C+D+I+F}{2}$	–			
			4n; 4n+2; 4n	$\frac{C+D+E+J}{2}$	–			
			4n+2; 4n; 4n	$\frac{C+H+E+F}{2}$	–			
			4n+2; 4n; 4n+2	$\frac{G+D+E+F}{2}$	–			
71 Immm	mmm	hkℓ with h+k+ℓ = 2n		C	–	¼	¼	¼
72 Ibam	mmm	hkℓ with	ℓ = 2n	C	–	¼	¼	¼
		h+k+ℓ = 2n	ℓ = 2n+1	D	–			
73 Ibca	mmm	hkℓ with	h = 2n, k = 2n	C	–	¼	¼	¼
		h+k+ℓ = 2n	h = 2n, k = 2n+1	E	–			
			h = 2n+1, k = 2n	D	–			
			h = 2n+1, k = 2n+1	F	–			
74 Imma	mmm	hkℓ with	k = 2n	C	–	¼	¼	1
		h+k+ℓ = 2n	k = 2n+1	F	–			
75 P4	4/m	hkℓ & $\bar{h}\bar{k}\ell$*		C+D	K+L	¼	¼	1
76 $P4_1$	4/m	hkℓ & $\bar{h}\bar{k}\ell$*	ℓ = 2n	C+D	K+L	1	1	¼
			ℓ = 2n+1	E+F	M+N			
77 $P4_2$	4/m	hkℓ & $\bar{h}\bar{k}\ell$*		C+D	K+L	1	½	½
78 $P4_3$	4/m	hkℓ & $\bar{h}\bar{k}\ell$*	ℓ = 2n	C+D	K+L	1	1	¼
			ℓ = 2n+1	E+F	M+N			
79 I4	4/m	hkℓ & $\bar{h}\bar{k}\ell$* with h+k+ℓ = 2n		C+D	K+L	½	½	½
80 $I4_1$	4/m	hkℓ & $\bar{h}\bar{k}\ell$* with h+k+ℓ = 2n		C+D	K+L	½	1	¼
81 $P\bar{4}$	4/m	hkℓ & $\bar{h}\bar{k}\ell$*		C+D	K+L	½	1	½
82 $I\bar{4}$	4/m	hkℓ & $\bar{h}\bar{k}\ell$* with h+k+ℓ = 2n		C+D	K+L	½	½	½
83 P4/m	4/m	hkℓ & $\bar{h}\bar{k}\ell$*		C+D	–	½	½	½
84 $P4_2/m$	4/m	hkℓ & $\bar{h}\bar{k}\ell$*		C+D	–	½	½	½
85 P4/n	4/m	hkℓ & $\bar{h}\bar{k}\ell$*	h+k = 2n	C+D	–	½	1	½
			h+k = 2n+1	E+F	–			
86 $P4_2/n$	4/m	hkℓ & $\bar{h}\bar{k}\ell$*	h+k = 2n	C+D	–	$-\frac{1}{4}$ to ¼	1	¼
			h+k = 2n+1	E+F	–			
87 I4/m	4/m	hkℓ & $\bar{h}\bar{k}\ell$* with h+k+ℓ = 2n		C+D	–	½	½	½
88 $I4_1/a$	4/m	hkℓ & $\bar{h}\bar{k}\ell$*	k = 2n	C+D	–	½	$-\frac{1}{4}$ to ¼	½
			k = 2n+1	E+F	–			
89 P422	4/mmm	hkℓ*		C	K	½	½	½
90 $P42_12$	4/mmm	hkℓ*	h+k = 2n	C	K	½	½	½
			h+k = 2n+1	D	L			

Table 2 (continued)

Space Group		Laue Group	Data Required	Parity Tests	A(hkℓ) Factor	B(hkℓ) Factor	Bounds x	Bounds y	Bounds z
91	$P4_122$	4/mmm	$hk\ell^*$	$\ell = 2n$	C	K	$\frac{1}{4}$	1	$\frac{1}{4}$
				$\ell = 2n+1$	$\frac{C+D+E+J}{2}$	$\frac{L+K+Q+N}{2}$			
92	$P4_12_12$	4/mmm	$hk\ell^*$	$2h+2k+\ell = 4n$	C	K	$\frac{1}{4}$	$\frac{1}{4}$	$\frac{1}{4}$
				$2h+2k+\ell = 4n+1$	$\frac{E+F+M+R}{2}$	$\frac{E+J+M+N}{2}$			
				$2h+2k+\ell = 4n+2$	D	L			
				$2h+2k+\ell = 4n+3$	$\frac{E+F+Q+N}{2}$	$\frac{I+F+M+N}{2}$			
93	$P4_222$	4/mmm	$hk\ell^*$		C	K	$\frac{1}{4}$	1	$\frac{1}{4}$
94	$P4_12_12$	4/mmm	$hk\ell^*$	$h+k+\ell = 2n$	C	K	$\frac{1}{4}$	1	$\frac{1}{4}$
				$h+k+\ell = 2n+1$	D	L			
95	$P4_222$	4/mmm	$hk\ell^*$	$\ell = 2n$	C	K	1	1	$\frac{1}{4}$
				$\ell = 2n+1$	$\frac{C+D+E+J}{2}$	$\frac{L+K+Q+N}{2}$			
96	$P4_12_12$	4/mmm	$hk\ell^*$	$2h+2k+\ell = 4n$	C	K	$\frac{1}{4}$	$\frac{1}{4}$	$\frac{1}{4}$
				$2h+2k+\ell = 4n+1$	$\frac{E+F+Q+N}{2}$	$\frac{I+F+M+N}{2}$			
				$2h+2k+\ell = 4n+2$	D	L			
				$2h+2k+\ell = 4n+3$	$\frac{E+F+M+R}{2}$	$\frac{E+J+M+N}{2}$			
97	I422	4/mmm	$hk\ell^*$ with $h+k+\ell = 2n$		C	K	$\frac{1}{4}$	$\frac{1}{4}$	$\frac{1}{4}$
98	$I4_122$	4/mmm	$hk\ell^*$ with $h+k+\ell = 2n$	$2k+\ell = 4n$	C	K	$\frac{1}{4}$	1	$\frac{1}{8}$
				$2k+\ell = 4n+1$	$\frac{C+D+L+O}{2}$	$\frac{C+H+L+K}{2}$			
				$2k+\ell = 4n+2$	D	L			
				$2k+\ell = 4n+3$	$\frac{C+D+K+P}{2}$	$\frac{G+D+L+K}{2}$			
99	P4mm	4/mmm	$hk\ell^*$		C	L	$\frac{1}{4}$	$\frac{1}{4}$	1
100	P4bm	4/mmm	$hk\ell^*$	$h+k = 2n$	C	L	$\frac{1}{4}$	$\frac{1}{4}$	1
				$h+k = 2n+1$	D	K			
101	$P4_2cm$	4/mmm	$hk\ell^*$	$\ell = 2n$	C	L	$\frac{1}{4}$	1	$\frac{1}{4}$
				$\ell = 2n+1$	D	K			
102	$P4_2nm$	4/mmm	$hk\ell^*$	$h+k+\ell = 2n$	C	L	$\frac{1}{4}$	1	$\frac{1}{4}$
				$h+k+\ell = 2n+1$	D	K			
103	P4cc	4/mmm	$hk\ell^*$	$\ell = 2n$	C	L	$\frac{1}{4}$	$\frac{1}{4}$	$\frac{1}{4}$
				$\ell = 2n+1$	D	K			
104	P4nc	4/mmm	$hk\ell^*$	$h+k+\ell = 2n$	C	L	$\frac{1}{4}$	$\frac{1}{4}$	$\frac{1}{4}$
				$h+k+\ell = 2n+1$	D	K			
105	$P4_2mc$	4/mmm	$hk\ell^*$		C	L	$\frac{1}{4}$	$\frac{1}{4}$	$\frac{1}{4}$
106	$P4_2bc$	4/mmm	$hk\ell^*$	$h+k = 2n$	C	L	$\frac{1}{4}$	$\frac{1}{4}$	$\frac{1}{4}$
				$h+k = 2n+1$	D	K			
107	I4mm	4/mmm	$hk\ell^*$ with $h+k+\ell = 2n$		C	L	$\frac{1}{4}$	$\frac{1}{4}$	$\frac{1}{4}$
108	I4cm	4/mmm	$hk\ell^*$ with $h+k+\ell = 2n$	$\ell = 2n$	C	L	$\frac{1}{4}$	$\frac{1}{4}$	$\frac{1}{4}$
				$\ell = 2n+1$	D	K			
109	$I4_1md$	4/mmm	$hk\ell^*$ with $h+k+\ell = 2n$		C	L	$\frac{1}{4}$	$\frac{1}{4}$	$\frac{1}{4}$
110	$I4_1cd$	4/mmm	$hk\ell^*$ with $h+k+\ell = 2n$		C	L	$\frac{1}{4}$	$\frac{1}{4}$	$\frac{1}{4}$
					D	K			
111	$P\bar{4}2m$	4/mmm	$hk\ell^*$		C	K	$\frac{1}{4}$	1	$\frac{1}{4}$
112	$P\bar{4}2c$	4/mmm	$hk\ell^*$	$\ell = 2n$	C	K	$\frac{1}{4}$	$\frac{1}{4}$	$\frac{1}{4}$
				$\ell = 2n+1$	D	L			
113	$P\bar{4}2_1m$	4/mmm	$hk\ell^*$	$h+k = 2n$	C	K	$\frac{1}{4}$	1	$\frac{1}{4}$
				$h+k = 2n+1$	D	L			
114	$P\bar{4}2_1c$	4/mmm	$hk\ell^*$	$h+k+\ell = 2n$	C	K	$\frac{1}{4}$	$\frac{1}{4}$	$\frac{1}{4}$
				$h+k+\ell = 2n+1$	D	L			
115	$P\bar{4}m2$	4/mmm	$hk\ell^*$		C	L	$\frac{1}{4}$	$\frac{1}{4}$	$\frac{1}{4}$
116	$P\bar{4}c2$	4/mmm	$hk\ell^*$	$\ell = 2n$	C	L	$\frac{1}{4}$	1	$\frac{1}{4}$
				$\ell = 2n+1$	D	K			
117	$P\bar{4}b2$	4/mmm	$hk\ell^*$	$h+k = 2n$	C	L	$\frac{1}{4}$	$\frac{1}{4}$	$\frac{1}{4}$
				$h+k = 2n+1$	D	K			
118	$P\bar{4}n2$	4/mmm	$hk\ell^*$	$h+k+\ell = 2n$	C	L	$\frac{1}{4}$	1	$\frac{1}{4}$
				$h+k+\ell = 2n+1$	D	K			
119	$I\bar{4}m2$	4/mmm	$hk\ell^*$ with $h+k+\ell = 2n$		C	L	$\frac{1}{4}$	$\frac{1}{4}$	$\frac{1}{4}$
120	$I\bar{4}c2$	4/mmm	$hk\ell^*$ with $h+k+\ell = 2n$	$\ell = 2n$	C	L	$\frac{1}{4}$	$\frac{1}{4}$	$\frac{1}{4}$
				$\ell = 2n+1$	D	K			
121	$I\bar{4}2m$	4/mmm	$hk\ell^*$ with $h+k+\ell = 2n$		C	K	$\frac{1}{4}$	1	$\frac{1}{4}$
122	$I\bar{4}2d$	4/mmm	$hk\ell^*$ with $h+k+\ell = 2n$	$2h+\ell = 4n$	C	K	$\frac{1}{4}$	$\frac{1}{4}$	$\frac{1}{4}$
				$2h+\ell = 4n+1$	$\frac{C+D+K+P}{2}$	$\frac{G+D+L+K}{2}$			
				$2h+\ell = 4n+2$	D	L			
				$2h+\ell = 4n+3$	$\frac{C+D+L+O}{2}$	$\frac{C+H+L+K}{2}$			
123	P4/mmm	4/mmm	$hk\ell^*$		C	–	$\frac{1}{4}$	$\frac{1}{4}$	$\frac{1}{4}$
124	P4/mcc	4/mmm	$hk\ell^*$	$\ell = 2n$	C	–	$\frac{1}{4}$	$\frac{1}{4}$	$\frac{1}{4}$
				$\ell = 2n+1$	D	–			
125	P4/nbm	4/mmm	$hk\ell^*$	$h = 2n, k = 2n$	C	–	$\frac{1}{4}$	1	$\frac{1}{4}$
				$h = 2n, k = 2n+1$	E	–			
				$h = 2n+1, k = 2n$	F	–			
				$h = 2n+1, k = 2n+1$	D	–			
126	P4/nnc	4/mmm	$hk\ell^*$	$h+k = 2n, k+\ell = 2n$	C	–	$-\frac{1}{4}$ to $\frac{1}{4}$	$-\frac{1}{4}$ to $\frac{1}{4}$	$\frac{1}{4}$
				$h+k = 2n,$ $k+\ell = 2n+1$	D	–			
				$h+k = 2n+1,$ $k+\ell = 2n$	F	–			
				$h+k = 2n+1,$ $k+\ell = 2n+1$	E	–			
127	P4/mbm	4/mmm	$hk\ell^*$	$h+k = 2n$	C	–	$\frac{1}{4}$	$\frac{1}{4}$	$\frac{1}{4}$
				$h+k = 2n+1$	D	–			
128	P4/mnc	4/mmm	$hk\ell^*$	$h+k+\ell = 2n$	C	–	$\frac{1}{4}$	$\frac{1}{4}$	$\frac{1}{4}$
				$h+k+\ell = 2n+1$	D	–			
129	P4/nmm	4/mmm	$hk\ell^*$	$h = 2n, k = 2n$	C	–	$\frac{1}{4}$	1	$\frac{1}{4}$
				$h = 2n, k = 2n+1$	F	–			
				$h = 2n+1, k = 2n$	E	–			
				$h = 2n+1, k = 2n+1$	D	–			
130	P4/ncc	4/mmm	$hk\ell^*$	$h+k = 2n, k+\ell = 2n$	C	–	$\frac{1}{4}$	1	$\frac{1}{4}$
				$h+k = 2n,$ $k+\ell = 2n+1$	D	–			
				$h+k = 2n+1,$ $k+\ell = 2n$	E	–			
				$h+k = 2n+1,$ $k+\ell = 2n+1$	F	–			
131	$P4_2/mmc$	4/mmm	$hk\ell^*$		C	–	$\frac{1}{4}$	$\frac{1}{4}$	$\frac{1}{4}$
132	$P4_2/mcm$	4/mmm	$hk\ell^*$	$\ell = 2n$	C	–	$\frac{1}{4}$	$\frac{1}{4}$	$\frac{1}{4}$
				$\ell = 2n+1$	D	–			
133	$P4_2/nbc$	4/mmm	$hk\ell^*$	$h = 2n, k = 2n$	C	–	$\frac{1}{4}$	1	$\frac{1}{4}$
				$h = 2n, k = 2n+1$	E	–			
				$h = 2n+1, k = 2n$	F	–			
				$h = 2n+1, k = 2n+1$	D	–			
134	$P4_2/nnm$	4/mmm	$hk\ell^*$	$h+k = 2n, k+\ell = 2n$	C	–	$-\frac{1}{4}$ to $\frac{1}{4}$	1	$\frac{1}{4}$
				$h+k = 2n,$ $k+\ell = 2n+1$	D	–			
				$h+k = 2n+1,$ $k+\ell = 2n$	F	–			
				$h+k = 2n+1,$ $k+\ell = 2n+1$	E	–			
135	$P4_2/mbc$	4/mmm	$hk\ell^*$	$h+k = 2n$	C	–	$\frac{1}{4}$	$\frac{1}{4}$	$\frac{1}{4}$
				$h+k = 2n+1$	D	–			
136	P4/mam	4/mmm	$hk\ell^*$	$h+k+\ell = 2n$	C	–	$\frac{1}{4}$	1	$\frac{1}{4}$
				$h+k+\ell = 2n+1$	D	–			
137	$P4_2/amc$	4/mmm	$hk\ell^*$	$h = 2n, k = 2n$	C	–	$-\frac{1}{4}$ to $\frac{1}{4}$	$-\frac{1}{4}$ to $\frac{1}{4}$	$\frac{1}{4}$
				$h = 2n, k = 2n+1$	F	–			
				$h = 2n+1, k = 2n$	E	–			
				$h = 2n+1, k = 2n+1$	D	–			
138	$P4_2/ncm$	4/mmm	$hk\ell^*$	$h+k = 2n, k+\ell = 2n$	C	–	$\frac{1}{4}$	1	$\frac{1}{4}$
				$h+k = 2n,$ $k+\ell = 2n+1$	D	–			
				$h+k = 2n+1,$ $k+\ell = 2n$	E	–			
				$h+k = 2n+1,$ $k+\ell = 2n+1$	F	–			

Table 2 (continued)

Space Group	Laue Group	Data Required	Parity Tests	A(hkℓ) Factor	B(hkℓ) Factor	Bounds x	Bounds y	Bounds z
139 I4/mmm	4/mmm	hkℓ* with h+k+ℓ = 2n		C	–	¼	¼	¼
140 I4/mcm	4/mmm	hkℓ*	ℓ = 2n	C	–	¼	¼	¼
		with h+k+ℓ = 2n	ℓ = 2n+1	D	–			
141 $I4_1$/amd	4/mmm	hkℓ*	k = 2n	C	–	¼	¼	1
		with h+k+ℓ = 2n	k = 2n+1	F	–			
142 $I4_1$/acd	4/mmm	hkℓ*	h = 2n,k = 2n	C	–	¼	¼	1
		with h+k+ℓ = 2n	h = 2n,k = 2n+1	E	–			
			h = 2n+1,k = 2n	D	–			
			h = 2n+1,k = 2n+1	F	–			
195 P23	2/m$\bar{3}$	hkℓ*		C	K	¼	¼	1
196 F23	2/m$\bar{3}$	hkℓ* with unmixed indices		C	K	¼	¼	¼
197 I23	2/m$\bar{3}$	hkℓ* with h+k+ℓ = 2n		C	K	¼	¼	¼
198 $P2_13$	2/m$\bar{3}$	hkℓ*	h+k k+ℓ					
			2n 2n	C	K	¼	¼	1
			2n 2n+1	F	M			
			2n+1 2n	E	N			
			2n+1 2n+1	D	L			
199 $I2_13$	2/m$\bar{3}$	hkℓ* with h+k+ℓ = 2n	h = 2n,k = 2n	C	K	¼	¼	¼
			h = 2n+1,k = 2n+1	F	M			
			h = 2n,k = 2n+1	E	N			
			h = 2n+1,k = 2n	D	L			
200 Pm3	2/m$\bar{3}$	hkℓ*		C	–	¼	¼	¼
201 Pn3	2/m$\bar{3}$	hkℓ*	h+k k+ℓ					
			2n 2n	C	–	$-\frac{1}{8}$ to ⅛	$-\frac{1}{8}$ to ⅛	¼
			2n 2n+1	D	–			
			2n+1 2n	F	–			
			2n+1 2n+1	E	–			
202 Fm3	2/m$\bar{3}$	hkℓ* with unmixed indices		C	–	¼	¼	¼
203 Fd3	2/m$\bar{3}$	hkℓ* with unmixed indices	h+k k+ℓ ℓ+h					
			4n 4n 4n	C	–	⅛	$-\frac{1}{8}$ to ⅛	1
			4n 4n+2 4n+2	D	–			
			4n+2 4n 4n+2	F	–			
			4n+2 4n+2 4n	E	–			
			4n 4n 4n+2	$\frac{C+D+I+F}{2}$	–			
			4n 4n+2 4n	$\frac{C+D+E+J}{2}$	–			
			4n+2 4n 4n	$\frac{C+H+E+F}{2}$	–			
			4n+2 4n+2 4n+2	$\frac{G+D+E+F}{2}$	–			
204 Im3	2/m$\bar{3}$	hkℓ* with h+k+ℓ = 2n		C	–	¼	¼	¼
205 Pa3	2/m$\bar{3}$	hkℓ*	h+k k+ℓ					
			2n 2n	C	–	¼	¼	¼
			2n 2n+1	F	–			
			2n+1 2n	E	–			
			2n+1 2n+1	D	–			
206 Ia3	2/m$\bar{3}$	hkℓ* with h+k+ℓ = 2n	h k					
			2n 2n	C	–	¼	¼	¼
			2n+1 2n+1	F	–			
			2n 2n+1	E	–			
			2n+1 2n	D	–			
207 P432	m3m	hkℓ*		C	K	¼	¼	¼
208 $P4_232$	m3m	hkℓ*		C	K	¼	1	¼
209 F432	m3m	hkℓ* with unmixed indices		C	K	¼	¼	¼
210 $F4_132$	m3m	hkℓ* with unmixed indices		C	K	⅛	¼	1
211 I432	m3m	hkℓ* with h+k+ℓ = 2n		C	K	¼	¼	¼
212 $P4_332$	m3m	hkℓ*	h+k k+ℓ					
			2n 2n	C	K	$-\frac{1}{8}$ to ⅛	$-\frac{1}{8}$ to ⅛	1
			2n 2n+1	F	M			
			2n+1 2n	E	N			
			2n+1 2n+1	D	L			

Space Group	Laue Group	Data Required	Parity Tests	A(hkℓ) Factor	B(hkℓ) Factor	Bounds x	Bounds y	Bounds z
213 $P4_132$	m3m	hkℓ*	h+k k+ℓ					
			2n 2n	C	K	$-\frac{1}{8}$ to ⅛	$-\frac{1}{8}$ to ⅛	1
			2n 2n+1	F	M			
			2n+1 2n	E	N			
			2n+1 2n+1	D	L			
214 $I4_132$	m3m	hkℓ* with h+k+ℓ = 2n	h = 2n,k = 2n	C	K	⅛	⅛	1
			h = 2n,k = 2n+1	E	N			
			h = 2n+1,k = 2n	D	L			
			h = 2n+1,k = 2n+1	F	M			
215 P$\bar{4}$3m	m3m	hkℓ*		C	K	¼	¼	1
216 F$\bar{4}$3m	m3m	hkℓ* with unmixed indices		C	K	¼	¼	1
217 I$\bar{4}$3m	m3m	hkℓ* with h+k+ℓ = 2n		C	K	¼	¼	¼
218 P$\bar{4}$3n	m3m	hkℓ*		C	K	¼	¼	¼
219 F$\bar{4}$3c	m3m	hkℓ* with unmixed indices		C	K	¼	¼	¼
220 I$\bar{4}$3d	m3m	hkℓ* with h+k+ℓ = 2n	h+k k+ℓ					
			2n 2n	C	K	¼	¼	¼
			2n+1 2n	E	N			
			2n+1 2n+1	D	L			
			2n 2n+1	F	M			
221 Pm3m	m3m	hkℓ*		C	–	¼	¼	¼
222 Pn3n	m3m	hkℓ*	h+k k+ℓ					
			2n 2n	C	–	$-\frac{1}{8}$ to ⅛	$-\frac{1}{8}$ to ⅛	¼
			2n 2n+1	D	–			
			2n+1 2n	F	–			
			2n+1 2n+1	E	–			
223 Pm3n	m3m	hkℓ*		C	–	¼	¼	¼
224 Pn3m	m3m	hkℓ*	h+k k+ℓ					
			2n 2n	C	–	$-\frac{1}{8}$ to ⅛	1	¼
			2n 2n+1	D	–			
			2n+1 2n	F	–			
			2n+1 2n+1	E	–			
225 Fm3m	m3m	hkℓ* with unmixed indices		C	–	¼	¼	¼
226 Fm3c	m3m	hkℓ* with unmixed indices		C	–	¼	¼	¼
227 Fd3m	m3m	hkℓ* with unmixed indices	h+k k+ℓ ℓ+h					
			4n 4n 4n	C	–	⅛	¼	1
			4n 4n+2 4n+2	D	–			
			4n+2 4n 4n+2	F	–			
			4n+2 4n+2 4n	E	–			
			4n 4n 4n+2	$\frac{C+D+I+F}{2}$	–			
			4n 4n+2 4n	$\frac{C+D+E+J}{2}$	–			
			4n+2 4n 4n	$\frac{C+H+E+F}{2}$	–			
			4n+2 4n+2 4n+2	$\frac{G+D+E+F}{2}$	–			
228 Fd3c	m3m	hkℓ* with unmixed indices	h+k k+ℓ ℓ+h					
			4n 4n 4n	C	–	⅛	¼	¼
			4n 4n+2 4n+2	D	–			
			4n+2 4n 4n+2	F	–			
			4n+2 4n+2 4n	E	–			
			4n 4n 4n+2	$\frac{C+D+I+F}{2}$	–			
			4n 4n+2 4n	$\frac{C+D+E+J}{2}$	–			
			4n+2 4n 4n	$\frac{C+H+E+F}{2}$	–			
			4n+2 4n+2 4n+2	$\frac{G+D+E+F}{2}$	–			
229 Im3m	m3m	hkℓ* with h+k+ℓ = 2n		C	–	¼	¼	¼
230 Ia3d	m3m	hkℓ* with h+k+ℓ = 2n	h = 2n,k = 2n	C	–	¼	¼	¼
			h = 2n,k = 2n+1	E	–			
			h = 2n+1,k = 2n	D	–			
			h = 2n+1,k = 2n+1	F	–			

Table 2 (continued)

Table 3. Generation of equivalent reflections, Laue group 4/m.

(A and B denote the structure factor components of a reflection with indices h, k, ℓ.)

Space Group	Parity	$A_{\bar{k}h\ell}$	$B_{\bar{k}h\ell}$
75		A	B
76	$\ell = 4n$	A	B
	$\ell = 4n + 1$	-B	A
	$\ell = 4n + 2$	-A	-B
	$\ell = 4n + 3$	B	-A
77	$\ell = 2n$	A	B
	$\ell = 2n + 1$	-A	-B
78	$\ell = 4n$	A	B
	$\ell = 4n + 1$	B	-A
	$\ell = 4n + 2$	-A	-B
	$\ell = 4n + 3$	-B	A
79		A	B
80	$2h + \ell = 4n$	A	B
	$2h + \ell = 4n + 1$	-B	A
	$2h + \ell = 4n + 2$	-A	-B
	$2h + \ell = 4n + 3$	B	-A
81		A	-B
82		A	-B
83		A	—
84	$\ell = 2n$	A	—
	$\ell = 2n + 1$	-A	—
85	$k = 2n$	A	—
	$k = 2n + 1$	-A	—
86	$h + \ell = 2n$	A	—
	$h + \ell = 2n + 1$	-A	—
87		A	—
88	$h + k + \ell = 4n$	A	—
	$h + k + \ell = 4n + 2$	-A	—

positive. A reflection of the type $kh\ell$ may be generated in a space-group-specific manner from a reflection of the type $hk\ell$ as shown in Table 4.

c) Laue group $2/m\bar{3}$.

From an asymmetric unit of 1/24 of the sphere of reflection — for example, all reflections with all indices positive and with $h \leqq \ell$, and $k \leqq \ell$ — all reflections with all indices positive must be generated. A study of cubic symmetry shows that all cubic space groups possess a 3-fold axis (not screw) through the origin. This results in the following relations which allow easy generation of the required additional reflections

$$A_{hk\ell} = A_{k\ell h} = A_{\ell hk} ,$$

and

$$B_{hk\ell} = B_{k\ell h} = B_{\ell hk} .$$

d) Laue group m3m.

The asymmetric unit here includes 1/48 of the sphere of reflection, for example, all reflections with all indices positive and $h \leqq k \leqq \ell$; again all reflections with all indices positive must be generated. Equivalent reflections fall into two groups

$$A_{hk\ell} = A_{k\ell h} = A_{\ell hk} \qquad A_{h\ell k} = A_{\ell kh} = A_{kh\ell}$$

and

$$B_{hk\ell} = B_{k\ell h} = B_{\ell hk} \qquad B_{h\ell k} = B_{\ell kh} = B_{kh\ell} .$$

Group 1 Group 2

Table 4. Generation of equivalent reflections, Laue group 4/mmm.

(A and B denote the structure factor components of a reflection with indices h, k, ℓ.)

Space Group	Parity	$A_{kh\ell}$	$B_{kh\ell}$
89		A	-B
90		A	-B
91	$\ell = 4n$	A	-B
	$\ell = 4n + 1$	B	A
	$\ell = 4n + 2$	-A	B
	$\ell = 4n + 3$	-B	-A
92	$\ell = 2n$	A	-B
	$\ell = 2n + 1$	-A	B
93	$\ell = 2n$	A	-B
	$\ell = 2n + 1$	-A	B
94		A	-B
95	$\ell = 4n$	A	-B
	$\ell = 4n + 1$	-B	-A
	$\ell = 4n + 2$	-A	B
	$\ell = 4n + 3$	B	A
96	$\ell = 2n$	A	-B
	$\ell = 2n + 1$	-A	B
97		A	-B
98		A	-B
99		A	B
100	$h + k = 2n$	A	B
	$h + k = 2n + 1$	-A	-B
101		A	B
102		A	B
103	$\ell = 2n$	A	B
	$\ell = 2n + 1$	-A	-B
104	$h + k + \ell = 2n$	A	B
	$h + k + \ell = 2n + 1$	-A	-B
105	$\ell = 2n$	A	B
	$\ell = 2n + 1$	-A	-B
106	$h + k + \ell = 2n$	A	B
	$h + k + \ell = 2n + 1$	-A	-B

Table 4 (continued)

Space Group	Parity	$A_{kh\ell}$	$B_{kh\ell}$
107		A	B
108	$\ell = 2n$	A	B
	$\ell = 2n + 1$	-A	-B
109	$2k + \ell = 4n$	A	B
	$2k + \ell = 4n + 1$	B	-A
	$2k + \ell = 4n + 2$	-A	-B
	$2k + \ell = 4n + 3$	-B	A
110	$2k + \ell = 4n$	A	B
	$2k + \ell = 4n + 1$	-B	A
	$2k + \ell = 4n + 2$	-A	-B
	$2k + \ell = 4n + 3$	B	-A
111		A	B
112	$\ell = 2n$	A	B
	$\ell = 2n + 1$	-A	-B
113	$h + k = 2n$	A	B
	$h + k = 2n + 1$	-A	-B
114	$h + k + \ell = 2n$	A	B
	$h + k + \ell = 2n + 1$	-A	-B
115		A	-B
116	$\ell = 2n$	A	-B
	$\ell = 2n + 1$	-A	B
117	$h + k = 2n$	A	-B
	$h + k = 2n + 1$	-A	B
118	$h + k + \ell = 2n$	A	-B
	$h + k + \ell = 2n + 1$	-A	B
119		A	-B
120	$\ell = 2n$	A	-B
	$\ell = 2n + 1$	-A	B
121		A	B
122	$2h + \ell = 4n$	A	B
	$2h + \ell = 4n + 1$	-B	A
	$2h + \ell = 4n + 2$	-A	-B
	$2h + \ell = 4n + 3$	B	-A
123		A	—
124	$\ell = 2n$	A	—
	$\ell = 2n + 1$	-A	—

Table 4 (continued)

Space Group	Parity	$A_{kh\ell}$	$B_{kh\ell}$
125	$h + k = 2n$	A	—
	$h + k = 2n + 1$	-A	—
126	$h + k + \ell = 2n$	A	—
	$h + k + \ell = 2n + 1$	-A	—
127	$h + k = 2n$	A	—
	$h + k = 2n + 1$	-A	—
128	$h + k + \ell = 2n$	A	—
	$h + k + \ell = 2n + 1$	-A	—
129		A	—
130	$\ell = 2n$	A	—
	$\ell = 2n + 1$	-A	—
131	$\ell = 2n$	A	—
	$\ell = 2n + 1$	-A	—
132		A	—
133	$h + k + \ell = 2n$	A	—
	$h + k + \ell = 2n + 1$	-A	—
134	$h + k = 2n$	A	—
	$h + k = 2n + 1$	-A	—
135	$h + k + \ell = 2n$	A	—
	$h + k + \ell = 2n + 1$	-A	—
136		A	—
137	$\ell = 2n$	A	—
	$\ell = 2n + 1$	-A	—
138		A	—
139		A	—
140	$\ell = 2n$	A	—
	$\ell = 2n + 1$	-A	—
141	$-h - k + \ell = 4n$	A	—
	$-h - k + \ell = 4n + 2$	-A	—
142	$h + k + \ell = 4n$	A	—
	$h + k + \ell = 4n + 2$	-A	—

A reflection in group 2 may be generated from a reflection of group 1 in a space-group-specific manner as shown in Table 5. This allows 5 additional reflections to be generated from each reflection of the asymmetric unit.

vi) Calculation of Patterson maps.

Patterson maps may be calculated by simply replacing structure factors by $|F_{obs}|^2$ and doing an electron-density-type map in the correct space group. The symbol for the Patterson group corresponding to a given space group may be obtained easily by placing either P, I, F, A, B, or C, depending upon the lattice of the space groups, in front of the symbol of the Laue group (for Laue group $2/m\bar{3}$, replace the Laue group symbol by m3). Therefore Patterson maps may be provided for simply by changing the space group number before initializing the trigonometric expressions.

Table 5. Generation of equivalent reflections, Laue group m3m.

(A and B denote the structure factor components of a reflection with indices h, k, ℓ.)

Space Group	Parity	A(Group 2)	B(Group 2)
207		A	-B
208	$h + k + \ell = 2n$	A	-B
	$h + k + \ell = 2n + 1$	-A	B
209		A	-B
210	$h + k + \ell = 4n$	A	-B
	$h + k + \ell = 4n + 1$	B	A
	$h + k + \ell = 4n + 2$	-A	B
	$h + k + \ell = 4n + 3$	-B	-A
211		A	-B
212	$h + k + \ell = 4n$	A	-B
	$h + k + \ell = 4n + 1$	B	A
	$h + k + \ell = 4n + 2$	-A	B
	$h + k + \ell = 4n + 3$	-B	-A
213	$h + k + \ell = 4n$	A	-B
	$h + k + \ell = 4n + 1$	-B	-A
	$h + k + \ell = 4n + 2$	-A	B
	$h + k + \ell = 4n + 3$	B	A
214	$h + k + \ell = 4n$	A	-B
	$h + k + \ell = 4n + 2$	-A	B
215		A	B
216		A	B
217		A	B
218	$h + k + \ell = 2n$	A	B
	$h + k + \ell = 2n + 1$	-A	-B
219	$h + k + \ell = 2n$	A	B
	$h + k + \ell = 2n + 1$	-A	-B
220	$h + k + \ell = 4n$	A	B
	$h + k + \ell = 4n + 2$	-A	-B

Table 5 (continued)

Space Group	Parity	$A_{(Group\ 2)}$	$B_{(Group\ 2)}$
221		A	—
222	$h + k + \ell = 2n$	A	—
	$h + k + \ell = 2n + 1$	-A	—
223	$h + k + \ell = 2n$	A	—
	$h + k + \ell = 2n + 1$	-A	—
224		A	—
225		A	—
226	$h + k + \ell = 2n$	A	—
	$h + k + \ell = 2n + 1$	-A	—
227		A	—
228	$h + k + \ell = 2n$	A	—
	$h + k + \ell = 2n + 1$	-A	—
229		A	—
230	$h + k + \ell = 4n$	A	—
	$h + k + \ell = 4n + 2$	-A	—

CALCULATION OF SETTINGS FOR AN EULERIAN-CRADLE-TYPE DIFFRACTOMETER

A crystal is correctly positioned for counting a reflection with indices h, k, and ℓ when the corresponding reciprocal lattice vector, $\underline{d}^* = h\underline{a}^* + k\underline{b}^* + \ell\underline{c}^*$, bisects the angle between the incident and diffracted x-ray beams when these beams form an angle of 2θ with one another. The angle θ is calculated simply from the Bragg equation. On an Eulerian cradle diffractometer two other angles, χ and ϕ, are needed to effect this arrangement. We will assume a crystal oriented with the $\underline{b}$ axis perpendicular to the plane of the incident and diffracted beams when χ and ϕ are set at zero. The $\underline{a}^*$, $\underline{c}^*$ plane then coincides with the plane of these beams. χ is then the angle between $\underline{d}^*$ and its projection onto the $\underline{a}^*$, $\underline{c}^*$ plane. ϕ is the angle between the projection of $\underline{d}^*$ onto the $\underline{a}^*$, $\underline{c}^*$ plane and the $\underline{c}^*$ axis, from $\underline{c}^*$ toward $\underline{a}^*$ being the positive angle.

The situation is diagrammed in Figure 4. One easily sees that $\ell^* = kb^* \cos \rho = \frac{k}{b}$. Then

$$\sin \chi = \frac{\ell^*}{d^*} = \frac{k}{2b \frac{\sin \theta}{\lambda}} . \qquad (1)$$

Next by the law of sines,

$$\sin \phi = \frac{G \sin(180° - \beta^*)}{d^* \cos \chi} = \frac{(ha^* + k\Delta G)(\sin \beta^*)}{2(\frac{\sin \theta}{\lambda})\cos \chi} , \qquad (2)$$

where ΔG is the displacement along $\underline{a}^*$ when the $k = 1$ layer of

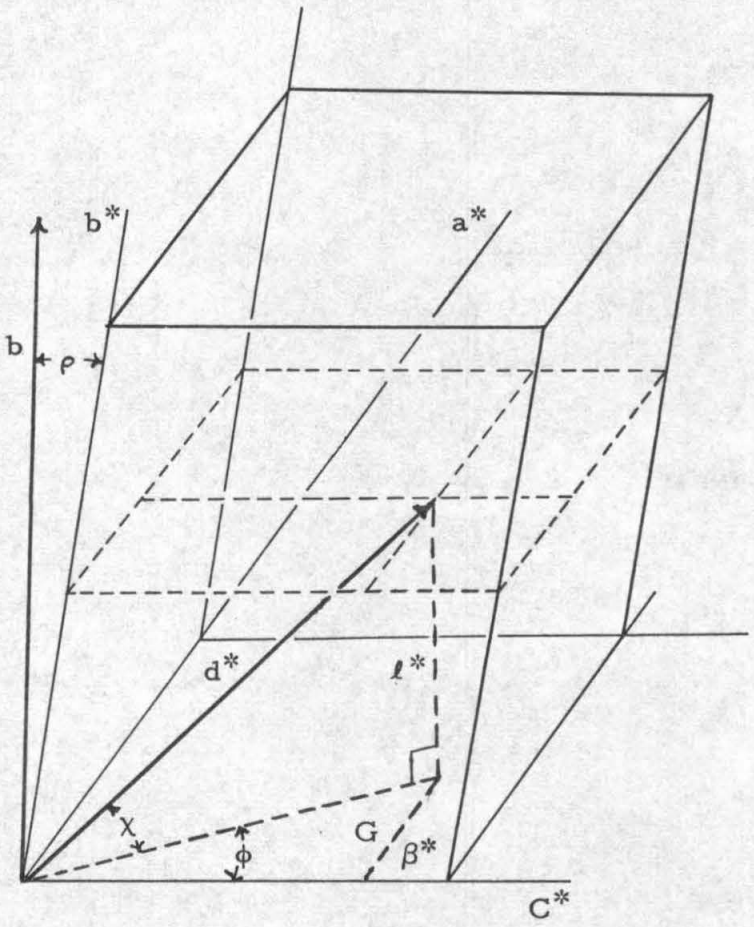

Figure 4. Definition of vectors and angles.

reciprocal space is projected on the k = 0 layer. It can be shown either by spherical trigonometry or by vector analysis that $\Delta G = \frac{-\cos\gamma}{\sin\beta^* \sin\gamma\, b}$. Substitution in 2 gives

$$\sin\phi = \frac{\left[ha^* + k\left(\frac{-\cos\gamma}{\sin\beta^* \sin\gamma\, b}\right)\right]\sin\beta^*}{2\left(\frac{\sin\theta}{\lambda}\right)\cos\chi} \quad .$$

Since $a^* = \frac{1}{a \sin\beta^* \sin\gamma}$ and $\cos\chi = \sqrt{1 - \frac{k^2}{4b^2\left(\frac{\sin^2\theta}{\lambda^2}\right)}}$,

the above reduces to

$$\sin\phi = \frac{h\left(\frac{1}{a\sin\gamma}\right) - k\left(\frac{\cos\gamma}{b\sin\gamma}\right)}{\sqrt{4\frac{\sin^2\theta}{\lambda^2} - \frac{k^2}{b^2}}} \quad . \qquad (3)$$

Expression 3 determines ϕ only to within ϕ and $180°-\phi$, since $\sin\phi = \sin(180°-\phi)$. We want the obtuse angle if

$$\underline{c}^* \cdot \underline{d}^* < 0 \ ,$$

and the acute if

$$\underline{c}^* \cdot \underline{d}^* > 0 \ .$$

Since $\underline{c}^* \cdot \underline{d}^* = ha^* c^* \cos\beta^* + kb^* c^* \cos\alpha^* + c^{*2}$

and $a^* : b^* : c^* = \frac{\sin\alpha}{a} : \frac{\sin\beta}{b} : \frac{\sin\gamma}{c}$,

the above condition reduces to

ϕ is obtuse if $h\left(\frac{\cos\alpha\cos\gamma - \cos\beta}{a}\right) + k\left(\frac{\cos\beta\cos\gamma - \cos\alpha}{b}\right)$

$$\ell\left(\frac{\sin^2\gamma}{c}\right) < 0 \quad . \tag{4}$$

Expressions 1, 3, and 4 allow the calculation of the required ϕ and χ angles for the general triclinic case.

In an orthogonal system, the calculation of ϕ may be considerably simplified. For this case

$$\sin\phi = \frac{\frac{h}{a}}{\sqrt{4\,\frac{\sin^2\theta}{\lambda^2} - \frac{k^2}{b^2}}} \quad ,$$

and ϕ is obtuse if ℓ is negative, acute if ℓ is positive.

References to Part II

1. See for example A. W. Hanson, H. Lipson, and C. A. Taylor, Proc. Roy. Soc., A218, 371 (1953).

2. M. Born and E. Wolf, "Principles of Optics," 381-400, Pergamon Press, London, 1959.

3. D. Duchamp, "User's Guide to the CRYRM Crystallographic System," California Institute of Technology, Pasadena, 1964.

4. D. Duchamp, Abstracts of the A. C. A. Bozeman Meeting, B-14, 29, 1964.

5. "International Tables for X-Ray Crystallography," Vol. 1, 373-575, The Kynoch Press, Birmingham, 1952.

Appendix I. PRELIMINARY INVESTIGATIONS OF SOME CRYSTALLINE COMPOUNDS.

i) $(C_2F_4)_2Fe(CO)_4$.

Crystals of the above compound were obtained from Dr. Martin J. Griffin of the E. I. du Pont de Nemours and Company through Professor J. D. Roberts. Crystals are pale yellow and sublime when exposed to the atmosphere. They are monoclinic with approximate cell parameters $\underline{a}$ = 26.79 A, $\underline{b}$ = 7.6 A, $\underline{c}$ = 27.8 A, and β = 124.4°. Reflections of the type $hk\ell$ are present only for $h + k = 2n$ and reflections of the type $h0\ell$ only for $\ell = 2n$, indicating that the space group is either Cc or C2/c. The density, measured by flotation methods, is 2.09 g. cm.$^{-3}$; the density calculated on the basis of 16 molecules per unit cell is 2.11 g. cm.$^{-3}$.

After a crystal had been mounted for taking intensity data, the discovery that Dr. Ronald Mason of Imperial College, London, had completed two-dimensional work and was collecting three-dimensional data on this compound led to the termination of this investigation (1).

ii) $[Fe_3(OCOCH_3)_7OH \cdot 3H_2O]NO_3$.

The above compound was prepared according to the method given by Starke (2). Crystals were obtained by evaporation from glacial acetic acid with a small amount of acetic anhydride added. Analysis of the resulting crystals showed the following: % C = 23.86, % H = 4.09, % Fe = 23.35, % N = 2.60; percentages calculated on the basis of $[Fe_3(OCOCH_3)_7OH \cdot 3H_2O]NO_3$ are: C, 23.55; H, 3.95;

Fe, 23.47; N, 1.96.

The crystals were found to be monoclinic with approximate cell parameters $\underline{a}$ = 11.78 A, $\underline{b}$ = 14.68 A, $\underline{c}$ = 15.21 A, and β = 90°50'. Reflections of the type h0ℓ are present only for ℓ = 2n and reflections of the type 0k0 only for k = 2n; therefore the space group is uniquely determined as $P2_1/c$.

Upon exposure to x-rays, the crystals were found to lose their diffracting power. Attempts to correct this by protecting the crystals from the oxygen of the air were successful. One poor set of hk0 photographs was obtained with a decaying crystal; the data from this set of photographs were used for Proposition 1. All other photographs were of even poorer quality. Since work on trimesic acid was showing interesting results at this time, work on this compound was put aside.

iii) $Hg(DPM)_2$.

An x-ray diffraction study of crystals of $Hg(DPM)_2$, the mercury complex of dipivaloylmethane, $(CH_3)_3CCOCH_2COC(CH_3)_3$, was undertaken in the hope of obtaining information about the coordination around the mercury atom. A sample of the compound was supplied by Dr. Chin-Hua S. Wu. Clear platy crystals were obtained by evaporation from ethanol solutions. They are triclinic with approximate cell parameters $\underline{a}$ = 10.27 A, $\underline{b}$ = 13.29 A, $\underline{c}$ = 9.9 A, α = 97°40', β = 92°, and γ = 110°45'. Using flotation methods, the density was found to be 1.50 g. $cm.^{-3}$; the density calculated on the basis of two molecules per unit cell is 1.51 g. $cm.^{-3}$.

The crystals were found to deteriorate when exposed to x-rays; some twinning problems were also encountered. The deterioration may be slow enough to allow at least one good exposure per crystal, provided the crystal is very well formed and is protected from the atmosphere. All photographs taken were unsuitable for the gathering of intensity data, since the spots were irregularly diffuse.

iv) $NC_6(H_3^?)Hg_3(ClO_4)_2 \cdot 4H_2O$.

Pale yellow crystals of a compound whose analysis was reported to correspond to the above empirical formula were obtained from Dr. T. H. Wirth. In order to obtain information about its structure, which is as yet unknown, a preliminary x-ray investigation was undertaken. Crystals were found to be monoclinic with approximate cell parameters $\underline{a}$ = 10.66 A, $\underline{b}$ = 17.22 A, $\underline{c}$ = 13.27 A, and β = 105.6°. Extinctions showed that the space group is $P2_1/c$. An approximate density determination agrees with a density of 5.45 g. $cm.^{-3}$, calculated on the basis of 8 molecules per unit cell. The crystals seem to hold up well under x-rays, and good, sharp photographs are readily obtainable.

References to Appendix I

1. R. Mason, Private communication to R. E. Marsh.
2. K. Starke, J. Inorg. Nucl. Chem., 13, 254 (1960).

Appendix II. A MOLECULAR PLANE FOURIER PROGRAM FOR THE BURROUGHS 220 COMPUTER.

i) Introduction.

This program is designed to calculate a Fourier section through a designated plane. Required input includes three-dimensional structure factor data, unit cell parameters, direction cosines of the designated plane in terms of the real cell axes, and the location of a center point for this plane. A first-dimension summation program (dependent on the space group) must also be entered.

The output is in the form of a rectangular grid, the points being spaced according to an interval (in Angstroms) specified by the user. The vertical and horizontal extent (in Angstroms) of the rectangle is also specified by the user. The program automatically takes the horizontal direction in the molecular plane to be that direction in which the first-dimension summation coordinate is a constant. This makes it necessary to do a first-dimension summation only once for each horizontal row and thereby simplifies and shortens the calculations. The equations for doing this are given in Part II of this thesis.

ii) Operational procedure.

1) Set PZT switch on console UP.

2) Read in main program.

   Computer halts with (rC) = 6666006666.

3) Set PZT switch on console DOWN.

4) Load key tape and press start.

Computer reads in and rearranges the key tape, does some preliminary calculations, and halts with (rC) = 7777007777.

5) Set up output.

Output is SPO, alphanumeric words.

6) Load first-dimension program and press start.

Computer reads in first dimension program and prints out:

a) Coordinates of the first point,
b) Vertical translation parameters,
c) Horizontal translation parameters.

Computer then halts with (rC) = 8888008888.

7) Load data tape and press start.

Fourier summation is carried out. Data is read in once for each row of the resultant map. (Data tape should have reflection strips at the beginning and end.) At the conclusion of the calculation, computer halts with (rC) = 9999009999.

iii) Performance of the Fourier summation.

For the purposes of this program, the Fourier expression for a particular space group is broken up in the usual way into the summation of certain triple trigonometric products. The structure factors are processed one by one by the first-dimension program, which multiplies them by the proper trigonometric term, divides them according to parity into different groups, and accumulates them in the proper place for the second- and third-dimension

summation. In accumulating these reflections, the first-dimension summation is performed.

The number of groups into which the input data for the second- and third-dimension summations have to be divided is determined by the number of different trigonometric expressions in the Fourier expression mentioned above. Up to four blocks of data can be stored in (0000)-(1039), (1040)-(2079), (2080)-(3119), and (3120)-(4159). The indices are indicated by the address, i.e., reflection $F_{0k\ell}$ must be stored in $26\,\ell + k + n(1040)$, where n can be 0, 1, 2, or 3 and the ℓ represents the third-summation index and the k represents the second-summation index. No indices are stored in the above blocks, only signed amplitudes. From the above, it follows that k_{max} and ℓ_{max} are 25 and 39 respectively. Thus the first-dimension program accumulates, in location $26\,\ell + k$, the expression

$$A_{k\ell} = \sum_{h} F_{hk\ell} \begin{pmatrix} \cos \\ \text{or} \\ \sin \end{pmatrix} 2\pi\, hx$$

where the summation is performed over all reflections having the parity assigned to that block. A first-dimension program, which is dependent upon space group, is part of the input to this program. It is easily written and usually consists of a hundred or less words.

After the first-dimension calculation is complete, the main program proceeds to calculate the values for the points along the particular row being calculated. Since the molecular plane is set up so that the first-dimension coordinate is constant along this row, the

first-dimension summation is only performed once for each row. The calculation of points along row is performed on a point by point basis. The terms accumulated by the first-dimension program are each multiplied by the appropriate trigonometric terms for the second and third summations (as designated by the trig code word) and accumulated according to the sign of the particular data block (as designated by the summation code word). The value for each point is given by

1st block

$$\pm \sum_{k\ell} A_{k\ell}' \begin{pmatrix} \cos \\ \text{or} \\ \sin \end{pmatrix} 2\pi ky \begin{pmatrix} \cos \\ \text{or} \\ \sin \end{pmatrix} 2\pi \ell z \pm$$

2nd block

$$\sum_{k\ell} A_{k\ell}'' \begin{pmatrix} \cos \\ \text{or} \\ \sin \end{pmatrix} 2\pi ky \begin{pmatrix} \cos \\ \text{or} \\ \sin \end{pmatrix} 2\pi \ell z \pm, \text{ etc.}$$

iv) The key tape.

a) Format.

(4950)	0 0000000xxx	Summation sequence
(4951)	± 000000. xxxx	x coordinate of center point
(4952)	± 000000. xxxx	y coordinate of center point
(4953)	± 000000. xxxx	z coordinate of center point
(4954)	0 0000000000	Not used
(4955)	0 xxxxxxxx00	Trig code word for 2nd and 3rd dim.
(4956)	0 000000xx. xx	d_H (Å) horiz. distance from center
(4957)	0 000000xx. xx	d_V (Å) vert. distance from center
(4958)	0 000000000x	Number of groups of data
(4959)	0 0000000000	Not used

(4960)	0 000000xxxx	Summation code word
(4961)	0 000000000x	If sine used in 1st dim. enter 1, else 0
(4962)	0 0000000000	Not used
(4963)	0 0000000000	Not used
(4964)	0 000000x. xxx	Increment (Å)
(4965)	0 . xxxxxxxxxx	Scale factor
(4966)	0 0000xxx. xxx	Length of a axis (Å)
(4967)	0 0000xxx. xxx	Length of b axis (Å)
(4968)	0 0000xxx. xxx	Length of c axis (Å)
(4969)	± 00000. xxxxx	Cos α_1 } Unit cell angles { $\alpha_1 = \sphericalangle$ b, c
(4970)	± 00000. xxxxx	Cos α_2 } Unit cell angles { $\alpha_2 = \sphericalangle$ a, c
(4971)	± 00000. xxxxx	Cos α_3 } Unit cell angles { $\alpha_3 = \sphericalangle$ a, b
(4972)	± 00000. xxxxx	Cos α } Direction cosines for
(4973)	± 00000. xxxxx	Cos β } molecular plane in terms
(4974)	± 00000. xxxxx	Cos γ } of cell axes
(4975)	0 00000000xx	Maximum index in 1st dim. summation
(4976)	0 00000000xx	Maximum index in 2nd dim. summation
(4977)	0 00000000xx	Maximum index in 3rd dim. summation

NOTE: No instructions of the form 6 xxxx xx xxxx are allowed before, during or after the key tape. This tape must consist of exactly 28 words.

The key tape is processed immediately after being read in. If it is desired to make changes manually, read in the key tape with the "step" switch and make changes immediately after.

b) Discussion.

4950: The summation sequence word (4950) determines which axes are summed over in the first, second, and third summations respectively (1 = h, 2 = k, 3 = ℓ). For

example, 213 signifies first dimension in k, second in h and third in ℓ. Pertinent parts of the key tape are rearranged in accordance with this word immediately after they are read in.

4951, 4952, 4953: These locations are for the x, y, and z coordinates of the point to be considered as the center of the map. They should be in fractional unit cell coordinates, positive or negative, and should be less than unity in absolute value.

4955: The trig code word (4955) determines which trig functions are used in the different blocks in the second and third summations (1 = cosine, 0 = sine). The first digit (1, 1) determines the second summation of the first block. If there are N blocks, the Nth digit (N, 1) determines the second summation of the Nth block; the N + 1 digit (N + 1, 1) determines the third summation of the first data block.

4956, 4957, 4964: The size of the plane section is determined by d_H and d_V. The distance out from the center of the plane in the horizontal (constant first-dimension summation parameter) direction is specified by d_H. Similarly d_V is the distance from the center in the vertical direction. Thus the resulting map is $2d_H$ wide by $2d_V$ long. Both d_H and d_V are required to be in Angstrom units and must be multiples of the increment (4964),

i.e. d_H, d_V = 0 mod (increment). The increment (4964), also in Angstrom units, gives the spacing between points in the horizontal and vertical directions.

4958: The number of data groups is entered here.

4960: The summation code word determines how the blocks are added together for output (1 = subtraction, 0 = addition). Only the last N digits are used, where N is the number of groups of data.

4961: If a sine function is used in the first dimension, a 1 should be entered here. Otherwise enter 0. This is to enable the program to avoid useless calculations.

4965: A scale factor (4965) should be entered if output will exceed four digits. Otherwise enter 9999999999. Provision is made only for four digits and a sign in the output. A point greater than 9999 in absolute value will not be output correctly.

4954, 4959, 4962, 4963: These locations are available for first-dimension code words if required. Otherwise they are not used.

4966, 4967, 4968, 4969, 4970, 4971: The lengths of the unit cell axes and the cosines of the interaxial angles should be entered here.

4972, 4973, 4974: The direction cosines of the normal to the molecular plane should be entered here. The program requires that cos α be the cosine of the angle between

the direct a axis and the normal to the molecular plane, similarly for cos β and the b axis and cos γ and the c axis. Direction cosines with respect to orthogonalized axes in the triclinic and monoclinic systems should not be used.

4975, 4976, 4977: The maximum indices of the first, second, third summation parameters are entered here to allow the program to economize on calculations.

v) First-dimension program.

a) General description. The first-dimension program must provide for three things:

1) Read in of data
2) Multiplication of data by the proper trigonometric term
3) Accumulation of the processed data in the appropriate place for use in the second- and third-dimensions.

It follows that the format for data input is dependent upon the first-dimension program.

b) Programming details. Space available for the first-dimension program is 4300-4490 inclusive. Cells 4200 to 4300 are available for the read in of data also.

The program stores sine and cosine of 2π hx as a function of h for use by the first-dimension program. (Here h is assumed to be the first-dimension-summation index.)

The $\underline{x}$ depends upon which row is currently being calculated and need not therefore concern the first-dimension programmer. The main program does the bookkeeping when changing row.

$\cos 2\pi hx$ is stored in 4800 + h.
$\sin 2\pi hx$ is stored in 4850 + h.

Values are stored from h = 0 to h = h_{max} in fixed point in the form ± . xxxxxxxxxx. A suggested method for looking up the trigonometric function is:

1) Enter the instruction which multiplies the reflection by the trig term as (0000 14 14xx).
2) With 00000000hh in (rA), store field (02) in the address portion of this multiply instruction.
3) Increment by 50 for a sign function.

Locations 4954, 4959, 4962, and 4963 on the key tape are not used for input to the main program and may be used to input into the first-dimension program. The main program clears locations 0000 through 4159 before branching to the first-dimension program. Processed data may therefore be accumulated by an "add to location" command.

If nothing is altered, the main program will enter the first-dimension program at location 4300. If program control switch 1 is on, the main program will enter at 4300 the first time and at 4306 all other times. Changing the point of entry is not simple, but can be done by changing two instructions

in the main program. The first-dimension program should enter the main program at location 4500.

No read in instruction is necessary for the first-dimension program tape if the first word is to be read into 4300. The last word on the tape should be (6 0000 30 1344).

Several first-dimension programs have been written and are available for use or as examples.

vi) Interpretation of results.

Output should be plotted on a square grid. The distance in Angstrom units between points is given by the increment word on the key tape. By choosing an appropriate grid, any desired scale may be easily obtained.

The fractional coordinates of any point in the plane may be easily calculated. To obtain the coordinates of a point, subtract the proper number of horizontal and vertical increments from the coordinates of the first point. For example, to find the x coordinate of the fourth point on row five, subtract three horizontal delta x's and four vertical delta x's from the x coordinate of the first point.

vii) Reproduction of the program tape.

To copy the program tape:

a) Set paper tape punch to SPO. (SPO switch on teletype down.)

b) Set PZT up and Program Control Switch # 2 ON.

c) Read in program.

A copy of the program will be immediately punched out on the tape punch. At the conclusion, the program will stop with

(rC) = 7270000727.

(PZT must remain up while the new program tape is being punched.)

d) If it is desired to do a Fourier calculation, proceed with step 3 in the operational procedure.

PROPOSITIONS

PROPOSITION 1

The locations of the three independent iron atoms in projection down the c axis of crystals of $[Fe_3(OCOCH_3)_7OH \cdot 3H_2O]NO_3$ are proposed. An investigation of the crystal structure of $[Fe_3(OCOCH_3)_6(OH)_2]_2[PtCl_6] \cdot 10H_2O$ is proposed.

Trinuclear acetate complexes have been known to exist for some time. Werner (1) found a complex with basic unit $[Cr_3(OH)_2(OCOCH_3)_6]^+$, and reported that the hydroxyl and acetate groups do not ionize. These compounds have been found to exist for iron and aluminum also (2, 3). A structure which has been suggested for these compounds is given below (4).

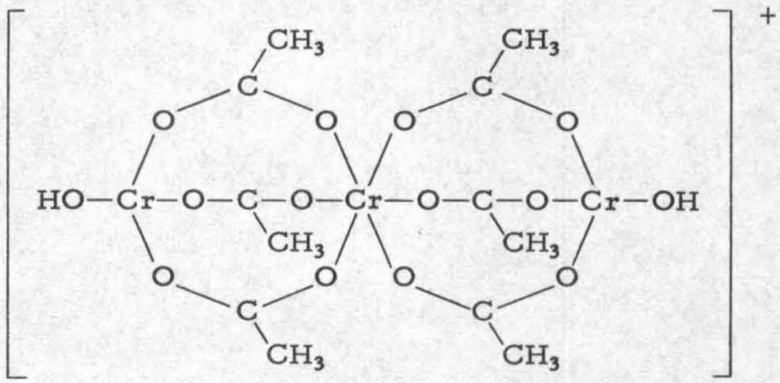

These compounds have been studied recently by Starke (5).

In hope of solving the structure of this complex, an x-ray investigation (see Appendix 1) of crystals of the compound $[Fe_3(OCOCH_3)_7OH \cdot H_2O]NO_3$ was undertaken, but encountered difficulties. A set of hk0 photographs of poor quality was obtained. To attempt to deduce some information about the structure, hk0 intensity

data was estimated using these photographs. Lorentz and polarization corrections were made, and hk0 Patterson and sharpened Patterson projections were calculated. From a study of these projections, $\underline{x}$ and $\underline{y}$ parameters are proposed for the three independent iron atoms. Structure factors were calculated using only iron atoms, and an electron density projection was calculated. This projection indicated slight shifts. The final proposed positions expressed in fractional unit cell coordinates are (0.103, 0.100), (0.060, 0.323), and (0.255, 0.323). Again structure factors were calculated using only the iron atoms. Observed and calculated structure factors are shown in Table 1.

An electron density difference projection was calculated, phasing according to the structure factors shown in Table 1 and subtracting out the contributions of the iron atoms to the structure factors. The two electron density projections are shown superimposed in Figure 1. The solid contours, which are at intervals of 200 arbitrary units beginning at 200, show the complete map; the dashed contours, at intervals of 100 arbitrary units beginning at 200, show the difference map.

To check on the locations of the iron atoms, an electron density projection was calculated phasing according to the iron atom at (0.255, 0.323). In this projection the other two atoms appeared and no other large peaks were observed.

Consideration of the above positions allows a linear configuration for the irons in the complex to be ruled out. Since the

Table 1. Observed and calculated structure factors.

h	k	F(obs)	F(cal)	h	k	F(obs)	F(cal)
2	0	87	- 80	9	3	< 17	- 20
3	0	61	138	10	3	< 18	3
4	0	77	-102	11	3	23	- 17
5	0	120	-175	12	3	35	- 23
6	0	36	66	13	3	15	- 17
7	0	56	- 25	14	3	< 12	- 10
8	0	78	- 68	0	4	75	17
9	0	77	103	1	4	162	- 93
10	0	50	44	2	4	74	- 71
11	0	26	- 33	3	4	110	96
12	0	61	44	4	4	< 11	29
13	0	24	7	5	4	< 13	4
14	0	60	- 51	6	4	58	94
15	0	13	2	7	4	53	10
1	1	175	-142	8	4	52	- 52
2	1	10	45	9	4	< 18	7
3	1	155	- 26	10	4	< 18	- 24
4	1	49	-128	11	4	51	- 47
5	1	28	63	12	4	< 16	12
6	1	< 13	55	13	4	< 15	12
7	1	30	- 43	14	4	< 12	- 6
8	1	46	61	1	5	61	-128
9	1	30	46	2	5	91	-120
10	1	48	- 48	3	5	26	32
11	1	< 18	3	4	5	116	-118
12	1	< 17	10	5	5	96	77
13	1	46	- 40	6	5	24	37
14	1	< 13	- 3	7	5	116	- 97
15	1	19	17	8	5	52	37
0	2	42	0	9	5	< 18	37
1	2	38	30	10	5	71	- 60

Table 1 (continued)

h	k	F(obs)	F(cal)	h	k	F(obs)	F(cal)
2	2	73	21	11	5	32	18
3	2	34	- 28	12	5	27	33
4	2	61	- 11	13	5	20	- 34
5	2	44	- 5	14	5	< 10	5
6	2	38	- 29	0	6	188	-168
7	2	< 14	- 4	1	6	74	8
8	2	42	15	2	6	46	52
9	2	21	0	3	6	109	- 89
10	2	< 18	8	4	6	23	62
11	2	25	14	5	6	116	108
12	2	< 17	- 3	6	6	32	- 45
13	2	< 16	- 4	7	6	46	15
14	2	< 13	1	8	6	46	46
1	3	24	- 40	9	6	70	- 67
2	3	146	- 79	10	6	< 18	- 28
3	3	29	- 70	11	6	27	24
4	3	24	- 33	12	6	17	- 30
5	3	42	- 4	13	6	< 13	- 5
6	3	17	30	14	6	17	35
7	3	< 15	51	1	7	73	66
8	3	80	39	2	7	83	34
3	7	91	51	1	11	< 17	49
4	7	100	59	2	11	83	- 88
5	7	20	- 17	3	11	20	- 42
6	7	41	- 36	4	11	24	48
7	7	26	- 19	5	11	38	- 41
8	7	< 18	- 44	6	11	< 18	- 8
9	7	30	- 27	7	11	55	72
10	7	38	14	8	11	< 18	- 5
11	7	< 17	10	9	11	< 16	- 13
12	7	< 15	12	10	11	32	36

Table 1 (continued)

h	k	F(obs)	F(cal)	h	k	F(obs)	F(cal)
13	7	19	25	11	11	13	- 18
0	8	43	25	12	11	19	- 30
1	8	81	22	0	12	39	31
2	8	27	9	1	12	24	- 10
3	8	< 14	- 9	2	12	< 18	- 16
4	8	24	- 18	3	12	< 18	25
5	8	15	- 20	4	12	30	9
6	8	45	- 17	5	12	< 18	- 20
7	8	32	- 5	6	12	18	18
8	8	< 18	5	7	12	< 18	- 2
9	8	< 18	10	8	12	28	- 14
10	8	< 18	12	9	12	< 16	14
11	8	< 16	9	10	12	< 13	3
12	8	< 14	2	1	13	< 18	- 14
13	8	< 11	- 2	2	13	41	- 28
1	9	31	- 20	3	13	44	- 25
2	9	29	51	4	13	< 18	- 13
3	9	19	28	5	13	23	- 1
4	9	30	- 20	6	13	< 17	12
5	9	21	20	7	13	35	20
6	9	24	0	8	13	< 16	16
7	9	49	- 40	9	13	18	9
8	9	24	- 2	10	13	< 11	1
9	9	< 18	4	0	14	< 18	- 38
10	9	< 17	- 17	1	14	44	- 17
11	9	21	10	2	14	43	- 2
12	9	< 13	17	3	14	41	- 2
0	10	< 16	- 37	4	14	< 18	22
1	10	100	75	5	14	< 17	29
2	10	50	64	6	14	38	9
3	10	60	- 90	7	14	< 15	6

Table 1 (continued)

h	k	F(obs)	F(cal)
4	10	21	- 14
5	10	19	13
6	10	70	- 86
7	10	26	- 6
8	10	44	52
9	10	< 17	- 17
10	10	33	17
11	10	21	48
12	10	< 11	- 16
8	14	15	1
9	14	< 11	- 18
10	14	24	- 15
1	15	< 17	37
2	15	< 17	- 22
3	15	21	- 1
4	15	< 16	36
5	15	< 16	- 21
6	15	< 15	- 14
7	15	< 13	22
8	15	< 12	- 17
9	15	< 12	- 15
0	16	< 16	28
1	16	16	- 29
2	16	19	- 28
3	16	21	41
4	16	< 15	1
5	16	< 13	- 15
6	16	21	- 38
7	16	< 10	1
1	17	< 14	- 6
2	17	19	33
3	17	36	21
4	17	< 12	- 6
5	17	< 11	11
0	18	31	11
1	18	13	8
2	18	< 10	3
3	18	33	- 2
4	18	10	- 8

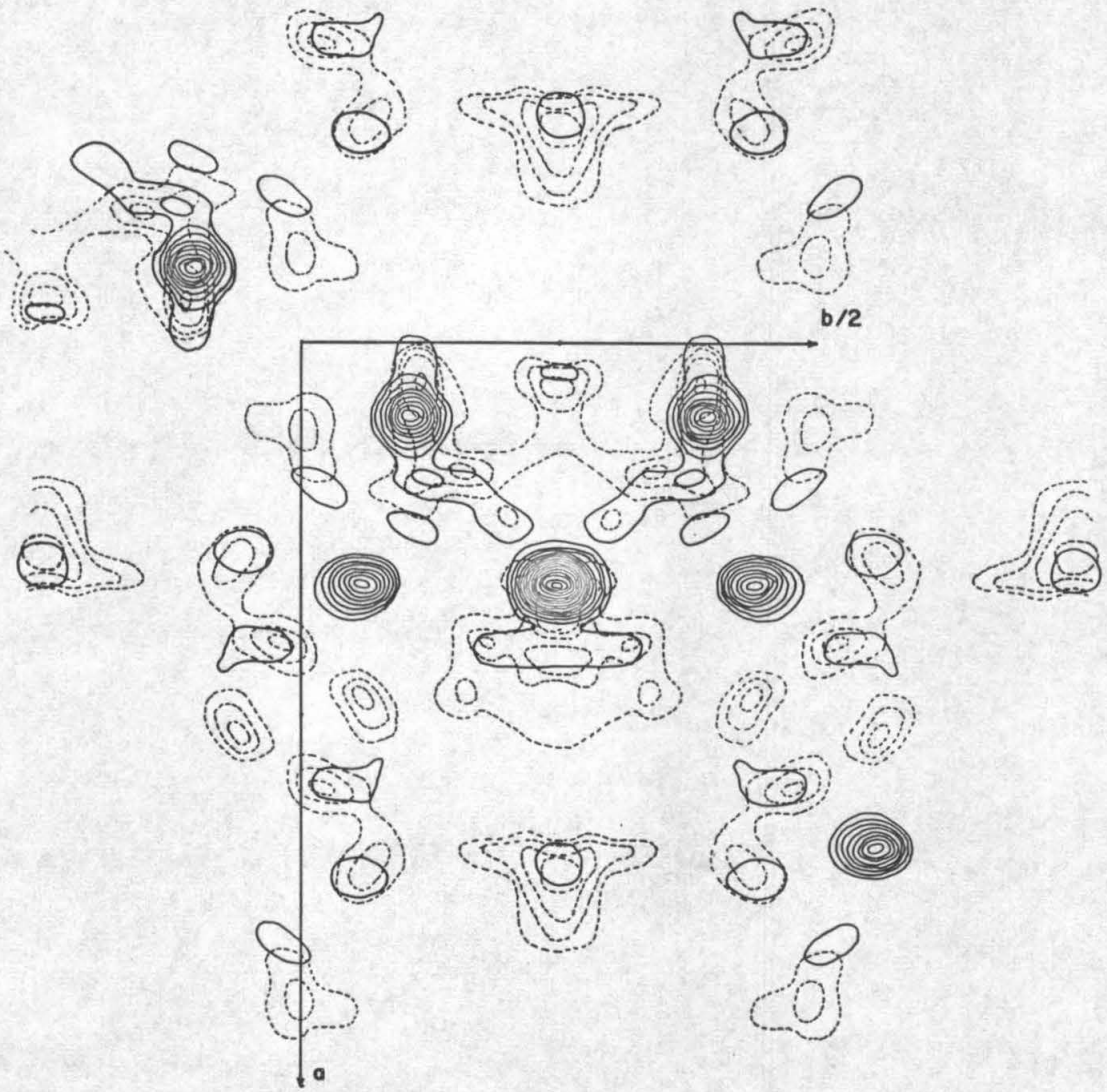

Figure 1. hk0 Fouriers.

structure shown previously would certainly be linear, it may be ruled out.

Chemical evidence will now be considered. Under absolutely anhydrous conditions, the conventional iron triacetate and not the complex reported here has been reported to crystallize from acetic acid (5). This indicates that the presence of water, or possibly hydroxyl groups, is necessary for the formation of the trinuclear complex. The $PtCl_6^=$ salt of these complexes has been shown to have a composition corresponding to $[Fe_3(OCOCH_3)_6(OH)_2]_2[PtCl_6]$ + 10 H_2O (6). Titration studies have shown that two acetate groups from a complex with eight acetate groups per complex are "free" acetic acid and can be titrated with $Ba(OH)_2$ (4). Also the hydroxyl groups in these complexes have been found to be inert in perchloric acid solution (7) and in other mineral acids (1). This evidence indicates that the formula for the complex being investigated should probably be written $([Fe_3(OH)_2(CH_3COO)_6] \cdot 2H_2O \cdot CH_3COOH)NO_3$ and that hydroxyl bridges may be important.

This is essentially where this proposition stood in December, 1962, when it was first presented by the author in connection with examination for candidacy. Recently the structure of $[Cr_3(OH)_2(CH_3COO)_6]Cl \cdot 8H_2O$ was determined by S. C. Chang and G. A. Jeffrey (8). The three chromium atoms are linked to the central oxygen atom in a planar type configuration as shown on the following page.

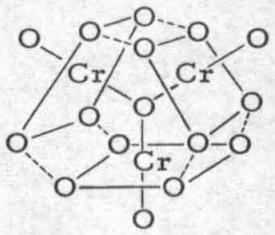

The positions found for the chromium atoms are in an arrangement analogous to that proposed previously by the author for the iron complex. The two structures are probably not exactly the same. The space group for the above structure is $P2_12_12$ which is different from that found for the iron complex (see Appendix 1 of this thesis). An investigation of the trinuclear iron complex is needed before further discussion.

The author proposes that an investigation of the $[Fe_3(OCOCH_3)_6(OH)_2]_2[PtCl_6]\ 10\cdot H_2O$ compound be undertaken. There is a good chance that by the investigation of this salt, the deterioration problem encountered with the nitrate salt could be by-passed. The additional information obtained by such an investigation would be valuable in understanding iron complexes, and could be compared with the chromium results. The configuration of the central oxygen of these complexes is also of interest.

References

1. A. Werner, Ber. Dtsch. Chem. Ges., 41, 3447 (1908).

2. R. Weinland and H. Reihlen, Z. Anorg. Chem., 82, 426 (1908).

3. G. Spacu and E. Popper, Kolloid Z., 103, 19 (1943).

4. W. D. Treadwell and W. Fisch, Helv. Chim. Acta, 13, 1209 (1930).

5. K. Starke, J. Inorg. Nucl. Chem., 13, 254 (1960).

6. R. Weinland, K. Kessler, and A. Bayerl, Z. Anorg. Chem., 132, 209 (1924).

7. A. T. Casey and K. Starke, Analyt. Chem., 31, 1060 (1959).

8. S. C. Chang and G. A. Jeffery, "Abstracts A. C. A. Winter Meeting," 1965, C-3, p. 26.

PROPOSITION 2

A cyclic structure with penta-coordinated aluminum has been given as the structure of the 1:1 complex of trimethyl aluminum with tetramethyltetrazene, $(CH_3)_2N-N=N-N(CH_3)_2$, (1). This structure is discussed and an alternative structure is proposed.

While studying reactions between tetramethyltetrazene and trialkyl aluminum complexes, Fetter and Bartocha (1) found a complex with formula $(CH_3CH_2)_3Al : (CH_3)_2N-N=N-N(CH_3)_2$ among the products of a reaction between triethyl aluminum and tetramethyltetrazene. Later Fetter, Brinckman, and Moore (2) showed that the corresponding trimethyl aluminum complex had also been produced in a similar reaction, but that it was not detected because of partial decomposition prior to elemental analysis. The methyl complex will be discussed here, but the discussion also applies almost exactly to the ethyl complex.

Elemental analysis shows that the complex is 1:1 (2). Molecular weights determined by cryoscopic methods are 199 g. $mole^{-1}$ and 193 g. $mole^{-1}$, as compared to 188 g. $mole^{-1}$ expected for a monomeric complex (2). The n.m.r. spectra of the complex show only two very sharp peaks of the ratio of approximately 4:3 with chemical shifts (in tau values) of 7.25 and 10.82 p.p.m. respectively. The large peaks represent the protons on methyl groups bound to nitrogen atoms; and the smaller, those on methyls bound to the aluminum atom. These spectra indicate that all hydrogen atoms of the aluminum methyl groups are equivalent, and similarly for hydrogen atoms on

nitrogen methyl groups. On this basis Fetter, Brinkman, and Moore gave the structure as a cyclic penta-coordinated aluminum complex as shown below.

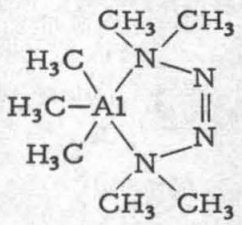

They proposed that asymmetric cleavage of the ring would be a reasonable precursor to the products which they observed on pyrolysis of the complex at about 90°. A complete mechanism for the pyrolysis was not proposed (2).

This structure may be objected to on steric grounds. Attempting to build a model of such a structure shows immediately that the methyl groups do not allow the aluminum atom and the amino nitrogen atoms to come much closer together than about 3 A; whereas the sum of the tetrahedral radii (3) predicts a distance of around 1.96 A.

Another interesting observation is that the chemical shift in uncomplexed tetramethyltetrazene is 7.21 p.p.m. (2). This is not very different from the 7.25 p.p.m. reported for the complex. Fetter, Brinkman, and Moore suggested that this was because the bonds were weak (2). Another alternative is that the nitrogen atoms to which the methyl groups are attached are not involved directly in the bonding to the aluminum atom.

An alternative structure is proposed in which the vacant orbital of a tetrahedrally coordinated trimethyl aluminum group interacts with the nitrogen atoms of the azo link in the tetramethyltetrazene as shown below. The tetramethyltetrazene molecule probably assumes

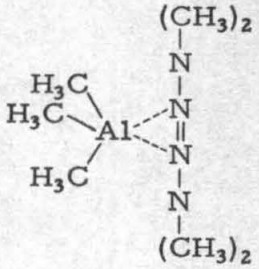

a trans-type configuration with the aluminum atom approaching normal to the plane of the nitrogen atoms. A cis-type configuration with the aluminum atom approaching in the plane is possible, but might be less favored. This structure agrees with the n. m. r. spectra and also doesn't have the steric problem which the cyclic form has. The aluminum atom may be regarded as tetrahedrally coordinated, as is usually found in aluminum compounds. Diazo groups are known to form strong bonds with certain metals; for example, in the cuprous chloride-azomethane complex, the Cu–N distances are reported to be somewhat shorter than the sum of the Pauling radii (4).

A first step leading to the various products produced by pyrolysis of this complex might also be suggested. Complexing with aluminum might well catalyze the formation of dimethyl amino radicals which would then react with the various species present to produce the variety of products observed. The dimethyl amino radical is fairly well known (5, 6, 7). It is usually produced by heating

tetramethyltetrazene to around 140–150° (8). The complexing might allow its formation in quantity at a lower temperature.

The determination of which complex, if either, is the actual structure will probably be difficult, since the complex is a liquid and is not very stable at temperatures above 0°C. (2). It is readily vacuum distilled so that perhaps vapor phase electron diffraction studies are possible. A lack of high symmetry in the complex would probably complicate such studies and also spectra studies. Study of the azo absorption frequencies might yield some information. Low temperature x-ray work may be the best method of attack for the problem of determining the structure of this interesting complex.

References

1. N. R. Fetter and B. Bartocha, Canad. J. Chem., 40, 342 (1962).

2. N. R. Fetter, F. E. Brinkman, and D. W. Moore, Canad. J. Chem., 40, 2184 (1962).

3. L. Pauling, "The Nature of the Chemical Bond," 246, Cornell, New York, 1960.

4. I. D. Brown and J. D. Dunitz, Acta Cryst., 13, 28 (1960).

5. J. S. Watson, J. Chem. Soc., 3677 (1956).

6. J. S. Watson and A. J. Waring, Canad. J. Chem., 38, 298 (1960).

7. F. O. Rice and C. J. Grelecki, J. Am. Chem. Soc., 79, 2679 (1957).

8. B. R. Cowley and W. A. Waters, J. Chem. Soc., 1228 (1961).

PROPOSITION 3

The pyrophosphate ion in the $Zr(P_2O_7)$ structure has been reported to have a P—O—P bond angle of exactly 180° (1). This structure is discussed and a possible alternative interpretation of the x-ray data is proposed in which a nonlinear P—O—P arrangement is allowed. The infrared spectra of this compound are discussed, and the presence of the POP symmetric vibration is proposed.

The structure of $Zr(P_2O_7)$ was determined by Levi and Peyronel (1), who also reported that the pyrophosphates of Si^{+4}, Ti^{+4} Sr^{+4}, Sn^{+4}, and Hf^{+4} are isomorphic to $Zr(P_2O_7)$. The $U(P_2O_7)$ structure was later reported to be of the same structural type (2). The crystals are cubic with $a_0 = 8.20$ A and reported space group T_h^6. As reported the structure consists of Zr atoms at the face-centered positions of a cube and the central oxygen atom of the pyrophosphate group at (1/2, 1/2, 1/2) with the group lying along a three-fold axis of the cube. The structure is shown in Figure 1, as described in Strukturbericht (3). Each of the Zr atoms is surrounded octahedrally by six oxygen atoms each from a different pyrophosphate group. The pyrophosphate groups are crystallographically required to have D_{3d} symmetry.

Several investigators have expressed doubt as to the correctness of the configuration of the pyrophosphate group in this structure in view of present day knowledge of such linkages (4, 5, 6). The crystal structure of $Na_4P_2O_7 \cdot 10H_2O$ has been accurately determined (7), and the pyrophosphate group was found to have C_2

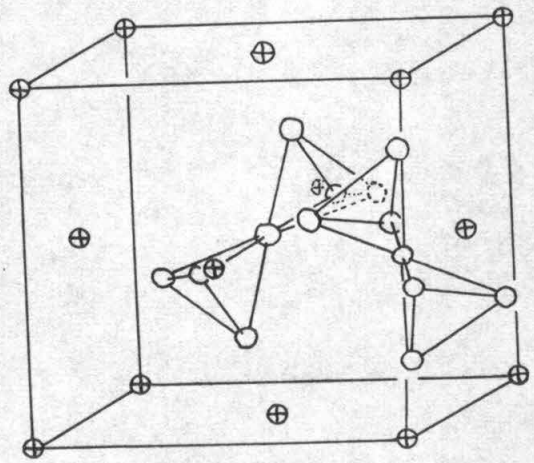

Figure 1. The $Zr(P_2O_7)$ structure (3), (all of the pyrophosphate groups are not shown).

symmetry with the parameters shown in Figure 2. In other

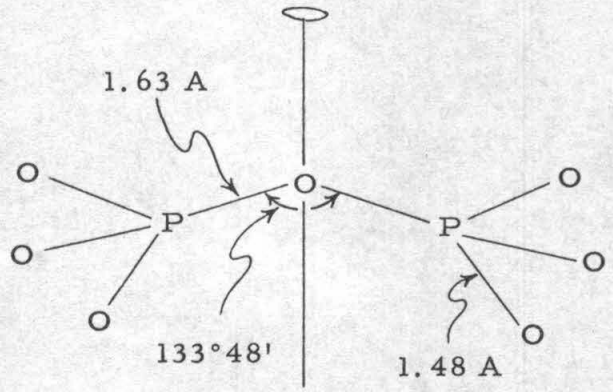

Figure 2. Pyrophosphate group in $Na_4P_2O_7 \cdot 1OH_2O$ (7).

phosphorus compounds "bent" P—O—P linkages have been found (8).

The spectra of the cubic pyrophosphates were studied by Steger and Leukroth (9). The infrared spectra which they reported for $Zr(P_2O_7)$ are shown in Figure 3. They discussed this spectra in terms of the Levi and Peyronel structure with a pyrophosphate ion of D_{3d} symmetry, proposed the following assignments for absorption maxima — 1058-1125 cm.$^{-1}$, as PO_3; 958-983 cm.$^{-1}$, as POP; 500, 548 cm.$^{-1}$, metal-oxygen — but did not mention the peak at 750 cm.$^{-1}$.

The infrared spectra shown in Figure 3 are not very different from spectra of other pyrophosphates. A band in the 700-750 cm.$^{-1}$ region is found in other pyrophosphates. In $Na_4P_2O_7 \cdot 1OH_2O$ infrared spectra a band was observed at 734 cm.$^{-1}$ (10). Similar bands are also present in spectra of the anhydrous pyrophosphates of Na, K,

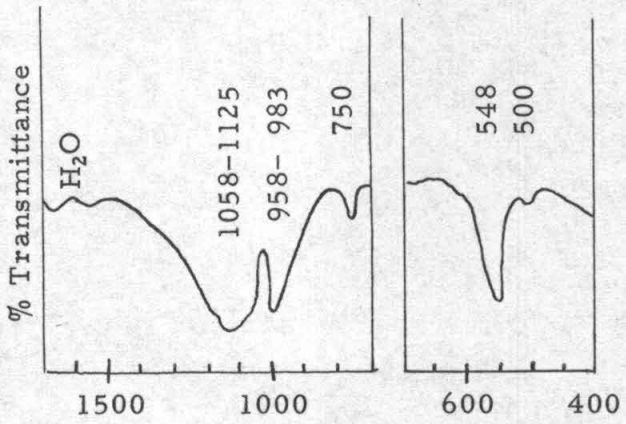

Figure 3. Infrared spectra of $Zr(P_2O_7)$ (9).

Mg, Ca, Sr, Ba, Pb, and Ag (11). A similar band was observed in organic compounds of the type 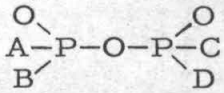 at 715-670 cm.$^{-1}$ (12). This band in all cases mentioned has been shown to be due to the POP symmetric mode (10, 11, 12).

It is proposed that the infrared band at 750 cm.$^{-1}$ in the $Zr(P_2O_7)$ spectra is also due to the POP symmetric mode. For a Levi and Peyronel type pyrophosphate group, the POP symmetric mode transforms according to the representation a_{1g} of the point group D_{3d} (9), and therefore should be inactive in the infrared. Coupling of the D_{3d} ion symmetry with the T_h crystal symmetry could mix this representation with the a_g and f_g representations of T_h (9), but these also indicate infrared inactive modes. However, if lower symmetry, e.g. C_{2v} or C_2, is allowed for the pyrophosphate ion, the POP symmetric mode is permitted in the infrared. If the above assignment is correct, the presence of the 750 cm.$^{-1}$ band is

further evidence that the symmetry of the pyrophosphate group in $Zr(P_2O_7)$ is less than D_{3d}.

Even if the acentric space group T^4, ($P2_13$), is assumed, the incorporation of a nonlinear POP linkage by modifying the cubic structure of Levi and Peyronel is not possible unless one assumes that the three-fold symmetry is statistical; i.e. the pyrophosphate group lies in a disordered position. In such a structure the Zr atoms would remain at the face centers and at the origin, and the "bent" pyrophosphate group would randomly assume three different orientations (six if the centric space group is used) to give statistical three-fold symmetry. It is proposed that this may be the actual structure of cubic $Zr(P_2O_7)$.

To test this hypothesis, a pyrophosphate group — in the staggered configuration with the dimensions found for the hydrated sodium salt (7) — was rotated geometrically inside a cube until the distances between the pyrophosphate oxygen atoms and the metallic ions at the face centers of the cube were about equal to 2.2 A. Positions derived in this manner are listed in Table 1. Using the space group T^4, structure factors were calculated. Structure factors were also calculated for the Levi and Peyronel structure. These were used to synthesize powder patterns by summing over the squares of the structure factors having the same Bragg angle. The patterns obtained by this calculation is given in Table 2 along with the powder pattern observed by Levi and Peyronel (1). The observed pattern as reported is not complete; some intensities missing in the listed

Table 1. Positions derived for the disordered structure.

Atom	x	y	z	T^4 Multiplicity	Pop. Factor
Zr	0	0	0	4	1
P_1	0.389	0.396	0.406	12	0.3333
P_2	0.595	0.609	0.605	"	"
O_1	0.362	0.231	0.459	"	"
O_2	0.469	0.422	0.256	"	"
O_3	0.270	0.520	0.462	"	"
O_1'	0.764	0.573	0.614	"	"
O_2'	0.499	0.603	0.751	"	"
O_3'	0.536	0.731	0.479	"	"
O''	0.530	0.446	0.523	"	"

pattern could be inferred from other parts of the paper and are listed in parentheses.

The agreement appears to be equally as good for both structures. More data are needed to tell whether the disordered structure proposed here is close to being the true structure for this compound. A single crystal investigation would probably show the orientation of the pyrophosphate groups, unless, of course, the actual disorder is more serious than that assumed in the above proposal.

The crystal structure of the $Me(IV)P_2O_7$ compounds was recently reinvestigated by Völlenkle, Wittman, and Nowotny (13) — again by powder methods. Their powder patterns indicated a larger

Table 2. Calculated and observed structure factors.

Indices	s	"Bent"	L & P	Obs. (1)
200	4	39,600	33,500	ms
210, 120	5	9,200	13,200	m
211	6	1,930	2,300	m
220	8	11,000	11,200	m
221	9	1,160	1,020	w
310, 130	10	15	0	—
311	11	13,700	11,700	s
222	12	6,400	11,200	mw
320, 230	13	1,430	1,600	mw
321, 231	14	2,400	2,050	(w)
400	15	9,800	3,800	(mw)
140, 410, 322	17	2,300	3,200	(mw)
411, 330	18	490	2,150	(mw)
331	19	8,300	3,700	m
240, 420	20	24,000	23,500	s
241, 421	21	297	160	(w)
322	22	120	230	w
422	24	9,800	12,500	s
340, 430	25	4,350	1,650	(w)
510, 150, 431, 341	26	395	210	—
511, 333	27	20,800	18,600	ss
250, 520, 432, 342	29	2,140	1,930	(w)
521, 251	30	1,230	2,300	ww
440	32	14,900	12,100	ms
522, 441	33	144	44	—
350, 433, 530	34	43	132	—
351, 531	35	7,050	4,600	ms
600, 442	36	9,100	7,900	ms
160, 610	37	307	980	—

Table 2 (continued)

Indices	s	"Bent"	L & P	Obs. (1)
532, 352, 611	38	1,630	2,150	w
620, 260	40	6,250	8,200	w
261, 621, 540, 450, 443	41	950	1,170	—
541, 451	42	470	535	—
533	43	5,180	3,970	ms
622	44	3,720	5,180	(ms)
630, 360, 542, 452	45	810	700	m
361, 631	46	435	1,840	ww
444	48	1,680	290	—
362, 632	49	950	400	—
543, 453, 710, 170, 550	50	325	15	—
711, 551	51	5,300	1,100	mw
640, 460	52	13,300	9,700	ms
270, 461, 641, 720	53	2,200	2,650	ww
271, 633, 552, 721	54	820	670	ww
462, 642	56	8,070	6,300	s
544, 722	57	175	22	—
370, 730	58	4	0	—
371, 553, 731	59	10,400	5,700	ss
463, 560, 643, 650	61	545	1,540	—
372, 561, 651, 732	62	243	946	—
800	64	5,270	4,580	—
810, 180, 470, 562, 652, 740	65	655	340	—
811, 741, 554, 471	66	450	290	—
733	67	2,860	1,290	—
280, 820, 644	68	7,600	4,800	s

s = strong, w = weak, m = medium

$\underline{s} = h^2 + k^2 + \ell^2$

cell — perhaps a super cell — with an axial length of 24.72 Å for ZrP_2O_7. This larger cell could be that of an ordered nonlinear POP structure, but the extra weak maxima which they observed in their powder patterns could also have been caused by a disorder similar to the one described above (14). Only an accurate single crystal investigation will tell the difference.

References

1. G. R. Levi and G. Peyronel, Z. Krist., 92, 190 (1935).

2. G. Peyronel, Z. Krist., 94, 311 (1936).

3. Strukturbericht, Z. Krist., 3, 140 (1937).

4. A. F. Wells, J. Chem. Soc., 55 (1949).

5. G. A. Barclay, E. G. Cox, and H. Lynton, Chem. and Ind., 178 (1956).

6. A. F. Wells, "Structural Inorganic Chemistry," 3rd ed, 58, Oxford, London, 1962.

7. D. M. MacArthur and C. A. Beevers, Acta Cryst., 10, 428 (1957).

8. See for example D. R. Davies and D. E. C. Corbridge, Acta Cryst., 11, 315 (1958).

9. Von E. Steger and G. Leukroth, Z. anorg. alleg. chem., 303, 169 (1960).

10. A. Mutschin and K. Maennchen, Z. anal. chem., 160, 81 (1958).

11. D. E. C. Corbridge and E. J. Lowe, J. Chem. Soc., 493 (1954).

12. R. B. Harvey and J. E. Mayhead, Canad. J. Chem., 33, 1555 (1955).

13. H. Völlenkle, A. Wittmann, and H. Nowotny, Monatsh. Chem., 94, 956 (1963).

14. See for example A. J. C. Wilson, "X-Ray Optics," 2nd ed, 112-128, Methuen, London, 1962.

PROPOSITION 4

A method is proposed whereby the optimal sequencing of sequential data collection devices may be determined. This proposition was written mainly with single crystal x-ray diffractometers in mind; however, the principles apply equally well to any sequential data collection device on which the sequence in which data points may be collected is variable. A minor course in linear programming taken by the author supplied the inspiration and mathematical background for this proposition.

In discussions of the best way to use automatic x-ray diffractometers, the sequencing problem has been approached by the trial-and-error, common-sense methods (1). The determination of an optimal sequence, given certain criteria dependent on the instrument, is however possible by mathematical methods.

We assume a data collection device which has m adjustments which may be varied between data points. Also we assume that n data points with known (or precalculated) settings,

$$(q_{11}, \cdots, q_{1k}, \cdots, q_{1m}), \cdots, (q_{j1}, \cdots, q_{jk}, \cdots, q_{jm}), \cdots,$$

$$(q_{h1}, \cdots, q_{nk}, \cdots, q_{nm}),$$

are to be collected. Initial machine settings are $q_{01}, \cdots, q_{0k}, \cdots, q_{0m}$. We first define a matrix C such that the element c_{ij} is the cost in going from data point $i - 1$ to data point j. The method of calculating c_{ij} will depend upon the data collection device involved. In general

an expression of the type

$$c_{ij} = \sum_{k=1}^{m} d_k |q_{i-1,k} - q_{jk}|$$

may be used if the cost of moving an adjustment is a function only of the amount moved. On semi-automatic devices, adjustments requiring human intervention will have different effects on the c_{ij} than those automatically changed. A person who has experience on a given machine usually knows how he would like to weigh machine wear, human labor, etc., to calculate the c_{ij}.

For simplification in calculation, we further require that the c_{ij} be integral — after calculating an initial C matrix with non-integral c_{ij} elements, the elements may be multiplied by an appropriate scale factor and rounded to produce the integral elements needed.

Next we define a sequencing matrix S in which $s_{ij} = 1$ if data point j immediately follows data point i - 1, and $s_{ij} = 0$ if not. Since each data point is to be collected only once, there can be only one non-zero element in each row and only one non-zero element in each column of the S matrix.

With this, the problem in mathematical terms is to find a set of non-negative integers s_{ij} which minimize

$$\sum_{ij} s_{ij} c_{ij} \qquad (1)$$

subject to the conditions

$$\sum_{i=1}^{n} s_{ij} = 1 \quad \text{for} \quad j = 1, \cdots, n$$

and

$$\sum_{j=1}^{n} s_{ij} = 1 \quad \text{for} \quad i = 1, \cdots, n \ . \tag{2}$$

The problem is now of the type encountered in integral linear programming (2); it is appropriately called a canonical integral linear program and is quite similar to the problem of finding the most efficient path through a network.

The "dual" problem is to find integers $d_1, \cdots, d_i, \cdots d_n$ and $f_1, \cdots, f_j, \cdots, f_n$ such that

$$\sum_{j} f_j - \sum_{i} d_i = \text{maximum} \tag{3}$$

subject to the conditions

$$f_j - d_i \geqq c_{ij} \quad \text{for all i and j} \ . \tag{4}$$

It can be shown (the duality theorem) that if the integers c_{ij} satisfy 1 and 2 and the integers d_i and f_j satisfy 3 and 4, then

$$\sum_{ij} s_{ij} c_{ij} = \sum_{j} f_j - \sum_{i} d_i \ .$$

From this, one sees that the two problems may be solved jointly.

The problem is now in a form in which it may be solved by one of the standard methods of integral linear programming, or it may be expanded to larger matrices and solved by the simplex method. The solution methods are iterative, and for a problem of n data points, the work involved is getting a solution on a computer is of the order of magnitude of inverting an $n \times n$ matrix. The solution which is obtained may not be unique, but there will be no other solution for which $\sum_{ij} s_{ij} c_{ij}$ is smaller.

A simple method for obtaining a solution will be illustrated in the following example. Given a C matrix

$$C = \begin{bmatrix} 3 & 4 & 1 & 3 \\ 2 & 5 & 6 & 1 \\ 4 & 3 & 7 & 2 \\ 1 & 3 & 1 & 5 \end{bmatrix},$$

we begin with a feasible solution in which $s_{ij} = 1$ for $i = j$ and $s_{ij} = 0$ for $i \neq j$,

$$S_o = \begin{bmatrix} 1 & 0 & 0 & 0 \\ 0 & 1 & 0 & 0 \\ 0 & 0 & 1 & 0 \\ 0 & 0 & 0 & 1 \end{bmatrix}.$$

We will proceed by introducing a new $s_{ij} = 1$; the elements of row i and column j which are presently unity must, of course, become zero, and corresponding element — required to complete the basic solution — will become unity. In order to decide which s_{ij} to make

unity we compute another matrix G with elements g_{ij} which tell how much $\sum_{ij} s_{ij} c_{ij}$ will change by making $s_{ij} = 1$; in this we consider only those g_{ij} for which $s_{ij} = 0$.

Therefore

$$G_o = \begin{bmatrix} - & -2 & -5 & -4 \\ -2 & - & -3 & -6 \\ -5 & -3 & - & (-9) \\ -4 & -6 & (-9) & - \end{bmatrix} .$$

By assigning $s_{ij} = 1$ for the pair of most negative g_{ij} (circled) we obtain another solution

$$S_1 = \begin{bmatrix} 1 & 0 & 0 & 0 \\ 0 & 1 & 0 & 0 \\ 0 & 0 & 0 & 1 \\ 0 & 0 & 1 & 0 \end{bmatrix} \quad \text{and} \quad G_1 = \begin{bmatrix} - & -2 & -2 & +2 \\ -2 & - & +3 & (-3) \\ +2 & (-3) & +9 & - \\ -2 & +3 & - & +9 \end{bmatrix} .$$

Reiterating, we obtain

$$S_2 = \begin{bmatrix} 1 & 0 & 0 & 0 \\ 0 & 0 & 0 & 1 \\ 0 & 1 & 0 & 0 \\ 0 & 0 & 1 & 0 \end{bmatrix} \quad \text{and} \quad G_2 = \begin{bmatrix} - & +2 & (-2) & +1 \\ +1 & +3 & +9 & - \\ +2 & - & +6 & +3 \\ (-2) & +6 & - & +9 \end{bmatrix} .$$

Reiterating, we obtain

$$S_3 = \begin{bmatrix} 0 & 0 & 1 & 0 \\ 0 & 0 & 0 & 1 \\ 0 & 1 & 0 & 0 \\ 1 & 0 & 0 & 0 \end{bmatrix} \quad \text{and} \quad G_3 = \begin{bmatrix} +2 & +7 & - & +7 \\ +5 & +3 & +7 & - \\ +3 & - & +7 & +3 \\ - & +3 & +2 & +5 \end{bmatrix}$$

We now have an optimal S since no $g_{ij} < 0$.

References

1. See for example C. T. Prewitt, Abstracts of the A. C. A. Bozeman Meeting, A-3, 19, 1964.

2. See for example D. Gale, "The Theory of Linear Economic Models," 132-179, McGraw-Hill Book Co., Inc., New York, 1960.

PROPOSITION 5

A method is proposed by which standard deviations may be assigned to intensity estimates obtained by visual comparison of spots on a film to spots on a standard intensity scale. The proposed method is developed with multiple film x-ray photographs in mind, but most ideas are equally applicable to any visually-estimated intensity measurements. Such standard deviations are very useful in the case of visually-estimated x-ray reflection intensities, since they may be carried through the data reduction process by standard propagation-of-error methods to yield a standard deviation in the final observed intensity; this standard deviation may then be used in least-squares weighting during refinement of the crystal structure.

If we assume that all spots are the same size and shape, the standard deviation in a visual intensity measurement is dependent on the differential sensitivity of the eye. This phenomenon has been extensively investigated by physiologists; the present state of the physiological knowledge on this subject has been summarized by Barlow (1). For medium range intensities, Weber's Law, $\frac{\Delta I}{I}$ = constant, seems to hold at least roughly, but this law has been shown to break down at the low and high ends of the intensity scale. From physiological experiments it has not been possible to get accurate mathematical expressions which hold for the full range of intensity. However, taking Weber's Law as a starting point, we may build up an expression of $\sigma(I)$ as a function of I which agrees with our

qualitative knowledge.

Our first approximation is

$$\sigma(I) = bI \quad . \tag{1}$$

Qualitative knowledge tells us that we must match a curve of the type shown below.

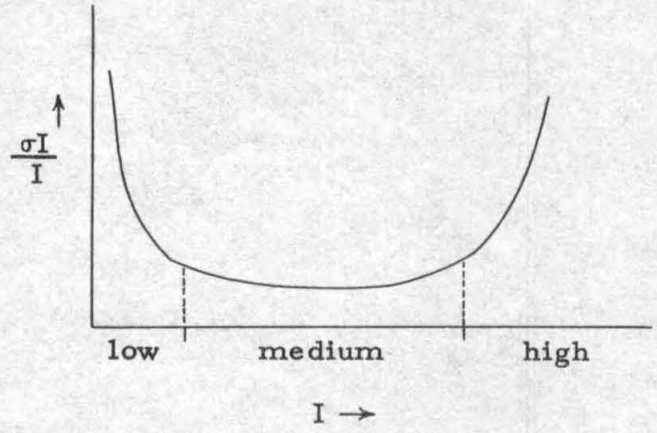

The low end may be taken into account by adding a constant to expression 1.

$$\sigma(I) = a + bI$$

This constant is of the order of $\frac{I_{min}}{3}$ where I_{min} is the minimum observable intensity value on the standard scale.

At the high intensity end of the scale (dark spots), testing of many different expressions has shown that adding the term $c \frac{I^2}{(I_{max} - I)^2}$ gives standard deviations agreeing with our qualitative knowlege; in

this, I_{max} is the value on the standard scale beyond which all readings are worthless, and c is about 0.1. The total expression is then

$$\sigma(I) = a + bI + c\,\frac{I^2}{(I_{max} - I)^2} \quad \text{for} \quad I < I_{max} \qquad (2)$$

and $\sigma(I) =$ a very large number for $I \geq I_{max}$

The constant b, which governs the size of the most important term in 2, is of order of magnitude 0.1. A determination of b for the particular case at hand is desirable if we are to have our standard deviations on an approximate absolute scale. In the multiple-film x-ray case, an exposure is taken by placing several films each against the other, the intensity difference between the same spot on different films being due only to absorption by the films. Assuming that all spots are read independently, let us consider how the value of b affects the spread of the frequency distribution of film factors calculated from pairs of intensities, both of which are of the size for which Weber's Law is presumed to hold. Since $\sigma(\ln x) = \frac{\sigma(x)}{x}$, substituting gives

$$\sigma(\ln I) = b \quad .$$

Therefore for this range, ln(I) is normally distributed with standard deviation b. Expressing the film factors as I_2/I_1, we get

$$\ln\left(\frac{I_2}{I_1}\right) = \ln I_2 - \ln I_1 \quad ,$$

and

$$\sigma \ln\left(\frac{I_2}{I_1}\right) = \sqrt{\sigma^2(\ln I_2) + \sigma^2(\ln I_1)} \ ,$$

if we assume no correlation between I_2 and I_1. Substituting gives

$$\sigma\left[\ln\left(\frac{I_2}{I_1}\right)\right] = \sqrt{2}\ b \ . \qquad (3)$$

Therefore it is possible to determine a value for b from a simple calculation of the spread of the distribution of the logarithm of the film factor.

$$\sigma\left[\ln\left(\frac{I_2}{I_1}\right)\right] = \sqrt{\frac{n}{n-1}\left[\frac{\Sigma\left[\ln\left(\frac{I_2}{I_1}\right)\right]^2}{n} - \left[\frac{\Sigma \ln\left(\frac{I_2}{I_1}\right)}{n}\right]^2\right]} \ .$$

Attempting to use the above to compute a value for b which will apply to the intensities from many films — as, for example, all layers about one axis, leads to trouble because the expectation value of $\ln\left(\frac{I_2}{I_1}\right)$ varies with angle of incidence of the x-rays to the film. This problem is avoided if for each set of films which is expected to have the same expectation value of $\ln\left(\frac{I_2}{I_1}\right)$, the quantity

$$n_i s_i^2 = \Sigma\left[\ln\left(\frac{I_2}{I_1}\right)\right]^2 - \frac{\left[\Sigma \ln\left(\frac{I_2}{I_1}\right)\right]^2}{n_i}$$

is calculated for each i. These quantities may then be combined to give

$$\sigma \ln \frac{I_2}{I_1} = \frac{\Sigma(n_i s_i^2)}{\Sigma n_i - 1} .$$

From the above, a value of b may be calculated. A suitable range for use in picking I values which lie in the medium range is $3I_{min} \leq I \leq .8I_{max}$.

The previous discussion has ignored spot shape, which on Weissenberg x-ray films is important. Testing has shown that we may raise the relative standard deviation of readings coming from regions on the film where α_1, α_2 splitting is causing smeared spots — relative to spots which do not have this problem — by multiplying expression 2 by the function

$$1 + de^{-g(0.5 - \sin^2 \theta)^2} ,$$

where θ is the Bragg angle. Reasonable values for d and g are 0.25 and 50 respectively. Another important point when dealing with α_1, α_2 splitting is that the $\sigma(I)$ for readings obtained from spots in which both the α_1 and α_2 contributions are resolved should be based on 2/3(I) since the total reading is a sum of two readings.

Reference

1. H. Barlow, J. Physiol., 136, 469-488 (1957).